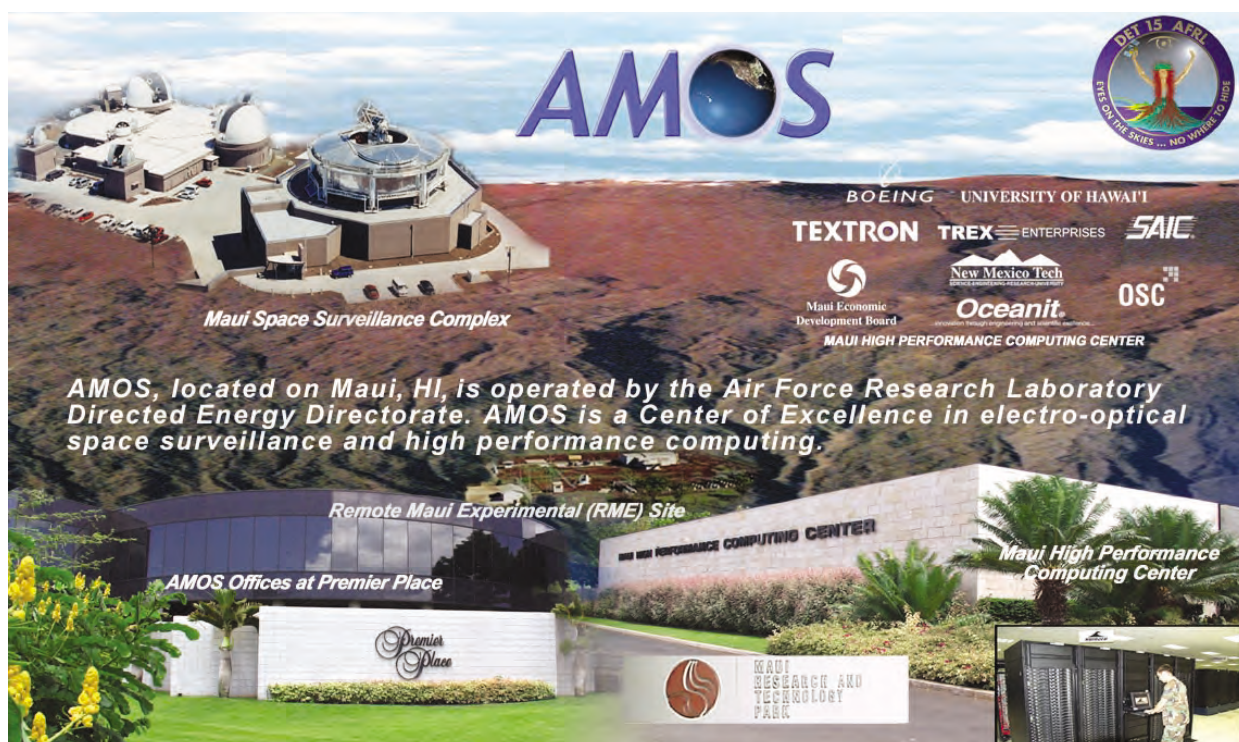# APPLICATION BRIEFS 2004

Air Force Maui Optical & Supercomputing Site (AMOS)

The views and conclusions contained in this document are those of the authors and should not be interpreted as necessarily representing the official policies or endorsements, either expressed or implied, of the Air Force Research Laboratory, the U.S. Government, the University of Hawaii, or the Maui High Performance Computing Center.

MAUI HIGH PERFORMANCE COMPUTING CENTER

550 Lipoa Parkway, Kihei-Maui, HI 96753
(808) 879-5077 • Fax: (808) 879-5018
E-mail: info@mhpcc.hpc.mil
URL: www.mhpcc.hpc.mil

An Air Force Research Laboratory Center Managed by the University of Hawaii.

Report Documentation Page		*Form Approved* *OMB No. 0704-0188*

Public reporting burden for the collection of information is estimated to average 1 hour per response, including the time for reviewing instructions, searching existing data sources, gathering and maintaining the data needed, and completing and reviewing the collection of information. Send comments regarding this burden estimate or any other aspect of this collection of information, including suggestions for reducing this burden, to Washington Headquarters Services, Directorate for Information Operations and Reports, 1215 Jefferson Davis Highway, Suite 1204, Arlington VA 22202-4302. Respondents should be aware that notwithstanding any other provision of law, no person shall be subject to a penalty for failing to comply with a collection of information if it does not display a currently valid OMB control number.

1. REPORT DATE **2004**	2. REPORT TYPE	3. DATES COVERED **00-00-2004 to 00-00-2004**

4. TITLE AND SUBTITLE **Application Briefs 2004**	5a. CONTRACT NUMBER
	5b. GRANT NUMBER
	5c. PROGRAM ELEMENT NUMBER
6. AUTHOR(S)	5d. PROJECT NUMBER
	5e. TASK NUMBER
	5f. WORK UNIT NUMBER

7. PERFORMING ORGANIZATION NAME(S) AND ADDRESS(ES) **Maui High Performance Computing Center (MHPCC),Air Force Maui Optical & Supercomputing Site (AMOS),550 Lipoa Parkway,Kihei-Maui,HI,96753**	8. PERFORMING ORGANIZATION REPORT NUMBER

9. SPONSORING/MONITORING AGENCY NAME(S) AND ADDRESS(ES)	10. SPONSOR/MONITOR'S ACRONYM(S)
	11. SPONSOR/MONITOR'S REPORT NUMBER(S)

12. DISTRIBUTION/AVAILABILITY STATEMENT
Approved for public release; distribution unlimited

13. SUPPLEMENTARY NOTES

14. ABSTRACT

15. SUBJECT TERMS

16. SECURITY CLASSIFICATION OF:			17. LIMITATION OF ABSTRACT	18. NUMBER OF PAGES	19a. NAME OF RESPONSIBLE PERSON
a. REPORT **unclassified**	b. ABSTRACT **unclassified**	c. THIS PAGE **unclassified**	**Same as Report (SAR)**	**60**	

Standard Form 298 (Rev. 8-98)
Prescribed by ANSI Std Z39-18

WELCOME

This is the tenth annual edition of Maui High Performance Computing Center's (MHPCC) *Application Briefs* which highlights some of the successes our customers have achieved this year.

MHPCC, established in September 1993, is an Air Force Research Laboratory (AFRL) Center managed by the University of Hawaii. A leader in scalable parallel computing technologies, MHPCC is primarily chartered to support the Department of Defense (DoD) and other government organizations.

MHPCC offers an innovative environment for High Performance Computing (HPC) applications. This includes:

- Computational Resources: Stable and secure parallel computing platforms for prototyping, benchmarking, and testing applications. MHPCC is ranked as one of the top HPC centers in the world in terms of computational capabilities.

- High-Speed Communications Infrastructure: OC12 connections (Hawaii), offering 620 megabit per second (Mbps) capacity, provide direct access to MHPCC resources — over the Defense Research and Engineering Network (DREN) and the Hawaii Intranet Consortium (HIC).

- Support Services: An expert staff provides MHPCC users with systems, network, and applications support in addition to assistance with code porting, optimization, and application development.

MHPCC is a well-established member of the High Performance Computing community, participating in collaborations and partnerships that extend its basic capabilities. MHPCC represents AFRL as a:

- Center within the Air Force Research Laboratory. MHPCC works closely with DoD and other government researchers to support Research, Development, Testing, and Evaluation (RDT&E) efforts.

- Distributed Center within the DoD High Performance Computing Modernization Program (HPCMP). MHPCC provides resources to the DoD research community, as well as Pacific Region DoD organizations, including the Air Force's Maui Space Surveillance Complex.

- Air Force Research Laboratory resource for the Air Force Maui Optical & Supercomputing Site (AMOS).

- Member of Hawaii's growing science and technology community.

MAUI HIGH PERFORMANCE COMPUTING CENTER
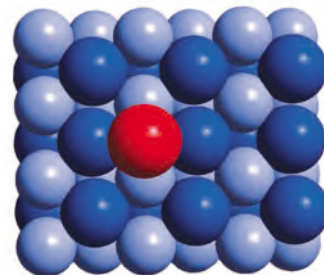
APPLICATION BRIEFS

The user application briefs in this publication represent selected research efforts that have taken place at MHPCC during 2004. Each application brief was written by an individual researcher or research team, and reflects their first-hand experiences using MHPCC resources. These articles reflect the diverse nature of our users and projects.
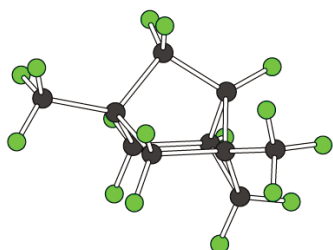
The Application Briefs in this document are the result of the efforts of more than 80 authors representing 30 organizations. We acknowledge the contributions of each of these individuals and are grateful for their work. We welcome back those authors who have become regular and frequent contributors. Joel T. Johnson is especially recognized for his tenth consecutive year of contributions to this publication. We also welcome those making their MHPCC Application Briefs debut this year.
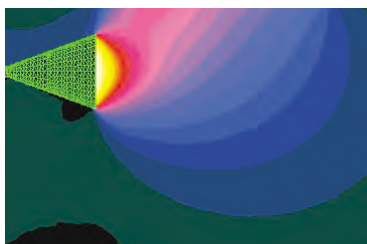
The shaded box at the top of each brief's first page is a short summary of the article. Author and/or organizational contact information can be found in the shaded box at the end of each brief. The notation at the bottom of each page indicates each project's primary functional area (DoD, Government, or Academic).
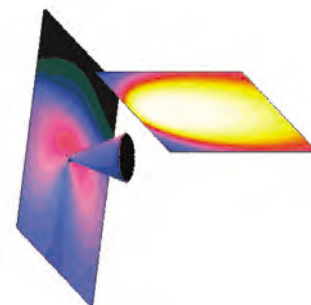
And finally, feedback regarding this publication is solicited. Please direct any communications to: *editor@mhpcc.hpc.mil.*
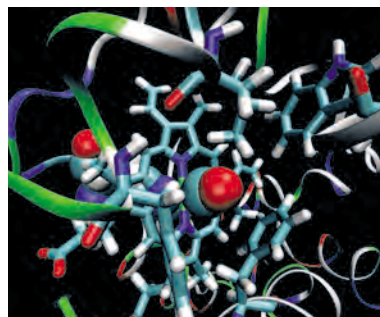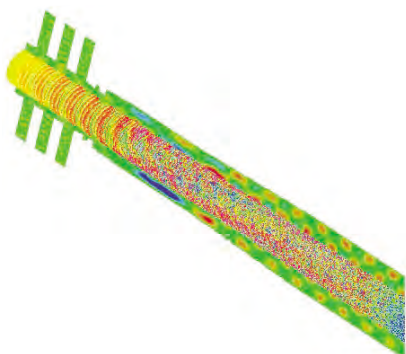
Thank you for your support.

iii

TABLE OF CONTENTS

TABLE OF CONTENTS CONTINUED

Theoretical Study of Nitrogenase.
Computational Evidence for Participation of the Central Nitrogen Atom
Michael L. McKee

The theoretical study of nitrogenase provides a detailed mechanism for the reduction of N_2 to NH_3. The central atom is considered to play an important role as reductant in the initial step. Between the first and second H-addition steps, the N-N bond of the N_2 substrate is predicted to cleave in a single step. The central nitrogen atom binds to one of the substrate nitrogen atoms. The N-N interaction gradually weakens after successive H-atom addition steps and breaks without exchanging central/substrate positions.

Background: Since the unexpected discovery in 2002 of a central light atom in the center of the FeMo cofactor of the nitrogenase protein by high resolution X-ray,[1] there has been a flurry of theoretical reports related to the mechanism of nitrogenase. The intense scrutiny is caused by fundamental curiosity of how nature breaks the strongest bond known, the $N{\equiv}N$ triple bond.

The reaction is also of immense practical value since the product, ammonia, is used in multi-million ton amounts every year. The current industrial process, known as the Haber-Bosch process, requires high pressures and high temperatures. The overall reaction involves the addition of eight protons and eight electrons (Equation 1) per N_2 molecule.[2] The iron atoms in the Fe_7S_9Mo cluster (resting state) have their spins anti-ferromagnetically coupled (S=3/2).

$$N_2 + 8e^- + 16MgATP + 8H^+ \rightarrow 2NH_3 + H_2 + 16MgADP + 16P_i \quad (1)$$
Equation 1.
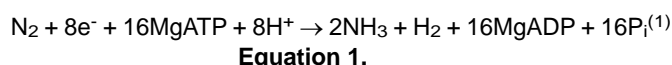
Before turnover of N_2 to NH_3 can start, it is generally believed that three or four electrons are required. In the present study, the ferromagnetic state (all irons have their spins parallel) is computed due to the difficulties encountered with the anti-ferromagnetic state. In addition, the proton/electron addition steps are coupled such that a hydrogen atom is added in each step. The resting form of the cluster is simplified to $Fe_8S_9N^+$, where all ligands are removed, the molybdenum atom is changed to iron, and the cluster is given a +1 charge to maintain the correct distribution of oxidation states in the cluster (Figure 1). Optimizations were carried out using density functional theory (B3LYP) with effective core potentials on iron atoms and flexible basis sets on all atoms.

Figure 1. Proposed active form of the FeMoCo cluster.

The active form of the cluster is considered to be $Fe_8S_6(SH)_2(SH_2)N^+$ which can bind N_2 by coordinating to two different iron atoms in di-bridging form (Figure 1). The active form of the cluster can eliminate H_2 or bind N_2. In the latter case, the migration of the hydrogen atom to the substrate nitrogen atom leads to complete cleavage of the N-N bond. The central nitrogen coordinates to one nitrogen atom of the substrate while the NH_2 group migrates to an iron atom (Figure 2). Subsequent H-atom additions lead to the elimination of two NH_3 groups. The present theoretical study provides insights into dinitrogen reduction by nitrogenase.

Figure 2. The substrate NN bond is broken.

References:
1) "Nitrogenase MoFe-Protein at 1.16 Resolution: A Central Ligand in the FeMo-Cofactor," O. Einsle, F. A. Tezcan, S. L. A. Andrade, B. Schmid, M.Yoshida, J. B. Howard, D. C. Rees Science 2002, 297, 1696-1700.
2) "Nitrogen Fixation: The Mechanism of the Mo-Dependent Nitrogenase," R. Y. Igarashi and L. Seefedt, Critical Reviews in Biochemistry and Molecular Biology 2003, 38, 351-384.

Author and Contact: Michael L. McKee
Organization: Department of Chemistry, Auburn University, Auburn, AL, 36849
URL: www.auburn.edu/~mckeeml
Resources: IBM SP2 *Typhoon* Cluster at MHPCC
Sponsorship: DOE/EPSCoR, MHPCC, Alabama Supercomputer Network

Pipeline Implementation of Cellular Automata for Structural Design on Message-Passing Multiprocessors

David B. Adams, Shahriar Setoodeh, Zafer G rdal, Layne T. Watson

The inherent structure of cellular automata (CA) is trivially parallelizable and can directly benefit from massively parallel machines in computationally intensive problems. This work examines both block synchronous and block pipeline (with asynchronous message passing) parallel implementations of cellular automata (CA) on distributed memory (message-passing) architectures. A structural design problem is considered to study the performance of the various cellular automata implementations. The synchronous parallel implementation is a mixture of Jacobi and Gauss-Seidel style iteration, where it is more Jacobi-like as the number of processors increase. Therefore, it exhibits divergence because of the mathematical characteristics of Jacobi matrix iteration for the structural problem as the number of processors increases. The pipeline implementation preserves convergence by simulating a pure Gauss-Seidel style rowwise iteration. Numerical results for analysis and design of a cantilever plate made of composite material show that the pipeline update scheme is convergent and successfully generates optimal designs.

Methodology: The problem of minimum compliance design with a volume constraint is investigated in this study. Compliance of a structure, by definition, is the work done by the external forces. To minimize the compliance for a structure with applied loads, the stiffness of the structure should be maximized while at the same time, the total volume must be kept less than a given value. This work considers fiber reinforced composite lamina with curvilinear fiber paths and treats the point-wise fiber orientation angle and density measure as continuous design variables.

Because of the close relationship cellular automata share with parallel Jacobi, Gauss-Siedel, and SOR methods, the work in parallel matrix iterative methods is very relevant to the parallelization of a CA. The Moore neighborhood used in this work corresponds to the nine point stencil used to derive the parallel Red/Black/Green/Orange SOR methods. Significant work has been done in the ordering and synchronization of Gauss-Seidel and SOR iterations to both improve their convergence properties and optimize their parallel implementations. The ideas of pipelining communication and optimal scheduling of processors have been examined in this other context. It has always been the case that the time required to update a single cell in the structure is very small compared to the communication time required to transmit the cell's state information. For this reason, a strip method or block method is preferred for parallelization to force the process to be compute bound instead of communication bound. The primary contribution of the present work is not in a novel parallelization of a CA, but rather to emphasize the need to maintain the convergence properties of the algorithm, as the number of processors increases for a simultaneous analysis and design CA. The point is that convergence for parallel CA simultaneous analysis and design can be preserved through the simple use of pipelined computation provided that the serial CA simultaneous analysis and design iteration converges (which need not obtain). Timings were performed at the Maui High Performance Computing Center on the P3 partition of *Tempest* consisting of 16-way, 375 Mhz Nighthawk-2 nodes, each with 8 Gbytes of shared memory.
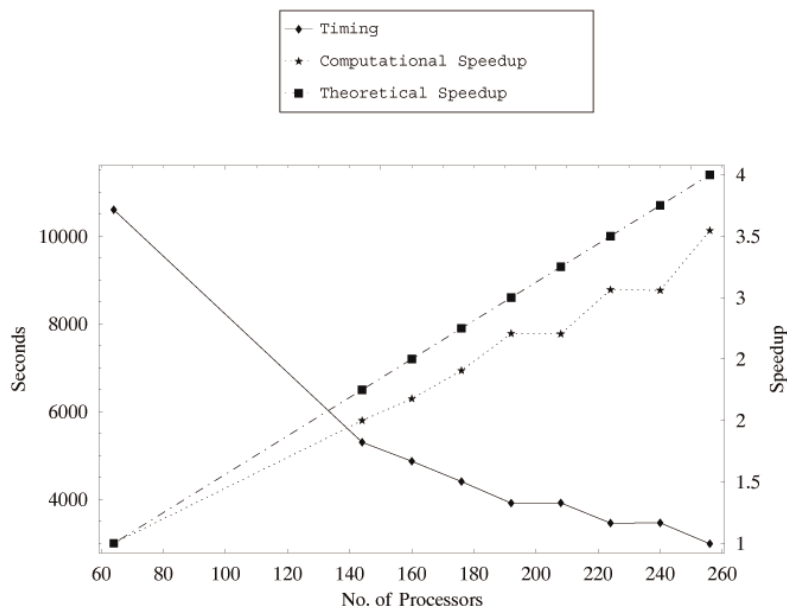
Figure 1. Execution time for the pipeline code was measured for a cell domain grid of 751 X 1501 cells. Timing results giving the relative speedup from 64 processors are shown with computation time to convergence measured in seconds.
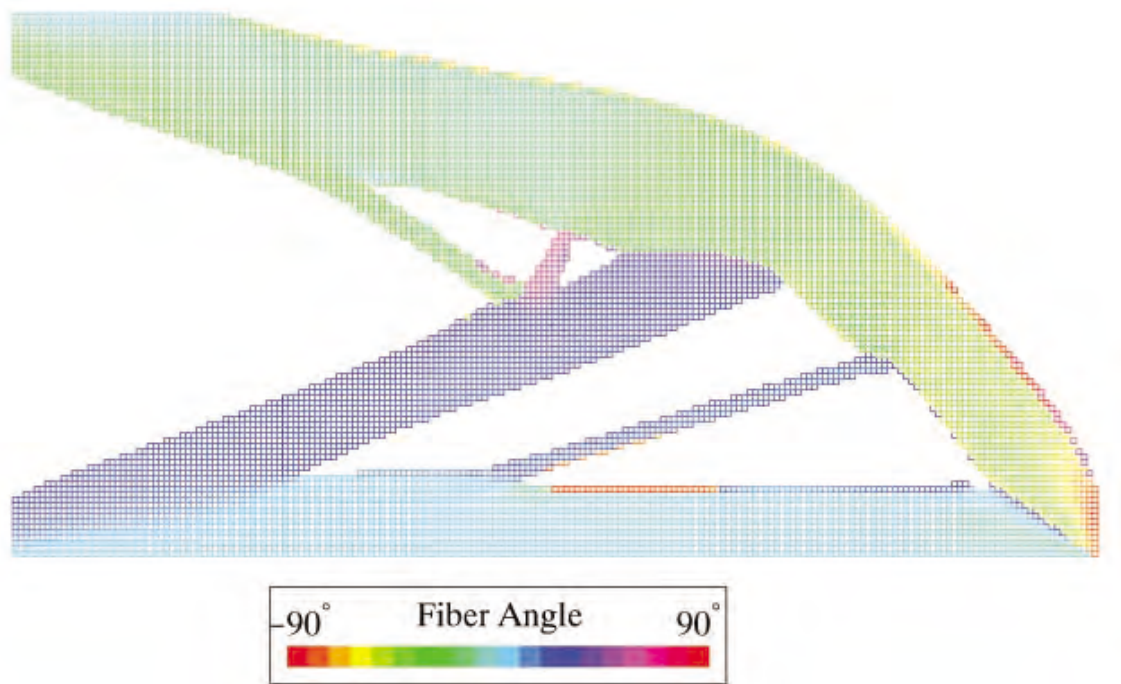
Figure 2. Sample CA design for a cantilever problem with 50% volume fraction. Cell color represents the optimal fiber angle.

Author and Contact: David B. Adams (Department of Computer Science)
Authors: Shahriar Setoodeh (Department of Engineering Science and Mechanics),
    Zafer G rdal (Departments of Aerospace and Ocean Engineering Science and Mechanics),
    Layne T. Watson (Departments of Computer Science and Mathematics)
Organization: Virginia Polytechnic Institute and State University, Blacksburg, VA, 24061-0106
Resources: IBM P3s on *Tempest* at MHPCC
Sponsorship: MHPCC, AFOSR Grant F49620-02-1-0090, and AFRL Grant F30602-01-2-0572

DoD

Elucidation of the Magic Number Protonated Water Cluster $H^+(H_2O)_{21}$

K. D. Jordan, R. A. Christie, R. S. Walters, T. D. Jaeger, M. A. Duncan, J. W. Shin,
N. I. Hammer, E. G. Diken, M. A. Johnson

The structural nature of the *magic number* protonated water cluster, $H^+(H_2O)_{21}$ has been elucidated through a combination of vibrational spectroscopy (Yale and Georgia groups) and electronic structure calculations (Pittsburgh group). The computations were carried out at the Maui High Performance Computing Center (MHPCC).

Background: Atomic and molecular clusters form a regime intermediate between that of independent atoms or molecules and the bulk phase. The finite size of clusters is responsible for their unique physical properties, such as "glass-like" phase transitions and magic number behavior. Molecular clusters serve as excellent model systems that can be investigated experimentally and theoretically using techniques not applicable to the bulk.

The protonated water clusters, $H^+(H_2O)_n$ are important both in terms of their role in natural processes and as a model for understanding the nature of the proton in aqueous chemistry. $H^+(H_2O)_n$ clusters have been postulated to be important species in the seeding of reactions in interstellar regions, as catalysts in the stratosphere, and in biomolecule reactions. Protonated water clusters also serve as model systems to aid in the understanding of proton transfer reactions in solution, an event of crucial importance in aqueous phase chemistry and biochemistry.

One of the most interesting properties of $H^+(H_2O)_n$ clusters is the magic number behavior first observed by Lin[1] and Searcy and Fenn[2] in the mid-1970s. In these studies, it was found that there were several cluster sizes which were significantly more likely to be observed in the mass spectrum than their neighbors. These are the so-called magic number clusters. Perhaps the most intriguing magic number is that observed at $n = 21$. The geometrical structure of this species has remained elusive up until now.

Methodology: In collaboration with the Duncan (Georgia) and Johnson (Yale) groups, we have undertaken a joint experimental/theoretical "attack" on the nature of the $H^+(H_2O)_n$ clusters.[3] Specifically, the Duncan and Johnson groups have characterized the $n = 6-29$ clusters using infrared predissociation spectroscopy, and we have used electronic structure methods to optimize the geometries and to calculate the vibrational spectra of selected isomers of these clusters. In the computational work we have employed the Gaussian 03 program[4], running in parallel over as many as 16 CPUs on the IBM Power3 computers at the Maui High Performance Computing Center.

The vibrational spectra from the Duncan and Johnson groups reveal that the $n = 21$ and 22 protonated water clusters display only a single line near 3700 cm^{-1} whereas the clusters on either side of these (i.e., for 11 = $n = 20$ and $n > 22$) display two lines in this spectral region which is associated with "free-OH" groups, that is OH bonds that are dangling "free" in space. The fact that only one absorption peak is observed in the free-OH stretch region for the $n = 21$ and 22 clusters implies that in these species all the free-OH groups are associated with water molecules in very similar Hydrogen-bonding environments. This eliminates a very large number of possible structures for these clusters.
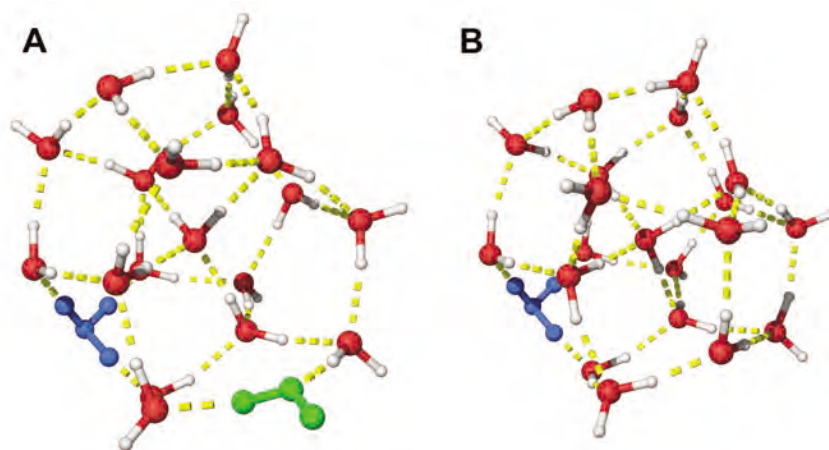
Figure 1. The geometric structures for the lowest-energy configurations of (A) $H^+(H_2O)_{20}$ and (B) $H^+(H_2O)_{21}$. In both structures, the proton is localized in the blue-colored H_3O^+ molecule. In Figure (A), the unique H_2O molecule which gives rise to the doublet peak in the spectrum of Figure 2 (A) is colored green.

Computations carried out on the *Squall* computer system at MHPCC show that the global minimum structures of the $n = 20$ and 21 clusters (depicted in Figure 1) give vibrational spectra in the free OH stretch region in close agreement with experiment (see Figure 2), in particular giving two peaks for the $n = 20$ cluster and a single peak in the free OH stretch region for the $n = 21$ cluster.

The global minimum of the $n = 21$ cluster may be viewed as being derived from a $(H_2O)_{20}$ dodecahedron, with an interior water molecule engaged in four Hydrogen-bonds to the dodecahedral cage. The proton is associated with a H_3O^+ entity located on the surface of the cluster. The $H^+(H_2O)_{20}$ cluster can be viewed as being formed from the $H^+(H_2O)_{21}$ cluster by loss of a surface water molecule, followed by reformation of one of the broken Hydrogen-bonds.

Summary: Although the experiments of the Duncan and Johnson groups combined with our theoretical calculations have provided new insight into the nature of protonated water clusters, they have also raised new questions, e.g., concerning the mobility of the proton, that we plan to tackle with the aid of new experiments and computational studies. Our results have been reported in the May 21st issue of Science.

References:
1) S. S. Lin, "Detection of Large Water Clusters by a Low Radio-Frequency Quadrupole Mass Filter," *Rev. Sci. Instrum.* 44, 1973, p. 516- 517.
2) J. Q. Searcy, J. B. Fenn, "Clustering of Water on Hydrated Protons in a Supersonic Free Jet Expansion," *J. Chem. Phys.*, 61, 1974, p. 5282-5288.
3) J. W. Shin, N. I. Hammer, E. G. Diken, M. A. Johnson, R. S. Walters, T. D. Jaeger, M. A. Duncan, R. A. Christie, K. D. Jordan, "Infrared Signature of Structures Associated with the $H^+(H_2O)_n$ (n = 6 to 27) Clusters," Science, 304, 2004, p. 1137-1140.
4) M. J. Frisch *et al.*, *Gaussian 03,* Gaussian, Inc., Pittsburgh, PA, 2003.
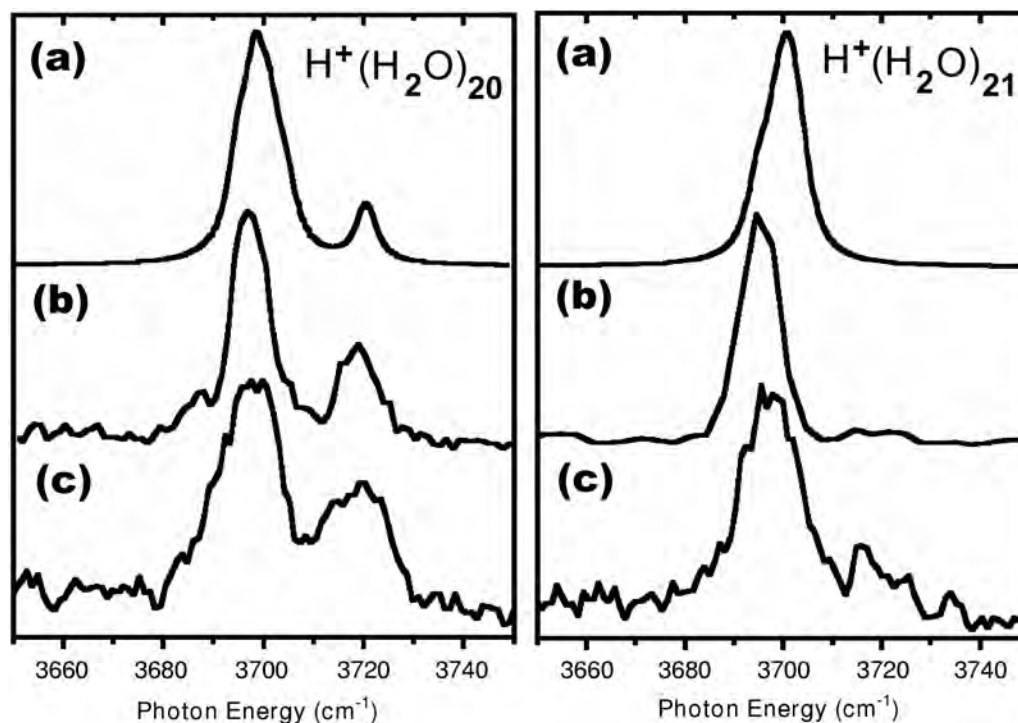
Figure 2. Calculated (a) and experimental [(b) Duncan group; (c) Johnson group] vibrational spectra of $H^+(H_2O)_{20}$ and $H^+(H_2O)_{21}$ in the free-OH region.

Author and Contact: K. D. Jordan
Author: R. A. Christie
Organization: Department of Chemistry, University of Pittsburgh, Pittsburgh, PA, 15260
Authors: R. S. Walters, T. D. Jaeger, M. A. Duncan
Organization: Department of Chemistry, University of Georgia, Athens, GA, 30602
Authors: J. W. Shin, N. I. Hammer, E. G. Diken, M. A. Johnson
Organization: Sterling Chemistry Laboratory, Yale University, P.O. Box 208107, New Haven, CT, 06520
Resources: IBM Power3 Processors at MHPCC

Global Optimization of Si_xH_y and Si_xF_y Clusters at the *Ab Initio* Level

John D. Head and Yingbin Ge

Computational methods used in this research found F ligands cause dramatic change to the Si frameworks suggesting that different ligands could be used to tune the optoelectronic properties of the Si nanoclusters.

Background: Nanometer-sized Si clusters have promising optoelectronic properties which could be useful for various technological applications such as solar cells. Since the bare Si clusters are highly reactive, practical devices will most likely consist of Si clusters passivated by some ligand. H and F atoms are prototypical passivating ligands. In our research we have been developing efficient strategies using non-empirical quantum chemistry calculations and genetic algorithms to globally search for the most stable Si_xH_y and Si_xF_y clusters. We obtained the diamond lattice-like global minima for the fully passivated $Si_{10}H_{16}$, $Si_{14}H_{20}$ and $Si_{18}H_{24}$ clusters and quite different structures for the incompletely passivated $Si_{10}H_{14}$, $Si_{14}H_{18,}$ and $Si_{18}H_{22}$ clusters shown in Figure 1. We have also found the $Si_{10}F_{16}$ and $Si_{10}F_{14}$ global minima shown in Figure 2. Surprisingly, the F ligands cause dramatic change to the Si frameworks suggesting that different ligands could be used to tune the optoelectronic properties of the Si nanoclusters.
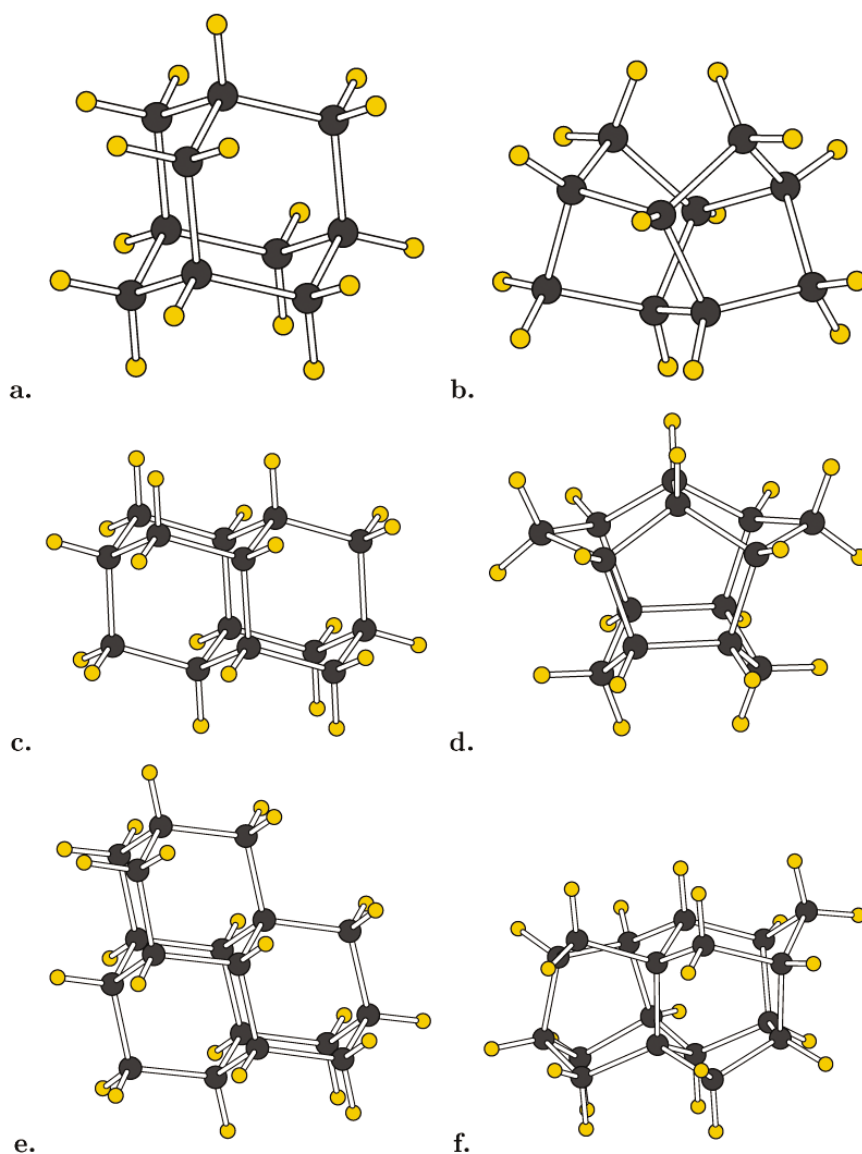
Figure 1. The MP2 global minima of various silicon hydride clusters: a. $Si_{10}H_{16}$, b. $Si_{10}H_{14}$, c. $Si_{14}H_{20}$, d. $Si_{14}H_{18}$, e. $Si_{18}H_{24}$, and f. $Si_{18}H_{22}$.

Research interests of this author include: Theoretical chemistry and electronic structure calculations of ground and excited state properties for large molecules, clusters, surfaces, and nanomaterials.
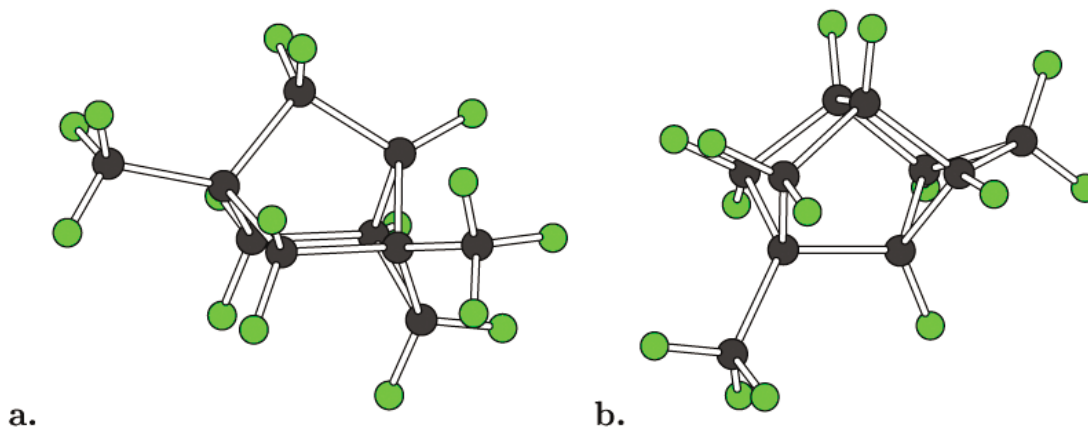
Figure 2. The B3LYP global minima of a. $Si_{10}F_{16}$ and b. $Si_{10}F_{14}$.

Author and Contact: John D. Head
Author: Yingbin Ge
Organization: University of Hawaii, Department of Chemistry, 2545 The Mall, Honolulu, HI, 96822-2275
Resources: *Squall* and *Tempest* at MHPCC
Sponsorship: University of Hawaii

DoD

Computation of Polarimetric Thermal Emission from the Sea Surface

Joel T. Johnson

The WindSAT radiometer of the Naval Research Laboratory was launched in January 2003, and is currently recording observations of the polarimetric thermal emission from the sea surface in 16 microwave channels. The brightness temperatures" measured in these channels can be used to retrieve wind speed and direction over the sea surface, along with other environmental information. Performing retrievals of sea wind vector requires knowledge of the process by which the rough sea surface produces microwave thermal emission. Although several physically based models exist, the approximations inherent in these models lead to uncertainties in the accuracy of their predictions. In this project, two approximate models of sea thermal emission are compared in order to assess their performance.

Methodology: The studies of this project involve predicting microwave thermal emission from a statistically described rough surface. A Monte Carlo simulation is used to capture brightness statistics, and two approximate electromagnetic theories are used for emission calculations. The more expensive of the two methods is the small slop approximation for surface scattering cross sections, which involves a quadruple integral in order to compute surface scattering cross sections at a single bistatic angle. An integration over all bistatic cross sections is further required to compute emitted power. Parallel computing resources are utilized to divide the multiple bistatic angles among 16 processors, as well as multiple azimuthal observation angles and surface realizations in the Monte Carlo simulation. The second approximate theory is a two-scale approximation and is much less expensive so that supercomputing resources are not required for its evaluation. Because of this advantage, the two-scale model is to be preferred if it can be shown to be of sufficient accuracy.

Results: Monte Carlo simulations have been completed for two distinct sets of surface statistics. Results are reported in terms of the direct surface emitted brightness temperature in the zeroth and second azimuthal harmonics (i.e., to capture wind direction effects), as well as the zeroth and second azimuthal harmonics of the reflected downwelling atmospheric brightness as a function of the zenith attenuation of the atmosphere. Figure 1 illustrates the comparison for a small height surface case, for which only sea surface waves shorter than two electromagnetic wavelengths are included in the simulated surfaces. Here the agreement between the active and passive (i.e., two-scale) small slope approximations is seen to be good, although some small differences are observed.
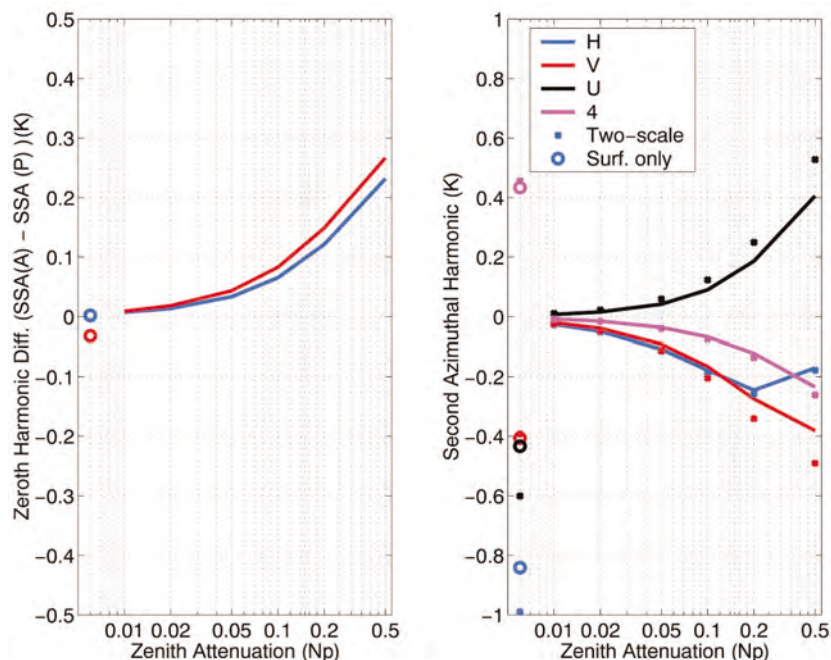
Figure 1. Comparison of active and passive (i.e., two-scale) models for surface (large circles and dots) and reflected atmospheric (lines and dots) brightnesses, versus zenith attenuation for the reflected atmospheric term. The left plot is the error in the zeroth azimuthal harmonic, while the right plot illustrates second azimuthal harmonic values from the two theories. The multiple curves in the plots indicate the four modified Stokes parameters measured by a polarimetric radiometer. Sea surfaces used contained only waves shorter than two electromagnetic wavelengths.

Figure 2 illustrates the comparison for the large height surface, where sea surface waves ranging up to 64 electromagnetic wavelengths are included in the simulation. Here the agreement between the two theories is seen to degrade, while remaining of acceptable accuracy for some applications. Further simulations will help to quantify the level of difference between the theories, as well as to suggest a practical theory for use in WindSAT sea wind vector retrievals.

Significance: The results of this project will influence future algorithms to be applied in performing wind vector retrievals from WindSAT data, as well as from future spaceborne polarimetric microwave radiometers.
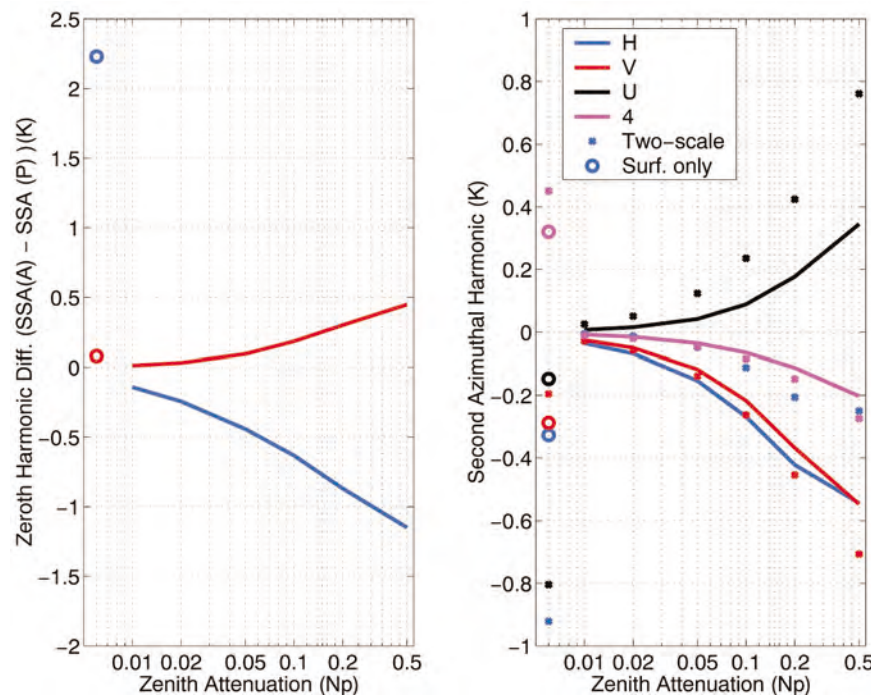
Figure 2. Same as Figure 1, except sea surfaces used contained only waves shorter than 64 electromagnetic wavelengths.

Author and Contact: Joel T. Johnson
Organization: Associate Professor, Ohio State University, 205 Dreese Laboratories, 2015 Neil Ave, Columbus, Ohio, 43210
URL: http://eewww.eng.ohio-state.edu
Resources: Up to 64 Power3 CPUs on the *Tempest* and 32 Nodes of the *Huinalu* Linux Cluster at MHPCC
Sponsorship: Department of Defense

DoD

High-Resolution Forecasts to Support AMOS Using MM5

Kevin Roe and Duane Stevens

The Hawaiian Islands contain a variety of microclimates in a very small region. Some islands have rainforests within a few miles of deserts; some have 10,000 foot summits only a few miles away from the coastline. Because of this, weather models must be run at a much finer resolution to accurately predict in these regions. NCAR's Mesoscale Model Version 5 (MM5) is run from a coarse 27 km resolution (surrounding an area of approximately 5000 by 5000 km) nested down to a 1 km resolution daily. Since the computational requirements are high to accomplish this in a reasonable time frame (as to still be a forecast) MM5 is run in parallel on MHPCC's IBM SP4s. Utilizing 32 processors the MM5 model is run daily over the above conditions in approximately six hours. These forecasts have been in place for over two years now and are being utilized by operators at the telescope on Haleakala, Maui.

Research Objectives: The telescope operations on Haleakala are highly dependent on weather conditions on the Hawaiian Island of Maui. If the wind speed is too high then the telescope cannot be utilized. Problems also exist if there are clouds overhead. Rainfall and relative humidity are also a factor in determining the capabilities of the telescopes. In order to effectively schedule telescope operations, an accurate weather prediction is extremely valuable. Current forecasts that are available from the National Weather Service (NWS) give good indications of approaching storm fronts but only at the coarse level (30-50 km resolution). Because of this and the location of the telescope on Maui this can be insufficient for their needs. The additional benefit of the telescope operators having access to an accurate forecast (even for only a day in advance) is that they can still perform some scheduling. If a storm is predicted they can plan maintenance for this time period. This allows them to function more effectively by giving them the capability to schedule downtime. This in turn saves time, improves operating efficiency, and potentially saves money.

Daily Operations: Every night at midnight Hawaiian Standard Time (HST), a PERL script is run to handle all the operations necessary to produce a forecast, prepare the data, and post it to the MHPCC Web page (http://weather.mhpcc.edu/mm5). The procedures the script executes are:

1) Determine and download the latest global analysis files from NCEP for a 48-hour simulation,
2) Begin processing by sending these files through MM5's REGRID program,
3) Take the output data files from REGRID and input into INTERPF,
4) Prepare the MM5 model for the current simulation,
5) Submit the MM5 run to MHPCC's IBM SP4 (*Tempest*) for execution (daily reservation starting at 1 A.M.),
6) Average daily run requires 5-6 hours for completion on 32 processors (1 P4 node),
7) Data is output in one-hour increments,
8) Data is processed in parallel to create useful images for meteorological examination,
9) Convert images to a Web viewable format,
10) Create the Web pages for these images, and
11) Post Web pages and images to MHPCC's Web site.

Figure 1. Maui Space Surveillance Site located atop Mt. Haleakala.

Web Output: Now that the above processes have created images, they must be made available for the telescope operators. This is accomplished by posting the images to the MHPCC Web page; specifically, http://weather.mhpcc.edu/mm5. This title page gives the user the option of what area and resolution they would like to examine. From the title page, the user can select the all island area at a 27 or 9 km resolution, one of the four counties (Hawaii, Maui, Oahu, and Kauai) at a 3 km resolution, or the summit of Haleakala at a 1 km resolution. Once one of the above has been selected, the user is transported to a web page that initially includes an image of the temperature in the selected area. On the regional Web page, the viewer can select to see the previous or next image through the use of a small JavaScript. If the viewer prefers, an animation of the images (in one hour increments) can be started and stopped. Finally, the user can select any of the images from a pull-down menu. If the viewer would like to change the field being examined, a pull down menu on the left side of the page will transport the user back to the main menu or allow them to choose a different field. Lastly, if the JavaScript becomes a problem for the viewer's browser, they have the option of being switched to a non-JavaScript equivalent version Web page.
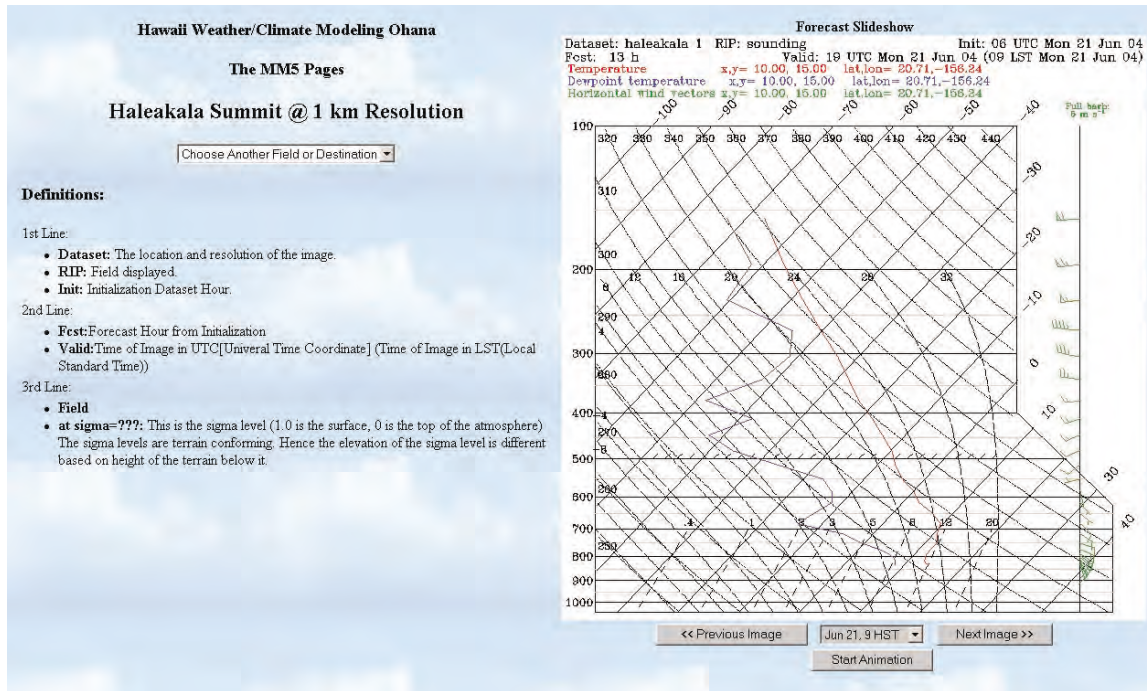
Figure 2. Website screen capture of weather modeling of the Haleakala Summit.

References:
1) J. Michalakes, "The Same-Source Parallel MM5, *Journal of Scientific Programming*, 8, (2000): 5-12.
2) J. Michalakes, S. Chen, J. Dudhia, L. Hart, J. Klemp, J. Middlecoff, and W. Skamarock, "Development of a Next Generation Regional Weather Research and Forecast Model," Developments in Teracomputing, Proceedings of the Ninth ECMWF Workshop on the Use of High Performance Computing in Meteorology, Eds., Walter Zwieflhofer and Norbert Kreitz, World Scientific, Singapore, (2000): 269-276.
3) J. Dudhia, "A Nonhydrostatic Version of the Penn State/NCAR Mesoscale Model, Validation Test and Simulation of an Atlantic Cyclone and Cold Front," Mon. Wea. Rev., 121, (1993): 1493-1513.
4) Yi-Leng Chen and J. Feng, "Numerical Simulation of Airflow and Cloud Distributions over the Windward Side of the Island of Hawaii, Part I: The Effects of Trade Wind Inversion," American Meteorological Society, (May 2001): 1117-1134.
5) Yi-Leng Chen and J. Feng, "Numerical Simulation of Airflow and Cloud Distributions over the Windward Side of the Island of Hawaii, Part II, Nocturnal Flow Regime," American Meteorological Society, (May 2001):1135-1147.
6) K. P. Roe and D. Stevens, "High Resolution Weather Modeling in the State of Hawaii," The 11th PSU/NCAR Mesoscale Model Users' Workshop, Boulder, C0, 2001.
7) K. P. Roe and D. Stevens, "High-Resolution Weather Modeling to aid AMOS," DoD HPCMP User Group Conference, Bellevue, WA, 2003.

Author and Contact: Kevin Roe
Organization: Maui High Performance Computing Center, 550 Lipoa Parkway, Kihei, Maui, HI, 96753
Author: Duane Stevens
Organization: Department of Meteorology, University of Hawaii at Manoa, 2525 Correa Road, HIG 350, Honolulu, HI, 96822
URL: http://weather.mhpcc.edu/mm5
Resources: IBM SP4 at MHPCC
Sponsorship: Air Force Research Laboratory

Hawaii Fire Danger Rating System, 2004

Francis M. Fujioka and Kevin P. Roe

Forest lands in Hawaii provide clean water and air for 1.2 million people, and habitat to rare plants and animals found nowhere else in the world. To help natural resource managers protect Hawaii's forests, the USDA Forest Service and MHPCC recently installed a new Hawaii Fire Danger Rating System at MHPCC, which combines the MM5 high resolution weather modeling framework with the National Fire Danger Rating System (NFDRS). The project built on previous work created terrain and fuels map databases necessary to evaluate fire danger.

Project Objectives: Upon completion, the Hawaii Fire Danger Rating System will incorporate high resolution weather and fire danger modeling subsystems to inform land managers of fire risks in Hawaiian forests and wildlands (Figure 1).[1] The System accounts for weather, fuels, and terrain characteristics in predicting fire ignition, spread, and heat energy release potential within a 48-72 hour forecast period. Wildland fire protection agencies will be able to create customized weather and fire danger maps on demand using an interactive web-based map service.
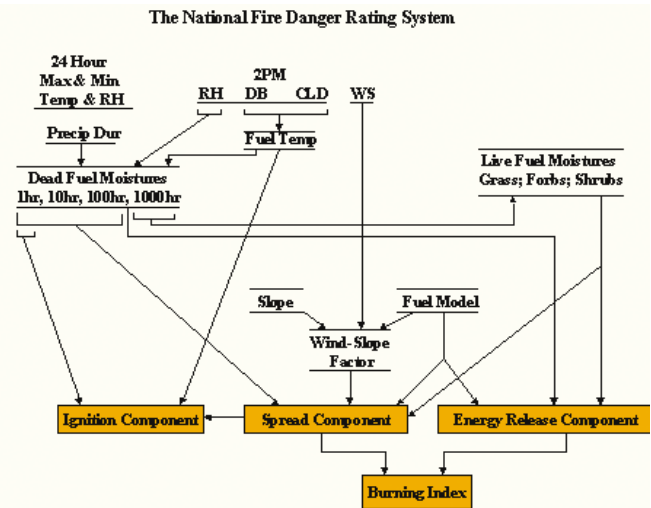

Figure 1. Wildfires in Hawaii typically burn through fine fuels such as the fuelbed shown here.

Figure 2. The Hawaii Fire Danger Rating System follows the design of the National Fire Danger Rating System. Ignition, spread, and energy release characteristics of a fire are determined from input streams of weather, fuel, and terrain data that describe the fire environment.

Methodology: The daily process of producing fire danger rating forecasts begins with MM5 model runs at MHPCC that produce fire weather forecasts for the counties of Kauai, Oahu, Maui, and Hawaii, at a grid interval of 3 km.[2] A fire danger rating post-processor uses the MM5 forecasts to calculate corresponding fire danger rating variables, integrating the additional effects of fuel and terrain conditions, which are assumed to be static. The weather data-relative humidity (RH), temperature (DB), cloudiness (CLD), and precipitation (Precip Dur) determine the moisture content of the dead fuel elements in the fuels map database, hence the ignition potential (Figure 2). An underlying fire behavior model within the NFDRS incorporates wind (WS) and topographic slope effects to estimate fire spread and energy release potentials. The Burning Index, derived from the Spread and Energy Release Components, is theoretically proportional to the expected flame lengths, given the fire environment inputs.

The fire danger rating components quantify the dimensions of the expected fire potential, thus providing fire protection agencies with information to respond with appropriate prevention, dispatching, and, if necessary, resource pre-positioning strategies. However, each agency may have its own critical thresholds of fire danger rating components that trigger management actions. This requires flexibility in extracting information from the danger rating system.

The Hawaii Fire Danger Rating System meets this requirement with a web-based geographic information system (GIS). The user can create weather and fire danger index maps for any time in the forecast period, and at the desired map scale (Figure 3). Other features such as roads, agency boundaries, place names, and even color satellite images may be selectively displayed, thus giving the user a wide variety of information to determine an appropriate management action.
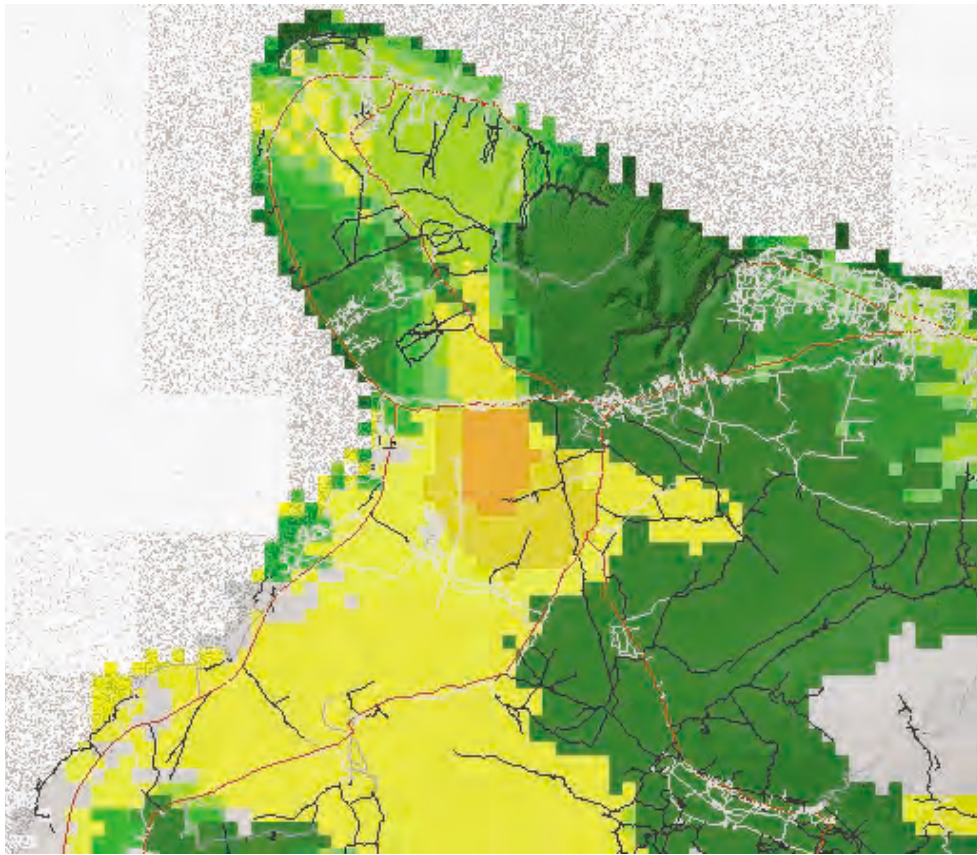
Figure 3. Forecast map of Energy Release Component for the North Kohala area of the Big Island. This map was created from the GIS Web server for the HFDRS.

Future Work: The Hawaii Fire Danger Rating System informs fire managers of potential fire problems. Once an incident occurs, good predictions of fire spread are needed, which requires even higher resolution weather, fuels, and topography. Future work will attempt to drive model grid intervals to less than one kilometer, and integrate the weather model with a fire behavior model.[3]

References:

1) F. M. Fujioka, D. R. Weise, and R. E. Burgan, "A High Resolution Fire Danger Rating System for Hawaii," Preprints, 3rd Symposium on Fire and Forest Meteorology, 9-14 January 2000, Long Beach, CA, American Meteorological Society, 103-106.
2) K. P. Roe and D. Stevens, "High Resolution Weather Modeling in the State of Hawaii," 11th PSU/NCAR Mesoscale Model Users' Workshop, Boulder, CO, 2001.
3) F. M. Fujioka, "PEGASUS: An Integrated Weather/Wildfire Modeling System," Preprints, 2nd Symposium on Fire and Forest Meteorology, 11-16 January 1998, Phoenix, AZ, American Meteorological Society, 38-41.

Author and Contact: Francis M. Fujioka
Organization: USDA Forest Service, 4955 Canyon Crest Drive, Riverside, CA, 92507
Author: Kevin P. Roe
Organization: Maui High Performance Computing Center, 550 Lipoa Parkway, Kihei, HI, 96753
Resources: IBM SP4s at MHPCC

Improving Interface Adhesion of Jet Engine Thermal Barrier Coatings

Karin M. Carling and Emily A. Carter

To achieve high thrust and fuel efficiency in a jet engine, the operational temperature is actually higher than the melting point of the metal engine components. To prevent parts from melting, they are covered with materials that protect them from the heat, so-called thermal barrier coatings (TBCs). These materials consist of several layers. The outer layer is a ceramic material which is a good thermal insulator, while the middle layer is a thermally grown oxide that acts as a corrosion barrier layer. These ceramics are bonded to the metal parts via a bond coat layer, which is a metallic alloy. With time and usage, the TBCs degrade and start to chip off, exposing the underlying metal to high temperatures that compromise the engine. This project uses quantum mechanics to investigate the adhesion and bonding of the interface between bond coat and thermally grown oxide, and how the interface properties are changed with the introduction of different elements at the interface. To begin with, we studied the adsorption of Hf on the clean NiAl(110) surface. Ultimately, we hope to suggest strategies to increase the adhesion between the bond coat and the ceramic, thus delaying the degradation of the TBCs.

Research Objective: This project focuses on characterizing the interface between the bond coat and ceramic layers of TBCs. Often, the bond coat is a NiAl alloy and this will give rise to a thermally grown aluminum oxide at the bond-coat-ceramic interface. Previous research with Ni as a model for the bond coat alloy showed that the metal-ceramic interface is the weakest point of the TBCs due to poor bonding between the metal and the ceramic across the interface, and that the adhesion of the interface improves with the introduction of early transition metal atoms at the interface.[1] Since most bond coats are based on NiAl alloys, here we use the binary NiAl alloy as the bond coat model and begin with investigating the adsorption of Hf atoms on the NiAl(110) surface.

Methodology: We use first-principles generalized gradient approximation (GGA) density functional theory calculations, as implemented in the plane-wave code VASP, and the PBE functional for the GGA. The interaction between electrons and ions is described with projector augmented wave (PAW) potentials. Periodic supercells allow efficient calculations of bulk, surface, and interface structures. Relaxation of ionic positions is performed to get the minimum energy structures.
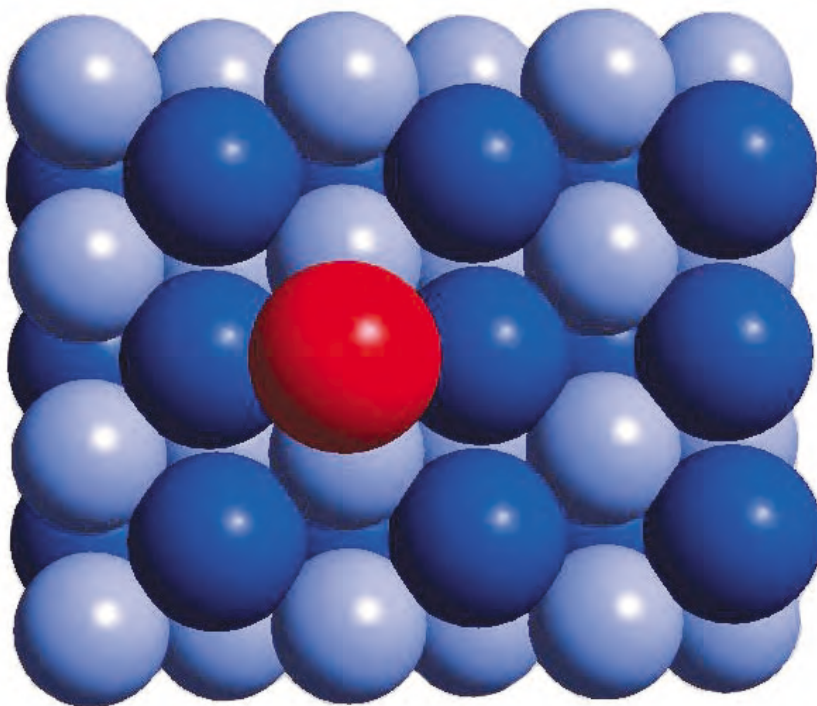

Figure 1. The Hf atom (red) is adsorbed in a Ni (light blue) bridge position on the NiAl(110) surface. Another stable, but less likely, adsorption site is the Al (dark blue) bridge.

Results and Significance: We find that the Hf atom has the most favorable adsorption energy when it is adsorbed in the Ni bridge site; see Figure 1. The Al bridge site will also be a stable adsorption site, but the energy of this site is more unfavorable than the Ni bridge. The surrounding Ni and Al atoms of the surface relax when the Hf is adsorbed. Generally, the Ni atoms relax towards the Hf, while the Al atoms move away. In the case of the Al bridge, the relaxations are large enough to move the two next-nearest-neighbor Ni atoms to a nearest-neighbor position, and the nearest-neighbor Al atoms become next-nearest-neighbors to the Hf atom. Also, all positions where the Hf atom has both Ni and Al atoms as close neighbors, e.g., any of the three-fold sites, are unstable. Our results indicate that the Hf atom is attracted to Ni atoms and repelled by Al atoms. The results from the adsorption of Hf on the clean NiAl surface give us the information needed to position Hf at the interface between NiAl and aluminum oxide, and to investigate the changes in adhesion of the interface with and without Hf present. This information will give a basis for recommendations from an atomistic, chemical point of view, on how to improve the design of TBCs to increase its lifetime and decrease the rate of spallation.

References:

1) E.A. Jarvis and E.A. Carter, Importance of Open-Shell Effects in Adhesion at Metal-Ceramic Interfaces, Physical Review B, 66, 100103 (2002).

Author and Contact: Emily A. Carter
Author: Karin M. Carling
Organization: Department of Chemistry and Biochemistry, University of California-Los Angeles, Box 951569, Los Angeles, CA, 90095-1569
URL: www.chem.ucla.edu/carter/
Resources: IBM SPs at MHPCC
Sponsorship: Air Force Office of Scientific Research

Chemistry of Gun Tube Erosion from First Principles

D. E. Jiang and Emily A. Carter

Experimental observations of eroded gun tubes show that carburization, sulfidation, and hydrogen embrittlement are potential causes for the erosion. We investigate the surface chemistry behind this problem via the state-of-the-art density functional theory (DFT) techniques.

Research Objective and Methodology: Firing a gun causes a harsh environment inside the gun tube: high temperature, high pressure, and reactive gases. As a result, the tube of the gun eventually erodes. Thermal effects, mechanical forces, and chemical corrosion may contribute to the process. Experimental observations of eroded gun tubes show that carburization, sulfidation, and hydrogen embrittlement are potential causes for the erosion. We investigate the surface chemistry behind this problem via the state-of-the-art density functional theory (DFT) techniques. We are also interested in determining a way to chemically pretreat iron surfaces to improve resistance to corrosive chemicals.

Results and Significance: We have studied carbon and hydrogen atoms interacting with bulk and surface iron,[1-4] and we have also examined carbon monoxide (CO) and hydrogen sulfide (H_2S) dissociation on iron and alloy surfaces.[5] We find that deposition of S on Fe surfaces via H_2S is kinetically and thermodynamically facile (see Figures 1 and 2). Our study provides understanding of the fundamental chemistry of gun tube erosion. We are currently investigating ceramic/alloy thin film coatings on iron. This may lead to the discovery of alternative protective coating materials for gun barrels.
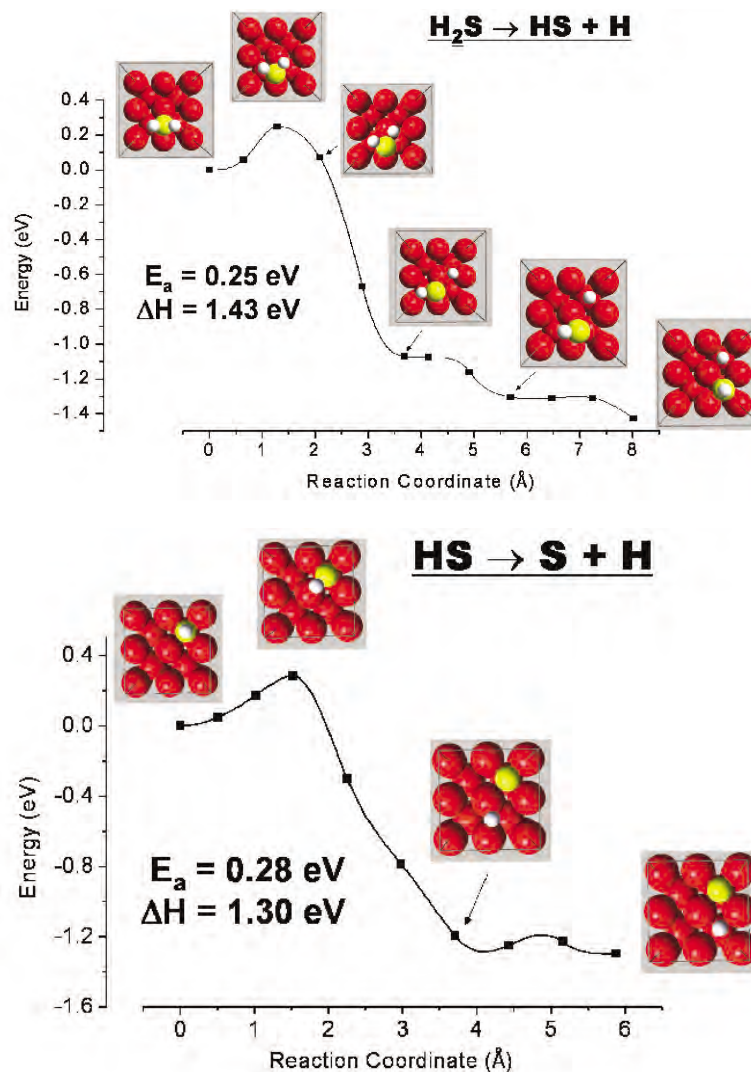
Figure 1. Minimum energy paths of sequential dehydrogenation steps of H_2S on Fe(100). Fe in red, S in yellow, and H in white.

References:

1) D. E. Jiang and E. A. Carter, Phys. Rev. B. 67, 214103 (2003).
2) D. E. Jiang and E. A. Carter, Surf. Sci. 547, 85 (2003).
3) D. E. Jiang and E. A. Carter, Phys. Rev. B., in press (2004).
4) D. E. Jiang and E. A. Carter, Acta Mater., in press (2004).
5) D. E. Jiang and E. A. Carter, Surf. Sci., submitted (2004).
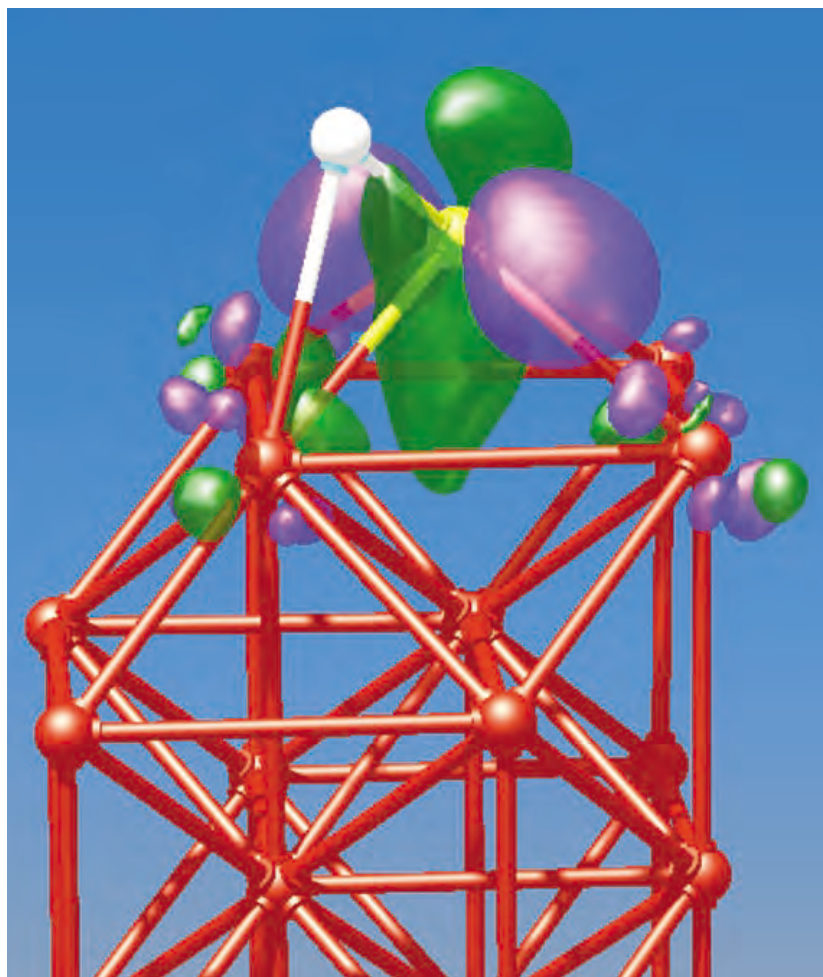
Figure 2. Isosurface plot of the charge density difference for HS/Fe(100) in the transition state. The iso-value is at -0.05 e/ ^{3} for the green surface and at 0.05 e/ ^{3} for the pink surface. Solid balls are atoms: H in white, S in yellow, and Fe in red.

Author and Contact: Emily A. Carter
Author: D. E. Jiang
Organization: Department of Chemistry and Biochemistry, University of California-Los Angeles, Box 951569, Los Angeles, CA, 90095-1569
URL: www.chem.ucla.edu/carter/
Resources: IBM SP3 and SP4 (*Tempest*) at MHPCC and SP3 (*Brainerd*) at the Army Research Laboratory, MSRC
Sponsorship: Army Research Office

Airborne Laser Atmospheric Decision Aid (ADA) Testing

Frank H. Ruggiero, Daniel A. DeBenedictis, Kevin P. Roe

The Airborne Laser (ABL) is being developed as one element of our Nation's Ballistic Missile Defense System. The ABL Element Office is developing an Atmospheric Decision Aid (ADA) to diagnose and forecast the location and magnitude of optical turbulence in the upper troposphere and lower stratosphere. The ADA will use as input real-time numerical weather prediction (NWP) forecasts provided by the Air Force Weather Agency (AFWA). This project evaluated the overall performance of the current operational model for use with the ADA as compared with the next generation model and whether the current model grid spacing used in AFWA operations is sufficient for the ADA. Results show the new generation of mesoscale model needs to improve its ability to forecast the lower stratosphere and that increasing the operational model grid spacing does not significantly improve optical turbulence forecasting.

Background and Objective: The Airborne Laser (ABL), an element of our Nation's Ballistic Missile Defense System (BMDS), will detect and destroy boosting ballistic missiles. The ABL Element Office is managing the development of an Atmospheric Decision Aid (ADA) to diagnose and forecast the location and magnitude of optical turbulence in the upper troposphere and lower stratosphere. Optical turbulence is the fluctuation of density in the atmosphere and acts to defocus laser beams and thus reduce their effective range. Layers of intense optical turbulence, while possibly stretching hundreds of kilometers in the horizontal, tend to occur on vertical scales of a centimeter to 100 meters. Mission planners responsible for the ABL will need to know the areas of strong optical turbulence fields in order to optimally locate the ABL's orbit to protect the asset while maximizing the lethality capability. The ABL ADA will provide mission planners with real-time forecasts of optical turbulence. The ADA uses output of a numerical weather prediction (NWP) model and runs a turbulence model[1] that quantifies optical turbulence from weather variables. The Air Force Weather Agency (AFWA) will send its real time operational mesoscale model forecasts to the ADA. Currently, the AFWA uses the Fifth Generation Penn State/National Center for Atmospheric Research Mesoscale Model (MM5)[2,3] as its operational model. It will soon transition to the new Weather Research and Forecast (WRF) Model for its operations. The objective of the work of this project is twofold. First, we have examined the effect of enhancing the vertical and horizontal resolution of MM5 on the resulting forecasts of optical turbulence. The second objective is to analyze the performance of the WRF model in predicting optical turbulence.

Results: In 2003-2004 we conducted validation runs of MM5 and WRF on the MHPCC IBM SP/RS6000 SP computer for two different field experiments where optical turbulence measurements were available. We found that increasing the MM5 horizontal and vertical resolution beyond the current operational AFWA settings did not significantly improve the optical turbulence forecasts.[4] Comparisons of optical turbulence forecasts between MM5 and WRF show that at this point in the stage of WRF development, MM5 and WRF are comparable in their ability to produce accurate input into the ADA.[5]
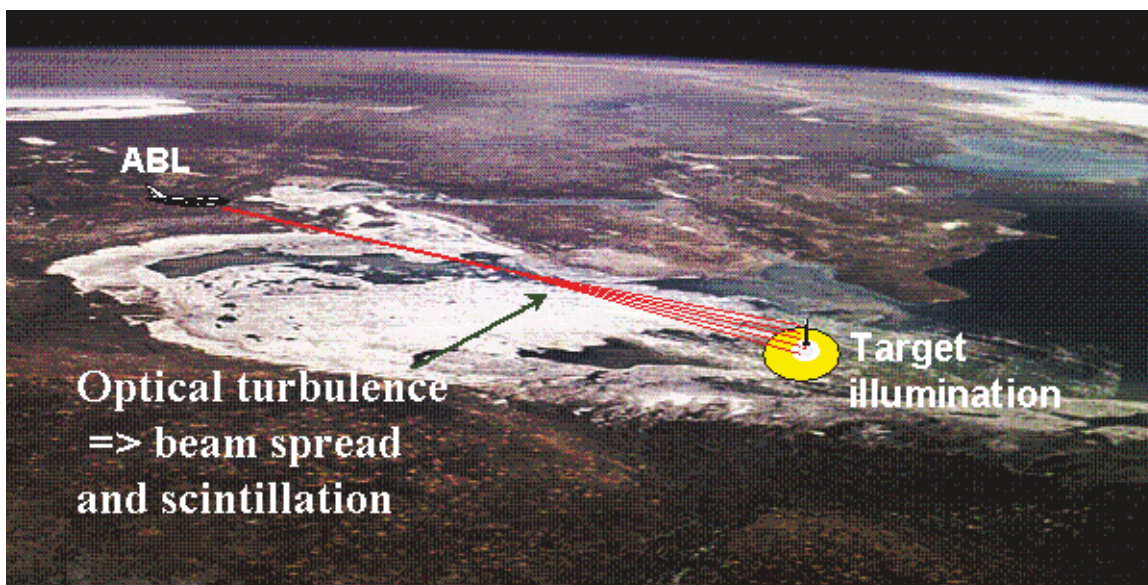

Figure 1. As the Airborne Laser dwells upon a target, optical turbulence will cause beam scintillation as well as beam spreading. This in turn will reduce the amount of power per unit area impacting the target and require a longer target dwell time.

References:

1) E. M. Dewan, R. E. Good, B. Beland, and J. Brown, "A Model for C_n^2 (Optical Turbulence) Profiles using Radiosonde Data," Phillips Laboratory Technical Report, PL-TR-93-2043, (1993), ADA 279399.

2) G. A. Grell, J. Duhia, and D. R. Stauffer, "A Description of the Fifth Generation Penn State/NCAR Mesoscale Model (MM5)," NCAR Tech. Note T/N-398 + STR, (1995); 122 pp, [Available from NCAR Information Services, P.O. Box 3000, Boulder, CO, 80307] (http://www.mmm.ucar.edu/mm5/documents/mm5-desc-doc.html).

3) J. Michalakes, "The Same-Source Parallel MM5, *Sci. Programming*, 8, (2000): 5-12. (http://www.mcs.anl.gov/~michalakes/JOSP-michalakes.ps).

4) F. H. Ruggiero, D. A. DeBenedictis, R. J. Lefevre, and S. Early, "Mesoscale Modeling Effects on Optical Turbulence Parameterization Performance," Preprints, 20th Conf., Weather Analysis and Forecasting and 16th Conf. on Numerical Weather Prediction, 12-15 January (2004), Seattle, WA.(http://ams.confex.com/ams/pdfpapers/69017.pdf).

5) F. H. Ruggiero, D. A. DeBenedictis, and K. Roe, "Comparison of WRF and MM5 for Optical Turbulence Prediction," Preprints, 2004 DoD High Performance Modernization Program Users Group Conference, 7-11 June, Williamsburg, VA.
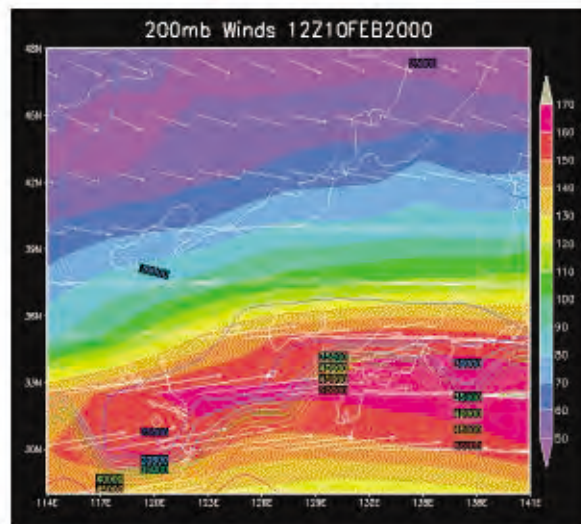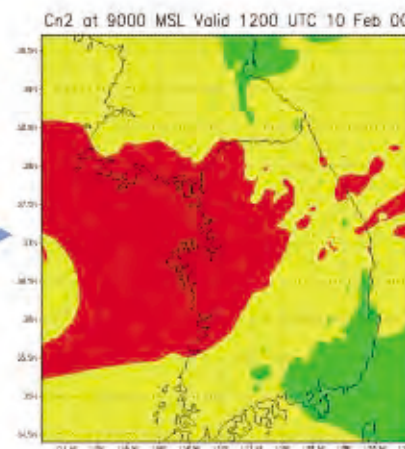
Figure 2. The Air Force Weather Agency at Offutt AFB, NE, is responsible for providing mesoscale atmospheric weather variables via DREN to the ABL's Atmospheric Decision Aid workstation (initially located at Kirtland AFB, NM) where optical turbulence will be forecasted for mission planning purposes.

Author and Contact: Frank H. Ruggiero
Organization: AFRL, Space Vehicles Directorate, Hanscom AFB, MA
Author: Daniel A. DeBenedictis
Organization: Titan/SenCom Corporation, Billerica, MA
Author: Kevin P. Roe
Organization: Maui High Performance Computing Center, 550 Lipoa Parkway, Kihei, Hi, 96753
Resources: IBM SP3/SP4 at MHPCC
Sponsorship: Air Force Research Laboratory and ABL Program Element Office

High Performance Computing and Visualization Support for Project Albert: Analysis of Simulations of Combat Operations and Operations Other Than War

Bob Swanson, Maria Murphy, Mike Coulman, Ron Viloria, Bruce Duncan

The Marine Corps Warfighting Laboratory's (MCWL) Project Albert involves research to assess the general applicability of the "New Sciences" to combat operations and operations other than war. While simulations based on these New Sciences (or complexity theory, which models behavior and interaction at the entity level) are considered part of an infant science, they do provide insight into evolving patterns of macroscopic behavior that result from collective interactions of individual agents. Simulations based on entity-level interactions represent a significantly different approach from the traditional attrition estimation techniques based on Lanchester equations, which assert that the loss rate of forces on one side of a battle is proportional to the number of forces on the other side. MCWL Project Albert is an effort to investigate how complexity theory may be applied to combat in a manner to augment and, perhaps in some cases, replace Lanchester modeling in the future.

Research Objectives: MCWL is continuing the development of a complex systems analyst's toolbox for exploiting emergent, collective patterns of behavior on the battlefield, and is currently using several multi-agent-based simulations of notional combat. Current models that are being employed include: Map Aware Non-uniform Automat (MANA), Pythagoras, Simulation Of Cooperative Realistic Autonomous Transparent Entities (SOCRATES), PAX, NetLogo, and the Irreducible Semi-Autonomous Adaptive Combat (ISAAC) model. These models simulate the interaction between two or more variable size forces of agents. The action of each agent is determined by a small rule set specified by parameters, such as the agent's ability to sense its surroundings and to communicate with other agents. Besides the common physical parameters measured by the model (such as range of fire and probability of kill), more abstract concepts are also modeled. Such concepts can include an agent's attraction to friendly and opposing forces and the influence of behaviors based on determinable thresholds, such as the tendency of an agent to follow orders. The magnitude and granularity of these independent variables provide the analyst with great flexibility in simulating various hypotheses. However, this same flexibility, coupled with the stochastic nature of the simulations, requires a significant computational capability to determine likely outcomes with any statistical significance. This requirement becomes even greater for the analyst who wants to study hypotheses over multiple varying independent parameters, a requirement that can easily overtax the capability of a single personal computer.

Methodology: The Maui High Performance Computing Center (MHPCC) Project Albert contractor team has performed computer systems and software engineering services in concert with military analysts from MCWL and other supporting contractors, to develop methodologies and tools needed for the large-scale analysis of agent-based distillation models. This development includes tools to define a problem set, request a job submittal, assist MHPCC personnel in running and managing the jobs, marshal the sometimes massive output of the jobs, and tools to help the end-user analyst visualize the numeric results created by these chaotic systems. The models are largely cross-platform in nature, but MHPCC has ported those models, where possible, to work on MHPCC's IBM Linux cluster, the IBM SP parallel supercomputer, and a cluster of Windows workstations unique and dedicated to Project Albert. The primary output of the many model runs is a set of numeric measures of battlefield effectiveness. In addition, tools produced at MHPCC can extract time/space results from certain models that add movie-like visualization capabilities of the battlefield state. The information generated from this exhaustive execution of model simulations, along with the associated mechanisms for visualization, will provide analysts with the tools required to investigate multiple hypotheses with statistical significance.
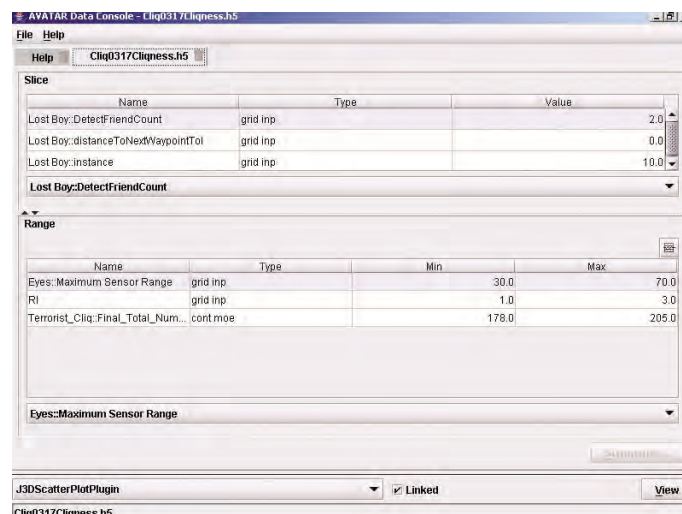

Figure 1. The AVATAR Data Console in use.

Results: The MHPCC contractor team has created a new Visualization system for Project Albert called "Albert Visualization Abstraction Toolkit for Analysis and Research (AVATAR). This tool will help provide visualization of the data generated by the chaotic systems modeled. This is a new visualization tool, written from the ground up, replacing the visualization tool provided in the past by MHPCC.

The AVATAR system is designed with a core "Data Console" that allows the user to select the portions of the data space they wish to view. It should be noted that a large set of runs from Project Albert can create millions of data points. The Console makes it easier for an analyst to grasp a large set of numeric information. Figure 1 shows the data console in use. The user can select inputs and outputs of the data farming runs either as "slices" or "ranges". A "slice" fixes an input variable at a specific value. A "range" allows specification of the minimum and maximum of either an input variable, or an output MOE.

The selected slices appear at the top of the display window, with the selected ranges appearing near the bottom. Pull-down menu selections allow the user to specify the single value for a slice. In the range area, pull-down menus allow the user to specify minimum and maximum allowed values. The bottom pull-down menu provides a list of the plugins available for plotting.

In order to view the selected information, the AVATAR system supplies a simple "plugin" interface. Thus, any Java programmer can produce a plotting plugin that views and/or analyzes the MOE data from Project Albert data farming runs. Several plugins have been created, with Figure 2 showing a 3-dimensional scatter plot of information. The Y direction (top to bottom) represents a MOE value (blue side casualties), while the X direction (left to right) represents a varying parameter (tendency to approach enemy). The depth of the image represents the random sample numbers injected into the model execution.

Work on the Data Console is complete, and customers have been testing various plugin technologies. Future development plans include providing a much richer set of plugins to the using community for both data visualization and data analysis.

Figure 2. An example of a 3-dimensional Plotting Plugin in use.

Significance: This initiative has led to a continuing evolution and refinement of the new generation of analytical models and tools for Department of Defense researchers. It is anticipated that MCWL will continue to require further development of simulation, visualization, and statistical methodologies that may enhance MCWL's ability to evaluate the applicability of these simulations to actual combat doctrine. These efforts will expand the existing infrastructure to incorporate new technologies.

Author and Contact: Bob Swanson
Authors: Maria Murphy, Mike Coulman, Ron Viloria, Bruce Duncan
Organization: Maui High Performance Computing Center, 550 Lipoa Parkway, Kihei, Maui, HI, 96753
Resources: IBM SP3, IBM Linux Supercluster, and Window Clusters at MHPCC
Sponsorship: Marine Corps Warfighting Laboratory (MCWL)

Simulation of 95 GHz Gyrotron Interaction Cavities

Peter J. Mardahl, Keith L. Cartwright, John J. Watrous

We are using the ICEPIC (Improved Concurrent Electromagnetic Particle-in-cell) simulation code to characterize the 100 KW ADS (Active Denial System) and the Airborne ADS program (JC32 Active Denial System ACTD) gyrotron. This gyrotron is the basis of the ADS effort to produce and field nonlethal weaponry for the warfighter. Its use will allow warfighters to control crowds without resorting to lethal weaponry and exposing the U.S. to negative diplomatic consequences as a result. The 100 KW system is already designed and fielded. Upcoming higher-power gyrotron designs strain the validity of traditional gyrotron simulation and modeling tools. These upcoming designs therefore represent expensive risks. ICEPIC, which makes fewer approximations about device physics, is being used to validate these designs, and will provide another test of these new designs before expensive experiments are constructed, reducing the risk and potential costs.

Introduction: ICEPIC predicts the performance of several high power microwave (HPM) devices currently in development for the U.S. Air Force. With an accurate simulation tool, devices such as (but not limited to) the relativistic klystron oscillator (RKO), the magnetically insulated line oscillator (MILO), the relativistic magnetron, and high frequency gyrotrons can be improved. ICEPIC simulates the electrodynamics (Maxwell's equations) and charged particle dynamics (relativistic Lorenz's force law) with second-order time and space accuracy in HPM sources. These simulations accurately predict RF-production and antenna gain when compared with experimental testing. In general, ICEPIC development has been driven by the desire to achieve high power in a compact RF device. This implies that the device is operated at high current and high space charge. Consequently, these devices are highly nonlinear. In addition, these devices have complex three-dimensional geometries with small features. ICEPIC may be used both for fine-tuning well-understood devices and for testing new designs.

Methodology: The ICEPIC gyrotron modeling effort is proceeding in two stages. First, ICEPIC will be used to characterize the existing 100 KW, 95 GHz gyrotron (shown schematically in Figure 1) presently in use in the functioning ADS prototype. High frequency (short wavelength) devices are very computationally expensive to model using ICEPIC, because ICEPIC must resolve the wavelength with 20 or more computational zones (cells) in order to model the physics accurately. The typical L-band tube, which operates in the gigahertz frequency range, is only a few wavelengths long. W-band tubes (such as the 95 GHz gyrotron) can be hundreds of wavelengths long. In 3D, the wavelength must be resolved in each dimension, which means that many billion cells would be needed to model the entire device. That is a practical impossibility, given computing resources available this decade. The only part of the device that really requires a full 3D ICEPIC model is the interaction region, which is only a very small fraction of the entire device.
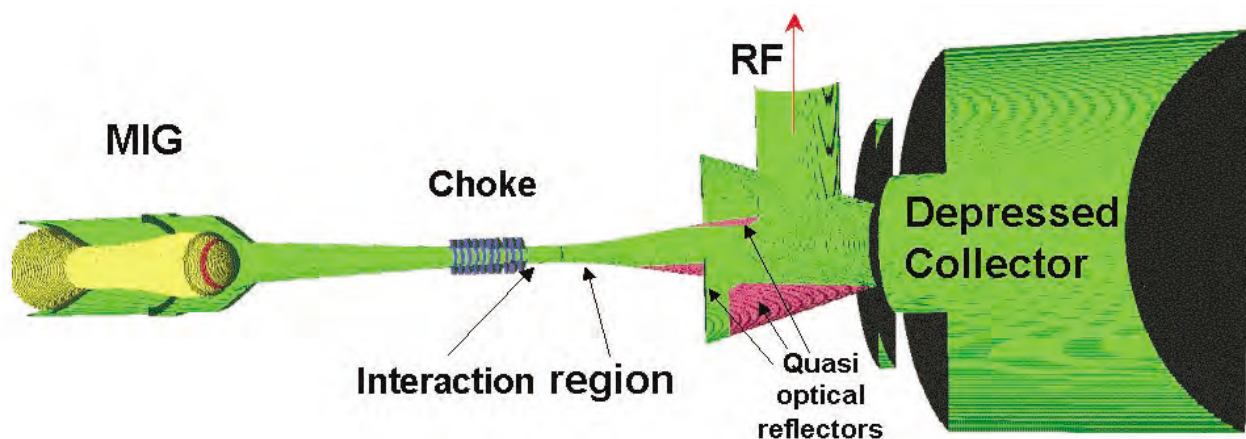
Figure 1. Shown is a schematic of the gyrotron. On the left is the Magnetron Injection Gun, which creates the energetic beam of electrons that drives the TE_{621} mode in the interaction region. Following that is the mode power extraction region, where quasi-optical reflectors transform the axially propagating TE_{621} into radially propagating electromagnetic waves, which leave the device. On the far right is the collector region, which gathers electrons from the spent beam and recovers some energy from the spent electrons, improving device efficiency.

Figure 2 shows the ICEPIC model of the interaction region, which includes some upstream and downstream components of the device. Figure 3 shows the gyrotron operating in the TE_{621} mode, which is the mode it was designed to use. Figure 4 shows an axial slice of the device in operation and the output power. The ICEPIC simulations have successfully matched device mode of operation, device operating frequency, and output power. Validation of the output power is a recent result and we are continuing to work on demonstrating predictive capability.

The next stage of the ICEPIC gyrotron modeling effort involves applying ICEPIC's demonstrated gyrotron simulation capability to test a new 2.5 MW gyrotron interaction cavity design before that device is built.
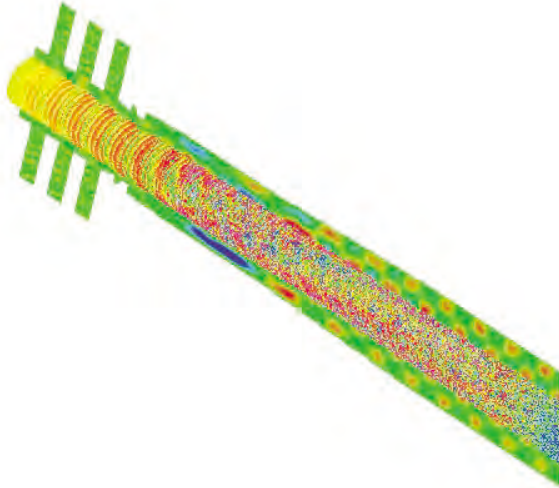

Figure 2. Shown is an image of an ICEPIC simulation of the gyrotron interaction region. The beam of electrons passes through and excites the TE_{621} mode.
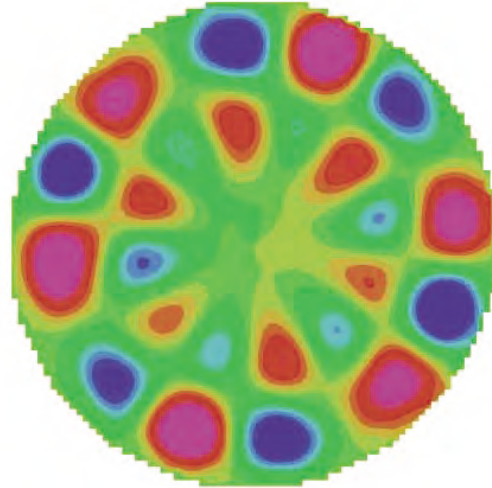

Figure 3. Shown is a transverse slice of the TE_{621} mode in the gyrotron, with colors indicating the magnitude of the azimuthal electric field.
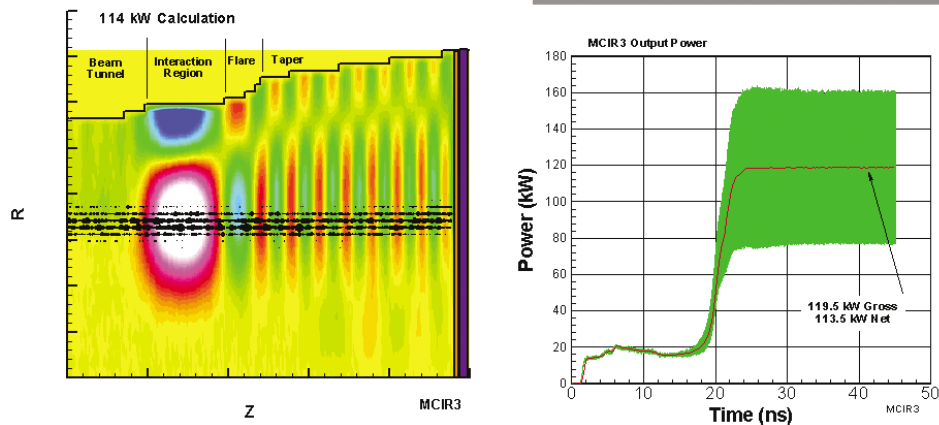
Figure 4. Shown on the left is an axial slice of the gyrotron in operation. On the right is a trace of the output power vs. time.

Reference:
1) R. E. Peterkin, Jr. and J. W. Luginsland, "Theory and Design of a Virtual Prototyping Environment for Directed Energy Concepts," *Computing in Science and Engineering* (March-April 2002).

Author and Contact: Peter J. Mardahl
Author: Keith L. Cartwright
Organization: AFRL/DE, Kirtland Air Force Base, 3550 Aberdeen Ave SE, NM, 87177-5776
Author: John J. Watrous
Organization: Numerex Corporation, Albuquerque, NM
Resources: IBM SMP and IBM Netfinity (MHPCC), IBM SMP (ARL, ERDC), SC40 and SC45 (ERDC).
Sponsorship: Department of Defense

Towards a High-Resolution Global Coupled Navy Prediction System

Julie McClean, Mathew Maltrud, Paul May, James Carton, Detelina Ivanova,
Prasad Thoppil, Elizabeth Hunke, Benjamin Giese

A computational project is underway to bring about the realization of a high-resolution global coupled atmosphere/ocean/ice prediction system for synoptic meteorological and oceanographic forecasting. A fully coupled near-global ocean/atmosphere prediction system at modestly high resolution has been constructed at the Naval Research Laboratory at Monterey (NRLMRY). The next steps in the development of this system are the inclusion of ice, improvement of the data assimilation scheme, and transitioning to higher resolution; university and national laboratory partners are advancing these goals.

Research Objectives: Towards the realization of a high-resolution global coupled air/sea/ice synoptic prediction system, we are continuing the development and testing, analysis and integration of realistic high-resolution ocean and coupled ocean/ice components, and an improved data assimilation scheme.

Methodology: A fully coupled near-global ocean/atmosphere prediction system has been constructed using resolutions of 0.75¡ in the atmosphere and 0.5¡ in the ocean (eddy-permitting) at the Naval Research Laboratory at Monterey (NRLMRY). The system consists of the Navy Operational Global Atmospheric System (NOGAPS) that incorporates the NRL Atmospheric Variational Data Assimilation Scheme (NAVDAS), the Los Alamos National Laboratory Parallel Ocean Program (POP), and the Navy Coupled Ocean Data Assimilation (NCODA), an optimal interpolation scheme (see Figure 1). An eddy-permitting fully global coupled ocean/ice simulation is underway using POP and the Los Alamos sea ice model known as CICE. Ensemble runs are being conducted using eddy-permitting global POP and the Simple Ocean Data Assimilation Scheme (SODA). SODA[1] also an optimal interpolation scheme, uses advanced error statistics that are flow dependent, anisotropic, and latitude-depth dependent. Finally, a short (two-year) high-resolution (0.1¡, 40-level) global POP simulation forced with daily NOGAPS fluxes is complete following a two-decade spin-up of this model using National Center for Environmental Prediction (NCEP) atmospheric fluxes.
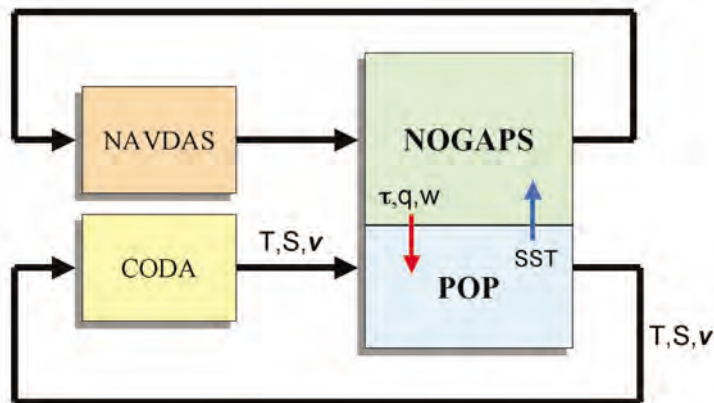

Figure 1. Naval Research Laboratory (Monterey) global coupled atmosphere/ocean prediction system.

Results: The high-resolution global ocean simulation was monitored in terms of its ability to reproduce the observed ocean state. Statistical quantities from data sets with global or near-global coverage such as those obtained from satellite altimeters were compared with model quantities. Results (Figure 2) indicate that the distribution and strength of simulated and observed sea surface height variability are in good agreement. Qualitatively, upper ocean flows are also well represented. Figure 3 shows trajectories of water parcels, released at 75 m throughout the global ocean, that move through the water column in three dimensions. High speeds are seen in western boundary currents such as the Kuroshio off of Japan and in the Gulf Stream off the eastern continental United States. Significant mesoscale eddy activity is seen globally; particularly note the effect of tropical instability waves in the off-equatorial eastern Pacific.

Shown here are the results of the coupled POP/CICE simulation initialized from uniform 2 m ice beginning in January 1979. Figures 4a and 4b show the ice thickness at the end of winter in the Arctic and Antarctica, respectively, from the coupled model with ice drift superimposed. In the Arctic, the thickest ice is found to the north of the Canadian Archipelago as is expected from observations.[2]

Significance: The high-resolution global integration is one of the highest horizontal and vertical resolution ocean simulations to be performed to date. It affords us the opportunity to study the ocean circulation, particularly mesoscale variability and processes as well as their interactions with the larger scales, in parts of the ocean that hitherto have not been simulated at such fine horizontal and vertical resolution. Similarly, the ice/ocean simulation is also one of the highest resolution coupled simulations to be performed to date on a global basis.
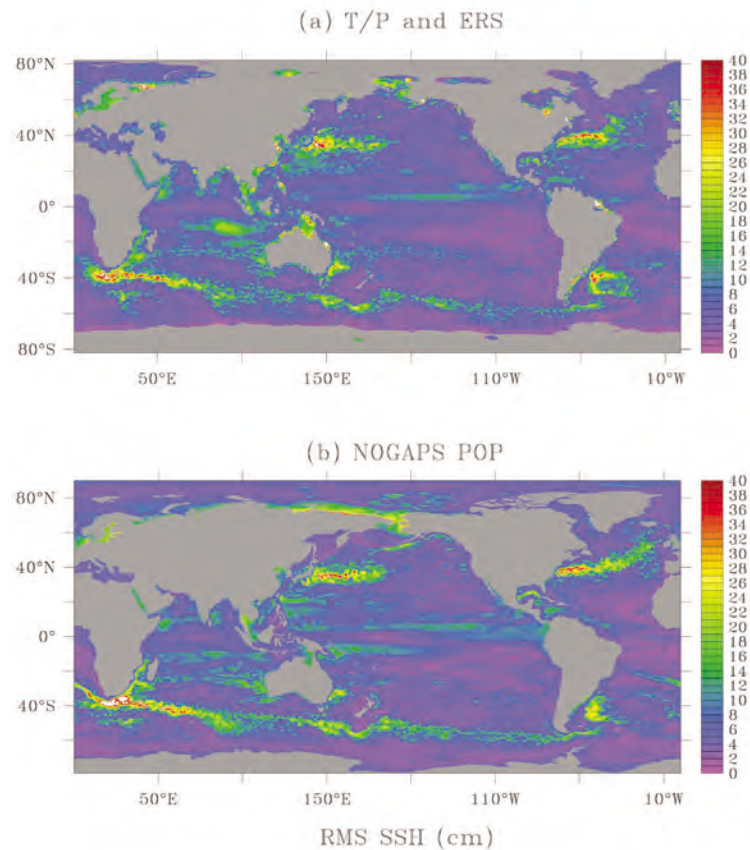

Figure 2. Root-mean-square (RMS) sea surface height (cm) from (a) altimetry and (b) POP (one-way NOGAPS surface forcing) for the year 2000.
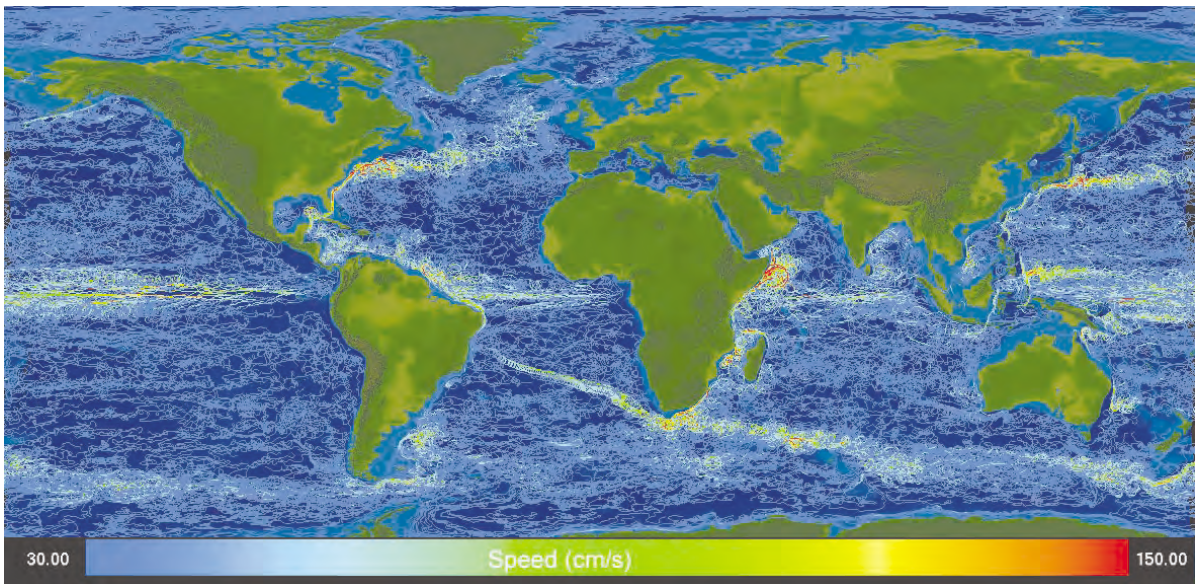

Figure 3. Trajectories of model water parcels initiated at 75 m throughout the global POP domain. Colors represent water parcel speeds (cm/s).
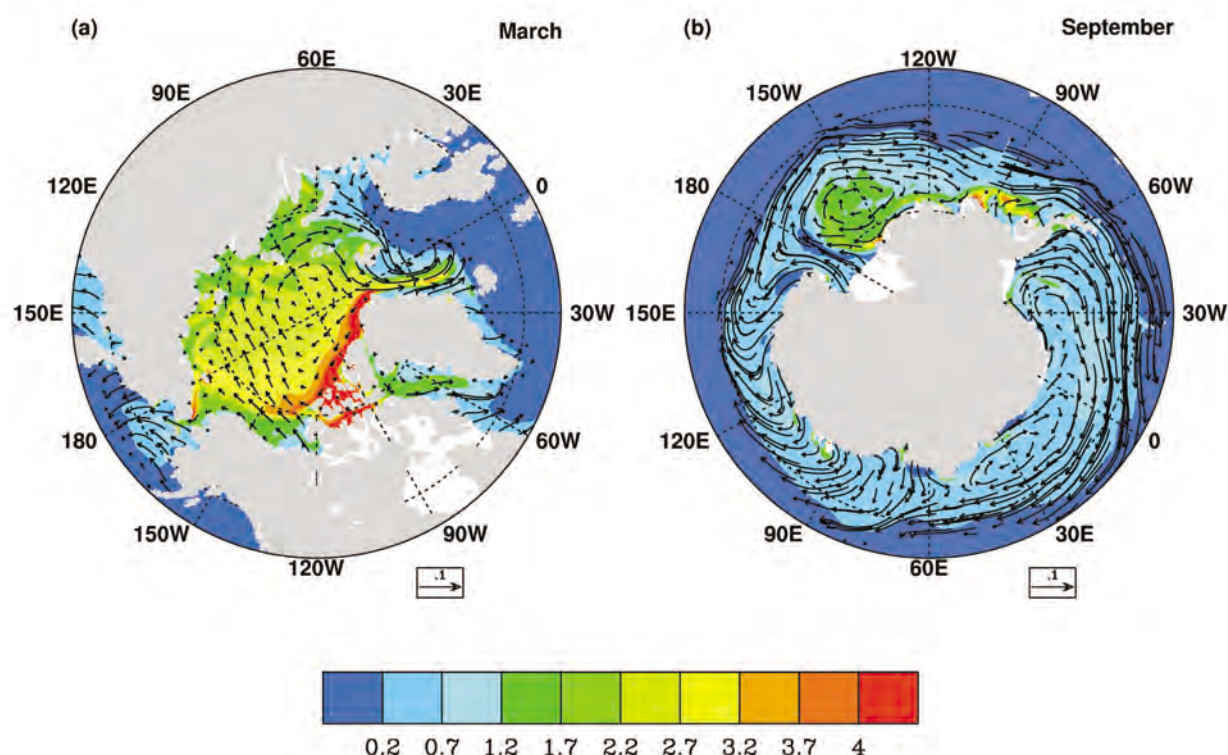
DoD

Figure 4. Monthly ice thickness (m) and ice drift (m/s) from the 0.4¡ coupled ocean/ice simulation at the end of winter in the (a) Arctic and (b) Antarctic in 1998.

References:
1) Carton, J. A., G. Chepurin, X. Cao, and B. S. Giese, 2000, A Simple Ocean Data Assimilation Analysis of the Global Upper Ocean, 1950-1995, Part 1: methodology, *Journal of Physical Oceanography*, 30, 294-309.
2) Bourke, R. H., and R. P. Garrett, 1987, Sea Ice Thickness Distribution in the Arctic Ocean, *Cold Regions Science and Technology*, 13, 259-280.

Author and Contact: Julie McClean
Authors: Detelina Ivanova, Prasad Thoppil
Organization: Department of Oceanography (OC/Mn), Naval Postgraduate School, Monterey, CA, 93943
Authors: Matthew Maltrud, Elizabeth Hunke
Organization: Los Alamos National Laboratory, Los Alamos, NM, 87545
Author: Paul May
Organization: Computer Sciences Corporation, 1900 Garden Road, Suite 210, Monterey, CA, 93940
Author: James Carton
Organization: Department of Meteorology, University of Maryland, College Park, MD, 20742
Author: Benjamin Giese
Organization: Department of Oceanography, Texas A&M University, College Station, TX, 77843-3146
Resources: IBM SP3/4 at MHPCC, IBM SP3 at NAVO, and Origin 3800 at ARL
Sponsorship: Office of Naval Research, High Performance Computing Modernization Program Grand Challenge Grant, Department of Energy, National Science Foundation

# Particle Simulation of Plume-Plume and Plume-Surface Interactions

A. D. Ketsdever, S. F. Gimelshein, D. C. Wadsworth

A FRL researchers have observed good agreement between simulation and experiment and this has provided credibility to important findings related to plume-plume and plume-surface interactions.

Background: Numerical modeling of two- and three-dimensional low Reynolds number gas flows from small nozzles has been performed using the direct simulation (DSMC) method. The objective of this effort is to gain an improved understanding of performance and plume interaction phenomena for low thrust devices, and thus improve the design and optimization process for a variety of micropropulsion systems. Simulations were performed for a wide range of flow parameters using the SMILE parallel DSMC code. Validation has been conducted through comparison of mass flow and thrust values obtained numerically with results of experimental measurements carried out recently by AFRL researchers. Good agreement observed between simulation and experiment provided credibility to important findings related to plume-plume and plume-surface interactions. In particular, a large effect of plume interaction on surface back force and net nozzle thrust has been shown for low Reynolds flows. The influence of the gas surface interaction accommodation coefficient on nozzle performance was also investigated. An example of the plume flow from a 4 cm diameter nozzle interacting with a plate is shown in Figures 1 and 2 where the pressure field and surface pressure distribution are shown for a throat Reynolds number of 60 and nitrogen propellant.

Figure 1. Interaction of nozzle plume with offset horizontal plate (flowfield pressure contours on plume symmetry plane).
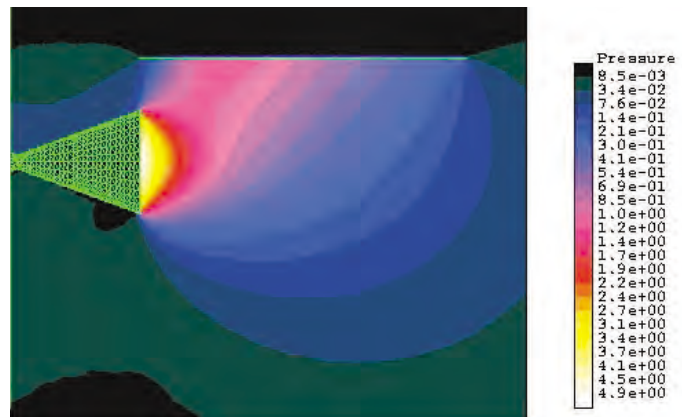
Publications:

1) A. Ketsdever, N. Selden, S. Gimelshein, A. Alexeenko, P. Vashchenkov and M. Ivanov, Plume Interactions of Multiple Jets Expanding into Vacuum: Experimental and Numerical Investigation, AIAA Paper, 2004, 1248.

2) A. Ketsdever, M. Clabough, S. Gimelshein, and A. Alexeenko, Experimental and Numerical Determination of Micropropulsion Device Efficiencies at Low Reynolds Numbers, Submitted to AIAA Journal.

Figure 2. Enhancement of plume backflow due to presence of plate (oblique view of surface pressure contours on nozzle, horizontal plate and nozzle backplate).
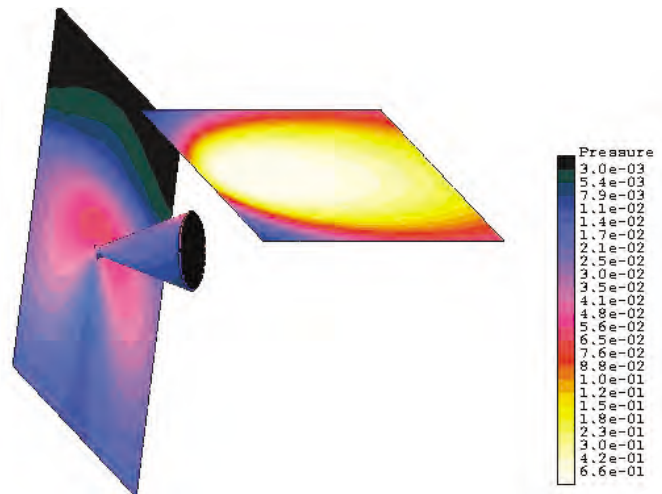
Author and Contact: A. D. Ketsdever
Organization: Senior Research Engineer, AFRL/PRSA, 10 E. Saturn Blvd, Edwards AFB, CA, 93524-7680A
Author: S. F. Gimelshein
Organization: Research Assistant Professor, Department of Aerospace and Mechanical Engineering, 201 Rapp Research Building, University of Southern California, Los Angeles, CA, 90089
Contact: D. C. Wadsworth
Organization: Scientist, ERC, Incorporated, 10 E. Saturn Blvd., Edwards AFB, CA, 93524

The Next Generation of Image Recovery Algorithm for the GEMINI Sensor

Kathy Schulze, Stuart M. Jefferies, Charles L. Matson

Efforts are underway to implement a new algorithm to replace bispectrum as the post processing algorithm for the GEMINI sensor while continuing to meet the operational requirements. The GEMINI sensor is part of the Air Force Research Laboratory s (AFRL) Air Force Maui Optical & Supercomputing Site (AMOS), located atop Mt. Haleakala, Maui, HI.

Background: Data reduction of short exposure imagery collected using the Air Force Research Laboratories (AFRL) Maui Space Surveillance System (MSSS) GEMINI sensor (Figure 1) is currently completed using a linear algorithm known as bispectrum. The bispectrum algorithm was selected for GEMINI data reduction in the mid-1990's and was implemented in parallel running on both the observatory and MHPCC computer systems. The bispectrum algorithm is capable of reducing ensembles of data very quickly, within a second or less, providing very fast turn-around time from data collection to recovery. Bispectrum recoveries can be used during data collection in a near-real-time (NRT) fashion to improve the raw data collection process as well as produce final data products for delivery to the Space Command customers. However, the bispectrum algorithm has several drawbacks that adversely affect the image recovery process. First, bispectrum requires an additional reference star measurement that can be difficult to collect correctly and second, the bispectrum algorithm performs poorly when the object being imaged isn't completely contained within the exposed frame. Efforts are underway to implement a new algorithm to replace bispectrum as the data reduction algorithm for the GEMINI sensor while continuing to meet the operational requirements.

Methodology: The future of image recovery algorithms for the GEMINI sensor lies in the implementation of a non-linear algorithm known as physically constrained iterative deconvolution or PCID.[1] Using PCID eliminates the requirement for the reference star measurements necessary for bispectrum and can also accommodate large objects with respect to the image frame. The drawback to non-linear algorithms, such as PCID, is that they are slow in producing results compared to linear algorithms and can be cumbersome to implement and execute due to their large memory and CPU needs. Implementing PCID to meet the operational goals of the MSSS GEMINI sensor requires an understanding of not only the data reduction requirements and algorithm, but also the host system architecture.

The GEMINI data reduction requirements fall into three categories: low, mid, and high resolution imagery. Low resolution imagery can be used effectively in the NRT feedback loop to improve the data collection process. Mid resolution imagery provides the Space Command customer intelligence information quickly after data collection. High resolution imagery is needed in cases where fine detail is required.

The PCID algorithm uses an ensemble (group) of short exposure images and solves for both the object and the point spread function (PSF) blurring each raw image at the same time. The algorithm solves for successively closer approximations of the object and PSFs by minimizing the error between the true measurement and a model of the measurement. The estimates of the object and PSF are refined with each iteration of the algorithm giving a closer approximation of the true measurement which in turn minimizes the error between the two quantities being compared. Completing more iterations of the algorithm improves the resolution of the image until the algorithm converges. Final convergence can require hundreds or even thousands of iterations. Processing options that increase memory and CPU requirements also improve the resolution of the recovery further complicating the implementation and slowing the execution of the PCID algorithm.
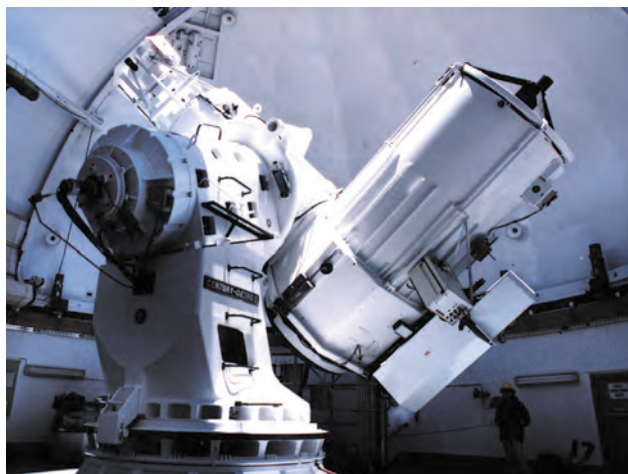

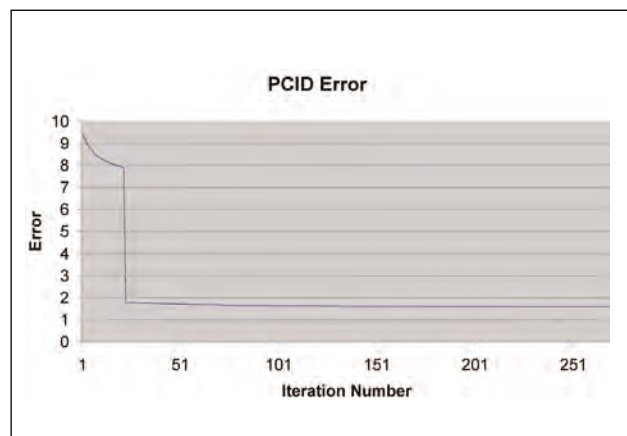**Figure 1.** GEMINI Sensor at the AFRL MSSS Site.

Figure 2. Residual error between the true measurement and the model of the measurement.

We expect to accommodate the low resolution imagery requirement to feed the NRT feedback to the data collection operators by minimizing the number of iterations of the algorithm and reducing or eliminating the use of processing parameters that increase the CPU and memory requirements. As shown in Figure 2, the residual error between the true measurement and the model of the measurement drops significantly within less than 100 iterations. The error continues to drop steadily but at a slower rate as the iterations progress. The sharp drop off in the error around iteration 25 is caused by the algorithm adjusting the minimization process based upon the selected processing parameters.

Figure 3 shows a representative raw frame before processing, followed by several recoveries. The recoveries were obtained by stopping the algorithm at the iteration number shown in Table 1.
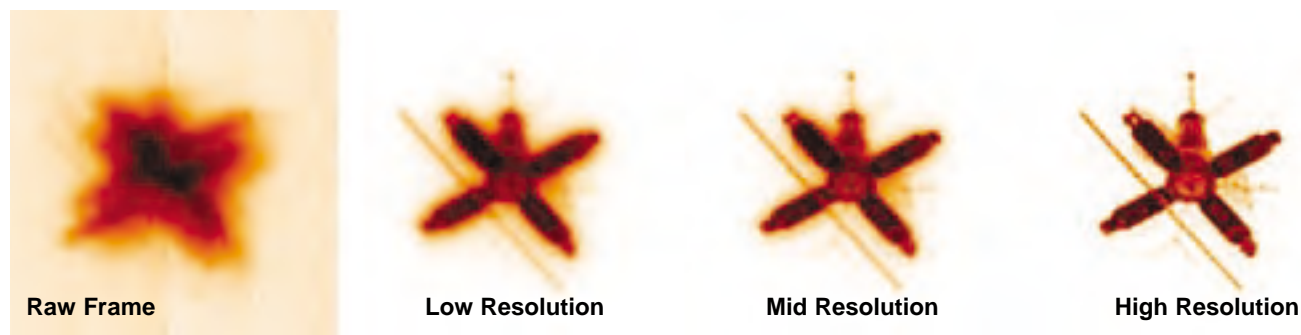

Raw Frame   **Low Resolution**   **Mid Resolution**   **High Resolution**

Figure 3. Representative new frame with recoveries.

Table 1 lists the number of iterations and processing time required for the above resolution types.

Resolution	Iterations	Processing Time
raw	0	0
low	20	0:30
mid	50	1:24
high	300	7:46

Table 1. Resolution type by iteration and time.

The MHPCC *Tempest* P3 or P4 nodes accommodate the PCID algorithm using the multiple program multiple data paradigm. While 30 seconds per recovery is still too slow to be usable for the GEMINI NRT aspect, research efforts are underway to reduce this time by a factor of 10.

Significance: Using the MHPCC highly parallel systems running PCID to support GEMINI sensor operations and data reduction at MSSS makes effective use of Maui Air Force Research Laboratory s assets to support the Space Command customer. Using PCID low resolution NRT will improve the quality of the collected data. Mid resolution imagery can be delivered within the required time limits and high resolution imagery will be available when required by allowing the algorithm to continue to process the data using additional processing parameters.

Before the advent of parallel computers with large capacity shared memory and fast inter-processor communications, image processing using non-linear algorithms was not practical for operational data reduction at MSSS.

 References:
1) K. J. Schulze, S. M. Jefferies, and C. L. Matson, "A Highly Parallel Physically Constrained Iterative Blind Deconvolution Algorithm: PCID," 2003, MHPCC Application Briefs, page 44.

Author and Contact: Kathy Schulze
Organization: KJS Consulting, 46 N Laelua, Paia, HI, 96779
Author: Stuart M. Jefferies
Organization: Maui Scientific Research Center, 590 Lipoa, Kihei, HI, 96753
Author: Charles L. Matson
Organization: Air Force Research Laboratory, Directed Energy Directorate, Kirtland AFB, NM, 87117
Resources: IBM SP3 and SP4 *Tempest* at MHPCC
Sponsorship: Air Force Research Laboratory

Intelligence Fusion

Greg Seaton, Brian Banks, Chad Churchwell

The Maui High Performance Computing Center (MHPCC) designed and is developing an intelligence fusion system for the Office of Naval Intelligence (ONI) to solve the problem of accessing and utilizing multiple intelligence sources accessible through different systems and interfaces (i.e., "stovepipes"). The intelligence fusion system combines, or fuses, intelligence from multiple, disparate sources into a single, coherent interface. The intelligence fusion process implements a universal ontological framework across the distinct sources, leveraging object-oriented technologies to provide fused intelligence to human analysts and artificial intelligence (AI) agents with the goal of generating high-value, actionable intelligence for the intelligence consumer. In addition to decision support, the intelligence fusion architecture allows subject matter experts (SME) to capture their valuable subject matter expertise to be leveraged by other analysts and AI agents.

Intelligence Fusion vs. Data Warehousing: Intelligence fusion is quite different from data warehousing. The data warehouse approach forces all data accessible to the end-user to be first processed through an extraction-transform-load (ETL) procedure and stored in a centralized and monolithic database. Intelligence fusion only accesses and retrieves the intelligence necessary to satisfy a request and does not require archiving or storing the resulting fused intelligence. The different data query and intelligence request approaches are illustrated in Figure 1a and Figure 1b.
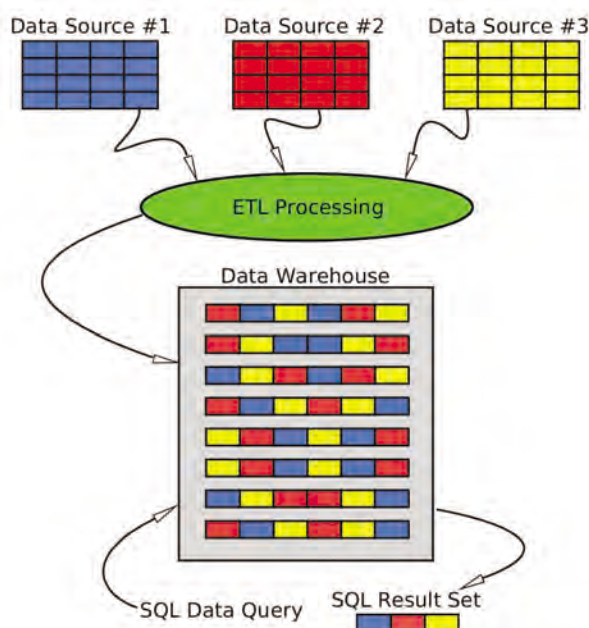
In a data warehousing effort, all of the data from the data sources must be extracted from the data sources, transformed into structures compliant with the data warehouse structures and loaded into the data warehouse. The resulting data warehouse requires storage space that will grow linearly throughout the life cycle of the warehousing project, requiring increasingly more administration and storage resources along with the complicated issue of data ownership and control.

In the MHPCC intelligence fusion system, based upon an ontological approach, all administration for the addition of a new intelligence source may be done by the fusion administrator in a GUI fusion management tool requiring no programmatic changes to the system and no client support resources.

Figure 1a. Data Queries in Data Warehouse Systems.

Object-Ontological Hybrid Approach to Intelligence Fusion: One of the issues with strict ontological-based systems is that many have not been user-friendly and have provided only command-line user interfaces. Any user of the system needed to have an in-depth understanding of the structure of the system ontologies as well as proficiency in the command-driven interface.

The MHPCC object-ontological hybrid approach to intelligence fusion couples the flexibility and power of an ontological approach with the usability and scalability of an object-oriented implementation.

Figure 1b. Intelligence Requests in Intelligence Fusion Systems.

This hybrid approach models the intelligence entities and sources into an ontology, maps the heterogeneous intelligence sources into a universal ontology, and implements an object layer for a GUI application to abstract and hide the implementation specifics of the underlying data topography from the analyst.

Core Intelligence Fusion System Components: The intelligence fusion system consists of five (5) primary components (Figure 2) in a services-oriented architecture (SOA).

Analyst Workspace
The analyst workspace GUI client application provides the analyst with a customizable workspace in which to commit intelligence entity and element requests, view request results, navigate relationships between intelligence entities and elements, and collaborate with other analysts.

Fusion Ontology Workspace
The fusion ontology workspace GUI client application allows the fusion analysts and administrators to map entity instances across disparate intelligence sources, define and extend element ontologies, and establish and administer security across the intelligence fusion system.

Subject Matter Expert Workspace
The subject matter expert (SME) workspace GUI client application allows the SME to capture expertise as formal rules. These rules may then be used by AI agents as well as by other analysts.

Ontology Service
The ontology service manages all ontological operations, including creation, modification, usage of the system ontologies, expert rules, and ontological mappings.

Intelligence Access Service
The intelligence access service manages all connections, access control, and intelligence retrieval for the intelligence sources in the intelligence fusion system.
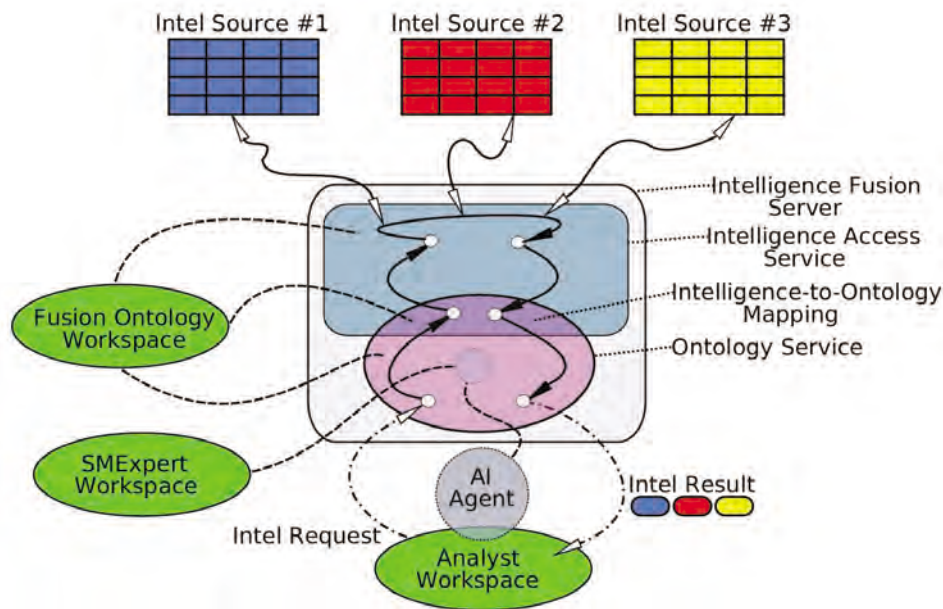

Figure 2. Core Intelligence Fusion System Components.

AI Agents: The MHPCC intelligence fusion system is architected to leverage multi-tiered AI agents across the collected intelligence sources to provide true 24/7 utilization of system resources. Expert AI agents, utilizing formalized subject matter expertise captured from SME analysts, may spider the ontological topography to identify and flag entities of interest for further automated analysis and/or consideration by human analysts.

The human analyst continues to be the most important asset in identifying and analyzing high interest entities. The intelligence fusion system is designed to provide these end-users with the functionality necessary to spend more time analyzing these higher-interest entities and less time sifting through mountains of data.

Intelligence Fusion and High Performance Computing: The MHPCC intelligence fusion architecture allows high performance computing (HPC), and more specifically, grid computing (GC), concepts to be leveraged for optimization of the intelligence fusion servers and AI agent utilization.

The intelligence fusion servers may be clustered in a load-balancing, high-availability, and extensible manner to provide the necessary computational and I/O performance to facilitate the use of the system by a theoretically unlimited user base (analysts and AI agents).

Summary: By leveraging an object-ontological hybrid approach, the intelligence fusion system provides the benefits of presenting the underlying intelligence topography as cogent and coherent objects to the end-user and leverages the power and flexibility of an ontological, knowledge-oriented framework.

In addition, the MHPCC intelligence fusion architecture allows for the implementation of HPC/GC approaches to provide a high-availability and extensible environment, optimizing computational resource usage and maximizing the amount of analytical processing on the target intelligence domain.

The goal of the MHPCC intelligence fusion system is to allow analysts to spend more of their valuable time analyzing high-interest entities and less time fighting the interface, ultimately resulting in more high-value, actionable intelligence for the intelligence consumer (Figure 3).
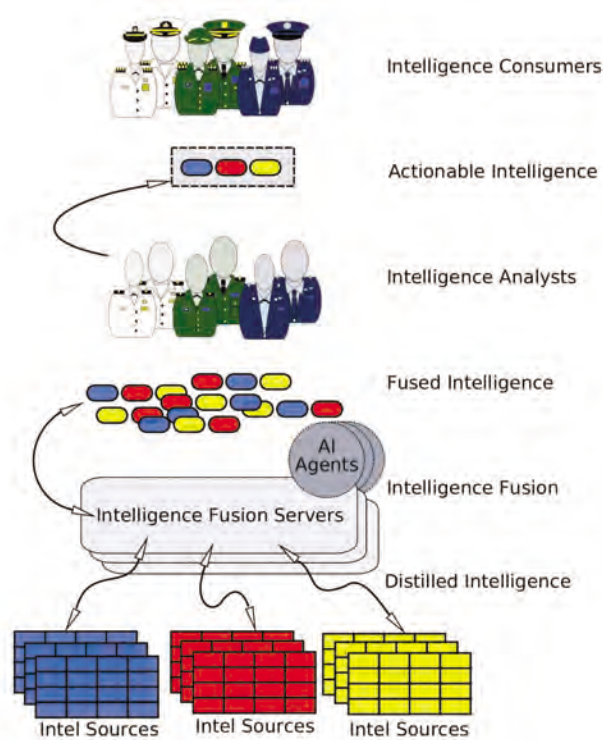

Figure 3. Intelligence Fusion and the Intelligence Consumer.

Author and Contact: Greg Seaton
Authors: Brian Banks, Chad Churchwell
Organization: Maui High Performance Computing Center, 550 Lipoa Parkway, Kihei, HI, 96753
Resources: IBM Power4 Systems and *Huinalu* Linux Cluster at MHPCC
Sponsorship: Office of Naval Intelligence (ONI)

Computational Proteomics at MHPCC: A Classical Molecular Dynamics Study of the Distal Residue in HemAT-*Hs*

James S. Newhouse, Tracey Allen K. Freitas, Maqsudul Alam

The heme-containing globular protein from the aerotaxis region of Halobacterium Salinarum[1] was studied in this work (which was part of the Computational Proteomics division of the Bioinformatics project at MHPCC). A 3D homology model of HemAT-*Hs*, as the protein is designated, based on the x-ray crystallographic structure of Sperm Whale Myoglobin (pdb: 1mbo) was created. The behavior of distal residues interacting with ligand O_2 , the protein working structure based upon the mentioned homology model, was characterized via force field Molecular Dynamics using VMD/NAMD.[2] The structure assumed a more realistic conformation during the molecular dynamics, allowing interpretation of the heme pocket environment that could be compared to experiment. The resulting picture of the heme pocket, combined with simulated site mutagenesis of the candidate distals helped to confirm, at least theoretically, a new distal candidate, Tyrosine 99, replacing the expected distal candidate, Glutamine 96 (see Figures 1 and 2).

Research Objectives: The objective of this research was to characterize by theoretical means (force field molecular dynamics in package VMD/NAMD) the behavior of distal residues in HemAT-*Hs*.

Significance and Vision: Characterization of this protein, from the signaling domain of aerotaxis, by theoretical methods, in aid of experiment, has proven the accuracy and efficacy of such methods. Computational Proteomics will be a major effort in the Bioinformatics project in collaboration with the University of Hawaii at MHPCC.
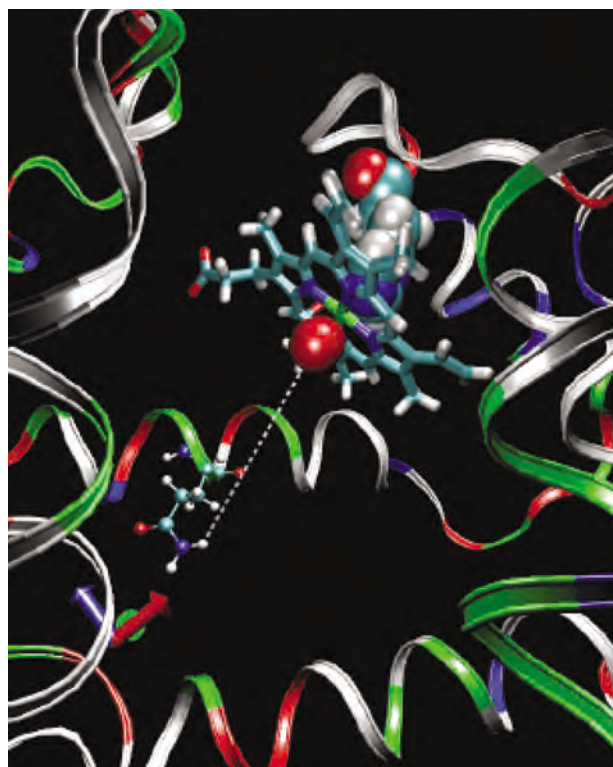

Figure 1. This figure depicts one candidate for the distal residue, Glutamine 96 (Q96 in the E Helix) which is about 11 Angstroms distant from O_2 at the end of 600 ps of MD, having drifted away from a distance of about 4.5 angstroms at the beginning. It is obviously not behaving as a distal residue. Simulation conditions: Water Solvated, 310.15¡ K (98.6¡ F).
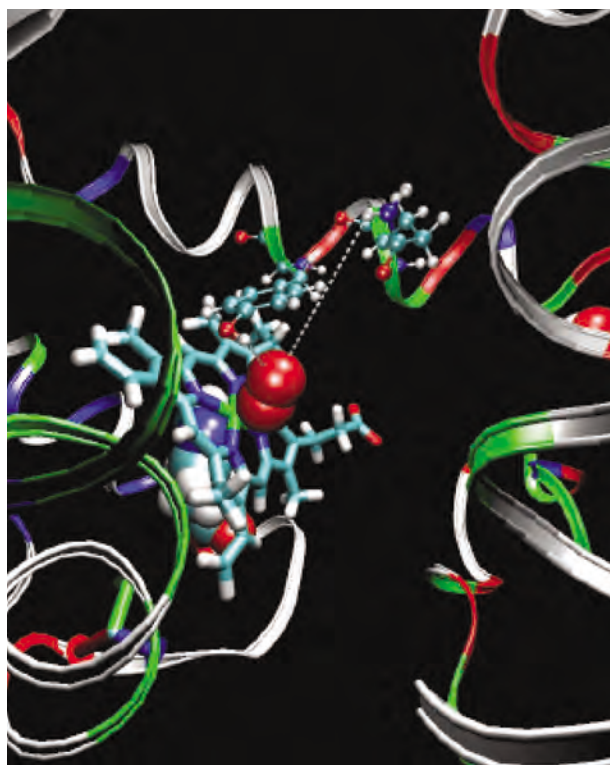

Figure 2. Comparison of Glutamine 96 and Tyrosine 99 as Distal Residues. At 50 ps Tyrosine 99 is about 3.1 angstroms from O_2 and Glutamine 96 is about 7.6 angstroms distant. Halobacterium *salinarum,* Sperm Whale Myoglobin Homology Model, Water Solvated, 310.15¡ K.

Methodology: Force field molecular dynamics employing the CHARMM force field was applied using VMD/NAMD.[2] In the simulation, protein, heme, and ligand were immersed in a cube of 5800 TIP3 water. 0.6 nanosecond of molecular dynamics were run at temperatures 310.15¡ K and 333.15¡ K on 128 processors of supercomputer *Tempest* at MHPCC. NAMD scales extremely well on many platforms, and the computer *Tempest* performed quite well. Some benchmarks for IBM Power3 NAMD runs are given.
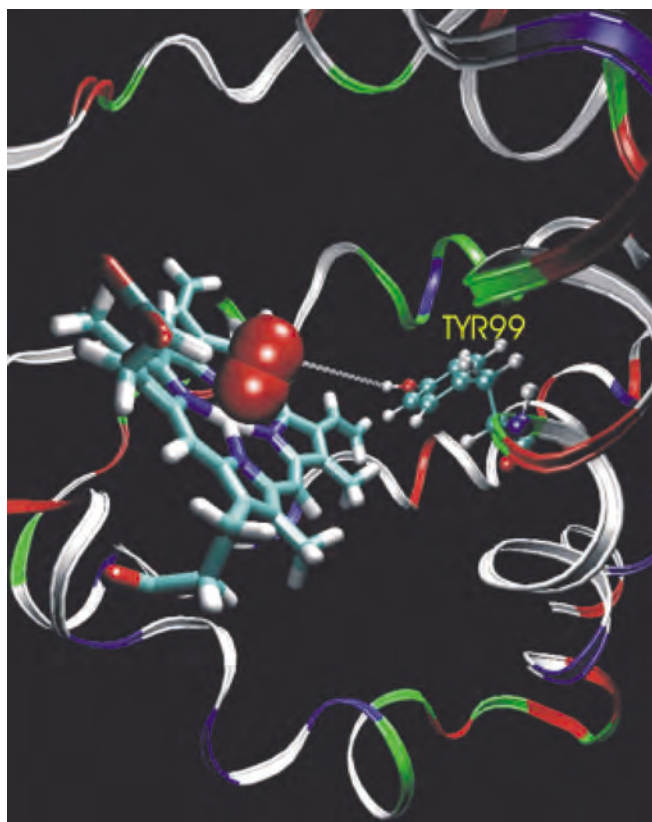
Figure 3. Site MutagenesisY99 --> A99 3M KCl, 1M NaCl, 310.15¡ K. Approach of Y99 to O_2 at 30 ps (6.511 Angstroms).

Benchmarks for Normal Molecular Dynamics Simulations:

Water solvated, 310.15¡ K 2000/600000 128 procs 12.9 Mb mem,	8.1 hours
Water solvated, 333.15¡ K 2000/600000 128 procs 12.6 Mb mem,	7.5 hours
5M KCl solution, 310.15¡ K 2000/600000 128 procs 14.6 Mb mem,	11.4 hours
5M KCl solution, 333.15¡ K 2000/600000 128 procs 14.3 Mb mem,	12.5 hours
1M NaCl, 4M KCl solution, 310.15¡ K 2000/600000 128 procs 14.7 Mb mem,	11.5 hours
1M NaCl, 4M KCl solution, 333.15¡ K 2000/600000 128 procs 14.7 Mb mem,	12.6 hours
1M MgCl2, 1M NaCl, 3M KCl solution, 310.15¡ K 2000/600000 128 procs 15.3 Mb mem,	11.4 hours

The Q96 (Glutamine) and Y99 (Tyrosine) positions were mutated, and 600 picosecond molecular dynamics simulations were run at 310.15¡ K in 3 M KCl and 1 M NaCl solution (see Figure 3), which simulated the environment growth conditions, on three different proteins.
Summarizing the closest approach of possible distal residue locations under Site Mutagenesis:

Site Mutagenesis Q96 --> A96
  A96 6.724 Angstroms at 0 ps then moves away
  Y99 6.511 Angstroms at 30 ps
  F68 4.51 Angstroms at 51 ps

Site Mutagenesis Y99 --> A99
  A99 3.270 Angstroms at 526 ps
  Q96 7.304 Angstroms at 0 ps then moves away
  F68 4.007 Angstroms at 43 ps

Site Mutagenesis Q96 --> I96
  I96 9.036 Angstroms at 252 ps
  Y99 6.241 Angstroms at 185 ps
  F68 2.986 Angstroms at 543 ps

Some Benchmarks for Site Mutagenesis Simulations:

a96, Water Solvated, 310.15¡ K 2000/600000 64 procs 14.6 Mb mem,		21.2 hours
a99, Water Solvated, 310.15¡ K 2000/600000 128 procs 13.8 Mb mem,		12.0 hours
a96, Water Solvated, 310.15¡ K 2000/600000 128 procs 15.4 Mb mem,		11.6 hours

Results: Molecular dynamics provided evidence of something unexpected. Instead of the putative distal residue, Glutamine 96, a different distal residue was identified. The distal candidate is Tyrosine 99 which shepherded the ligand O_2 in the simulations. Subsequent laboratory tests (site mutagenesis) confirmed this unexpected result. A theoretical simulation, obtained on a supercomputer, led the experiment in the right direction.

References:

1) Hou S., Freitas T., Larsen R. W., Piatibratov M., Sivozhelezov V., Yamamoto A., Meleshkevitch E. A., Zimmer M., Ordal G. W., Alam M., Globin-Coupled Sensors: A Class of Heme-Containing Sensors in Archaea and Bacteria, Proc. Natl. Acad. Sci. USA (2001), 98, 9353-9358.

2) NAMD package http://www.ks.uiuc.edu/Research/namd from the Theoretical and Computational Biophysics Group at the University of Illinois, Laxmikant Kal , Robert Skeel, Milind Bhandarkar, Robert Brunner, Attila Gursoy, Neal Krawetz, James Phillips, Aritomo Shinozaki, Krishnan Varadarajan, and Klaus Schulten. NAMD2: Greater Scalability for Parallel Molecular Dynamics, *Journal of Computational Physics*, 151:283-312, 1999, "NAMD was developed by the Theoretical and Computational Biophysics Group in the Beckman Institute for Advanced Science and Technology at the University of Illinois at Urbana-Champaign."

Author and Contact: James S. Newhouse
Organization: Maui High Performance Computing Center, 550 Lipoa Parkway, Kihei, HI, 96753
Authors: Tracey Allen K. Freitas and Maqsudul Alam
Organization: University of Hawaii at Manoa, 2538 The Mall, Snyder 111, Honolulu, HI, 96822
Resources: IBM Power3 *"Tempest"*, SGI Onyx 3400 *"Mano"*, and SGI Octane dual R12000 *"Lyra" at* MHPCC

Environment for Design of Advanced Marine Vehicles and Operations Research (ENDEAVOR) Project

Robert Dant, D. J. Fabozzi, J. Bergquist, Jonathan Dann, Carl Holmberg,
Bryan Hieda, Scott Splean, Jane Salacup

As the Nation transforms its military force structure for the 21st Century, there is a pressing need to re-evaluate the nature of naval ships and their design. New advanced hull types can both decrease drag and detectable signature, while increasing both speed and stability − providing obvious operational and budgetary pay-offs. The benefits of advanced hull designs also have a commercial spin-off in high-speed transport and ferries (see Figure 1). The ENDEAVOR project aims to provide an integrated capability to rapidly create an Advanced Marine Vehicle (AMV) design at the concept level, to assess AMV performance, and to determine operational characteristics. The Air Force Research Laboratory's Maui High Performance Computing Center (AFRL/MHPCC) is working to design, test, and integrate naval architecture tools and simulation software with oceanographic and marine vessel databases on a high performance computing system. Eventually, this system will be available over the Internet for use by customers from their desktop computers.

Research Objectives: The objective of this research effort is to integrate a number of existing software tools into a single, high-performance design environment. By utilizing a supercomputer server environment, the ENDEAVOR system will shorten the cycle time of an iterative design and test process, enabling designers to quickly optimize complex designs. This capability will give users more freedom to consider a wider range of concepts against the time given to a product's design phase.

Methodology: The technologies involved included the following: 1) PC-based client software with which a user manipulates the parameters for their designs and test conditions via a convenient GUI, 2) a web services infrastructure through which the client software submits designs to be processed and stored, 3) material and environmental databases in which to record and recall user vehicle designs and tests, and 4) physics-based codes hosted on a high performance parallel computing system to support complex design evaluations and testing.

Figure 1. Sea Flyer (HYSWAC - Hybrid Small Waterplane Area Craft) in a "flying" mode, with artist's underwater view of lifting body.

Results: AFRL/MHPCC fielded a suite of software servers across both Linux and PC hardware servers. The Linux server provides standard and encrypted web content, Java servlet applications, Simple Object Access Protocol (SOAP) web services, and database management system services. The PC server provides a mirror functionality, supporting Microsoft-based technologies such as Office and Windows-based algorithms.

These servers support a variety of client-server capabilities (see Figure 2), which have been organized into the following sub-projects:

1) Ocean Environment: provides a Geographic Information System (GIS), an Ocean Wave Model, and environmental statistics (see Figure 3).
2) AMV Product DB: provides an interactive database of AMVs manufactured and deployed throughout the world, and displayed through a GIS environment. This also contains a field-based searchable interface.
3) Mission Model: allows for AMV mission requirements, design verification, and mission planning support.
4) AMV Designer: allows users to create and store AMV designs.

5) Integration Desktop: allows users to integrate third party code into the ENDEAVOR visual programming environment.
6) Service Manager: allows users to deploy integrated applications and process models to AFRL/MHPCC for remote execution via SOAP-based web services
7) Performance Analysis: allows users to analyze AMV performance for certain environmental conditions and mission requirements.
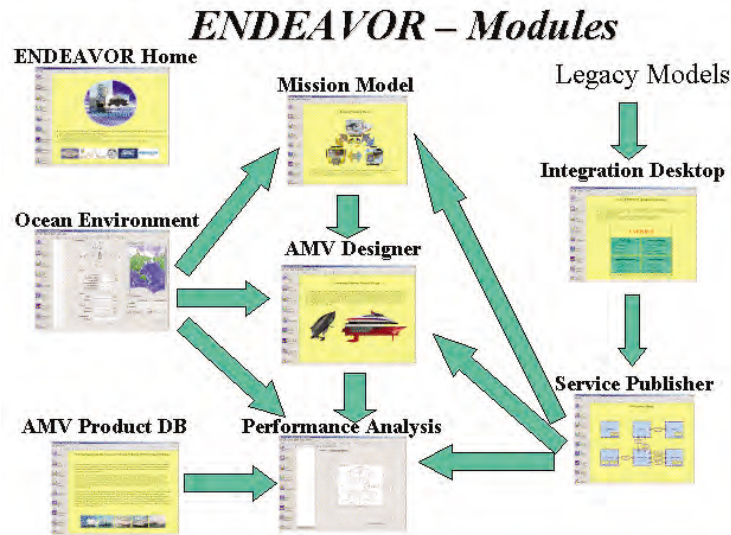

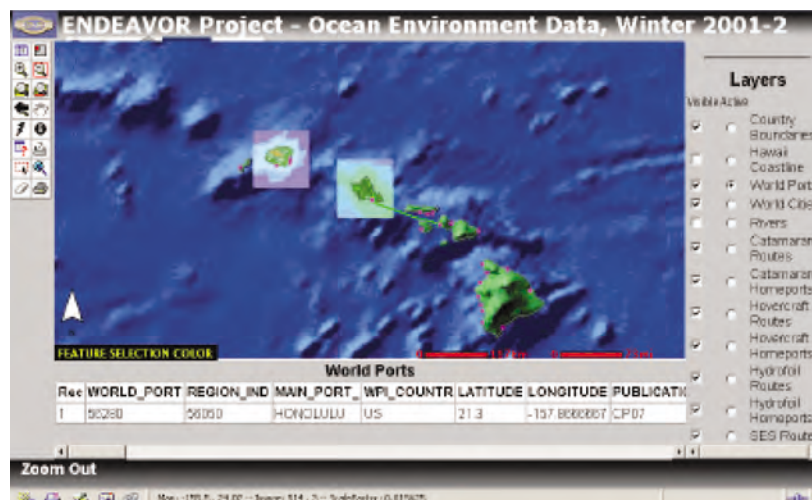**Figure 2.** Project ENDEAVOR Software Modules.

Figure 3. Project ENDEAVOR Geographic Information System (GIS).

Significance: The U.S. Navy is currently investigating a host of novel concepts, with promises of more to come. The benefits of advanced hull designs also have a commercial spin-off in high-speed transport and ferries. For regional transportation, people and cargo in offshore islands can have quick and easy access to other islands, which is of particular interest for the challenging sea conditions between the Hawaiian Islands. The impact to the global and local economy can potentially be significant. As the ENDEAVOR system matures, designers can realistically explore new possibilities hidden in unproven concepts.

Author and Contact: Robert Dant
Authors: D. J. Fabozzi, J. Bergquist, Jonathan Dann, Carl Holmberg, Bryan Hieda, Scott Splean, Jane Salacup
Organization: Maui High Performance Computing Center, 550 Lipoa Parkway, Kihei, HI, 96753
Resources: DELL PowerEdge 2650 (2 Processors)
Sponsorship: Office of Naval Research (ONR)

Cargo Tracking Data Warehouse System Performance Enhancements

Chad Churchwell, Aaron Steigerwald, Marc Lefebvre, Brian Banks, Todd Lawson

The MHPCC team was tasked to enhance the performance of the data warehouse that the Office of Naval Intelligence (ONI) uses to monitor international cargo traffic. By utilizing numerous advanced database architectural features and by leveraging the high performance computing assets at MHPCC, data loading, data retrieval, and data analysis processes were streamlined providing a faster performing, more scalable, and easier to maintain data warehouse solution. MHPCC's *Tempest* (IBM SP3/SP4) and *Huinalu* (IBM Linux Supercluster) computing resources were utilized for implementation and testing.

Research Objectives: The Office of Naval Intelligence (ONI) uses a data warehouse to store and analyze cargo contents and movements in the Nation's premier cargo tracking system. The MHPCC undertook the task of enhancing the original implementation with the primary objectives of improving data load and retrieval times. Using advanced technologies and techniques, MHPCC Application Engineers have developed an architecture that not only facilitates rapid data loading and retrieval, but is scalable and maintainable as well. The effort utilized MHPCC's *Tempest* and *Huinalu* computing resources for implementation and testing. The *Tempest* resource consisted of one IBM Power4 node containing 32 processors and 32 GB of RAM, and the *Huinalu* resources consisted of 32 nodes each containing two Intel 933 processors and 1 GB of RAM.

Methodology: The ONI data warehouse effort focused on three key areas. The first involved a redesign of the data warehouse's schema and architecture, which is the foundation of the system and significantly affects performance and maintainability. The second addressed the need for an appropriate Extraction, Transformation, and Loading (ETL) tool that executes and maintains mappings between the traditional On-Line Transaction Processing (OLTP) database source and data warehouse. The third effort focused on the loading process, which introduced an intermediate step in the form of a staging environment in order to minimize system downtime while new data are loaded into the data warehouse.

Figure 1. Cargo Ships.

The use of MHPCC's computing resources was grouped into functional areas. The flexible *Huinalu* nodes were grouped according to need, and were used for ETL tool activities and others for database access and development. The *Tempest* node was used primarily to house the numerous databases used for development and testing.

Results: The design of a data warehouse's schema and underlying storage configuration impacts every aspect of an On-Line Analytical Processing (OLAP) system, which is a generic term for ONI's cargo tracking system, and is crucial to its success. Details such as the type of schema and configuration of the underlying storage objects must be tailored to the operational nuances of the system. The following list highlights the different technologies and architectural methods employed in implementing ONI's data warehousing solution:

Star Schema:
This type of schema facilitates rapid data retrieval within the data warehouse. A detailed knowledge of how the data interacts and the types of queries made against it are required for its design.

Data Partitioning and Sub Partitioning:
The storage of data can be partitioned, i.e., logically and physically organized by a data field such as a date. In this instance, queries containing date components can significantly reduce the amount of data searched. Improved data loading and maintenance simplification is also achieved using partitioning. MHPCC engineers used a mathematically formulated date field to organize ONI's partitions.

Data Aggregation:
Data sets that are commonly accessed and queried can be aggregated into objects that expedite data retrieval. ONI's data warehouse architecture takes advantage of these structures, improving query response time.

Database Management System (DBMS) Optimizer Customization:
A DBMS optimizer controls how every query made against the data warehouse will be executed. ONI's data warehouse uses an optimizer that was tailored to its operational characteristics and in turn improves performance.

Automated Query Regeneration:
The data warehouse was configured to take advantage of a technology whereby the DBMS determines whether or not to automatically rewrite the user's query in order to provide quicker results. The DBMS is able to do this based on statistics and information it gathers about the sets of data the user queries.

Bitmap Indexing:
Indexing data fields improves query performance. Bitmap indexes, as opposed to b-tree indexes, are applicable when the data sets they are applied to are of a finite nature. Their use improves query performance while reducing management overhead and have been used extensively throughout ONI's data warehouse.
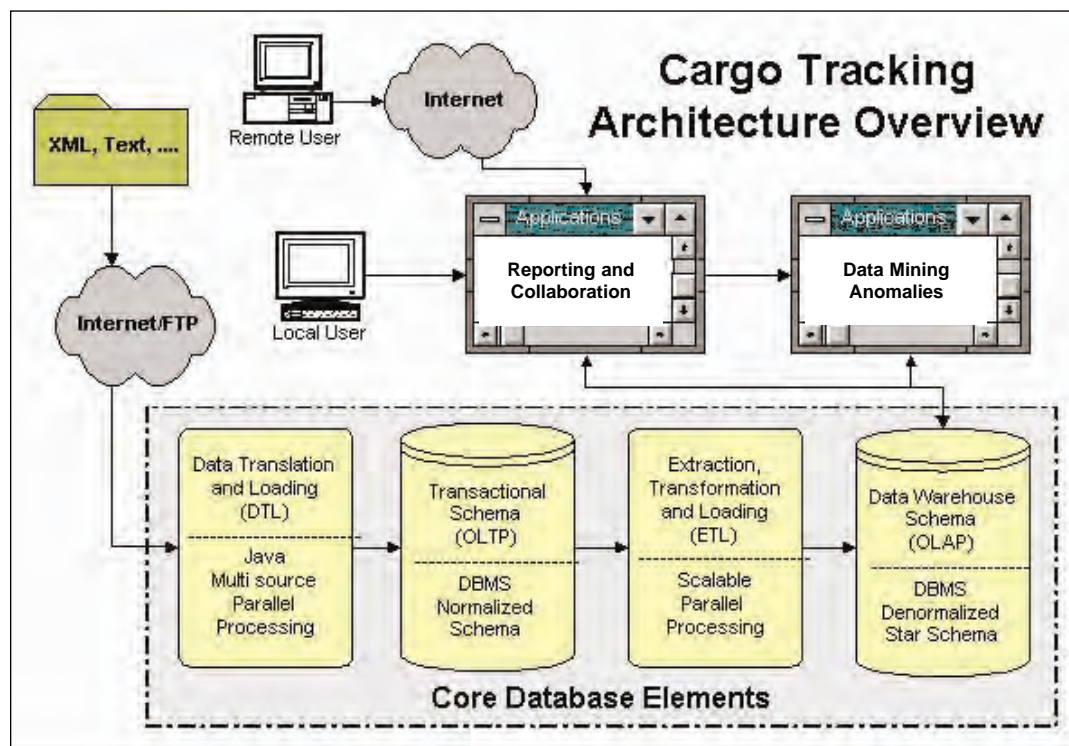

Figure 2. Architecture Overview for Cargo Tracking.

There are several important aspects to selecting and implementing a successful ETL tool. Every data warehouse requires some form of ETL tool, which pulls data out of a source database, processes and manipulates it, and inserts it into a data warehouse. The data warehouse is an aggregation of the source database and has a completely different schema that is optimized for rapid data retrieval, hence the need for data processing and manipulation. The ETL tool selected for ONI's system streamlines the mappings between source and destination (data warehouse) data relationships. It also facilitates the aggregation of selected source data fields, such as multiple cargo descriptions, into one. Other technical details, such as the reuse of data record keys, proved extremely helpful during testing and validation. One critical phase of ETL tool integration is the data-mapping phase. MHPCC staff utilized internal and external subject matter expertise to efficiently and effectively map and aggregate source data fields to their data warehouse counterparts.

MHPCC engineers utilized a combination of technologies and techniques to develop an innovative solution that provides scalability and minimizes system downtime during data loading. The initial challenge was to reduce data loading times, and consequently system downtimes, that were directly proportionate to the amount of data being loaded as well as the number of records stored in the data warehouse. The first major component of the solution involved incorporating a staging environment into the system's architecture. The staging environment includes a modified version of ONI's operational data warehouse that accepts ETL inputs while the ETL is processing data, a time consuming task. The second component utilizes a data partitioning scheme and the ability to move low-level database storage objects between databases, which enables the transfer of monthly blocks of data between the staging and operational data warehouses. The users experience no interruptions while the ETL loads data into the staging environment and minimal interruption while the updated storage objects are transferred into the operational data warehouse. This solution is highly scalable. Given any type of computing hardware, loading and system down time will remain constant whether 50 K or 50 M records are loaded per day. As a result, users will never experience   fluctuations in performance and downtime is minimal.

The implementation and testing of all data warehouse enhancements were made possible utilizing MHPCC's *Tempest* and *Huinalu* computing resources. *Tempest,* a 32 IBM Power4 processor, 32 GB RAM node, housed virtually all databases used during development and testing. It allowed engineers to experiment with different techniques requiring varying degrees of processing power. The *Huinalu* nodes, each containing two Intel 933 processors and 1 GB RAM, executed ETL processes and served as a development environment for our geographically separated team members. The ability to easily reconfigure different clusters of *Huinalu* nodes afforded the team the flexibility it needed during different stages of the project.

Significance: ONI's premier cargo tracking system's data warehouse has undergone significant enhancements at the MHPCC. Its schema and system architecture have been modified to improve data loading and retrieval times using a variety of cutting edge technologies and techniques. An ETL tool was selected and implemented that streamlines mappings and eases their future maintenance. The data loading solution affords improved scalability and reduces system downtime. ONI's analysts benefit from the enhancements by having consistent and fast access to crucial data, while ONI's information technology support staff benefit from improved system scalability and maintainability.

Author and Contact: Chad Churchwell
Authors: Aaron Steigerwald, Marc Lefebvre, Brian Banks, Todd Lawson
Organization: Maui High Performance Computing Center, 550 Lipoa Parkway, Kihei, HI, 96753
Resources: *Tempest* (IBM SP3/SP4) and *Huinalu (*IBM Linux Supercluster*)* at MHPCC
Sponsorship: Office of Naval Intelligence (ONI)

Numerical Simulations of Asymmetries in Photo-Ionization Using Ultrashort Intense Laser Pulses

Szczepan Chelkowski and Andr D. Bandrauk

Using numerical solutions of time-dependent Schr dinger equation (TDSE) for a hydrogen and a helium atom in a linearly polarized, few-cycle laser field, we calculate the photoelectron left/right asymmetry measured by two opposing detectors placed along the laser polarization vector, with laser focus in the center. We find a very simple dependence of this asymmetry on carrier-envelope (C.E.) phase ϕ for laser intensities slightly below the tunneling regime which may allow us to measure (or to calibrate) and to stabilize the C.E. phase. In this regime there exists a wide intensity range. The zero asymmetry occurs at the same phase equal to $\pi/3$. We show that the direction of photo-emission can be controlled by the C.E. phase. These important results were not expected from simple theoretical models; they demonstrate the importance of numerical simulations in describing the laser-matter interactions at high laser intensities.

Research Objectives: High-power ultra-short laser pulses with durations as short as a few optical cycles are now available as research tools.[1,2] While long monochromatic pulses are completely characterized by their polarization, frequency and the temporal shape of their envelope, short pulses require at least one additional parameter since the electric field envelope of few-cycle pulses varies significantly during one cycle. Typically the temporal shape of the laser electric field is represented as a product of Gaussian-like envelope times trigonometric function. The phase of this function becomes a physically important parameter for pulses shorter than four optical cycles and is called the carrier envelope (C.E.) phase ϕ or the absolute phase. We show in Figure 1 the laser electric field:

$$E(t)=\varepsilon_0(t)\cos(\omega t+ \phi),$$

where $\varepsilon_0(t)$ is the pulse envelope (described by a Gaussian function), for two C.E. phases, $\phi=0$ and $\phi=\pi/2$. Recently, significant progress has been achieved in stabilizing the C.E. phase.[2]

When such a few-cycle laser pulse interacts with atomic gas its C.E. phase will affect significantly various physical process,[1] but it leaves a particularly simple signature in angular distributions of photo-ionized electrons.[3-6] The goal of our investigation is to find the laser pulse parameters which are most convenient for measurement of the C.E. phase ϕ. This task was required to solve about a thousand times the time-dependent Schr dinger equation (TDSE) which necessitates a huge amount of computer time.
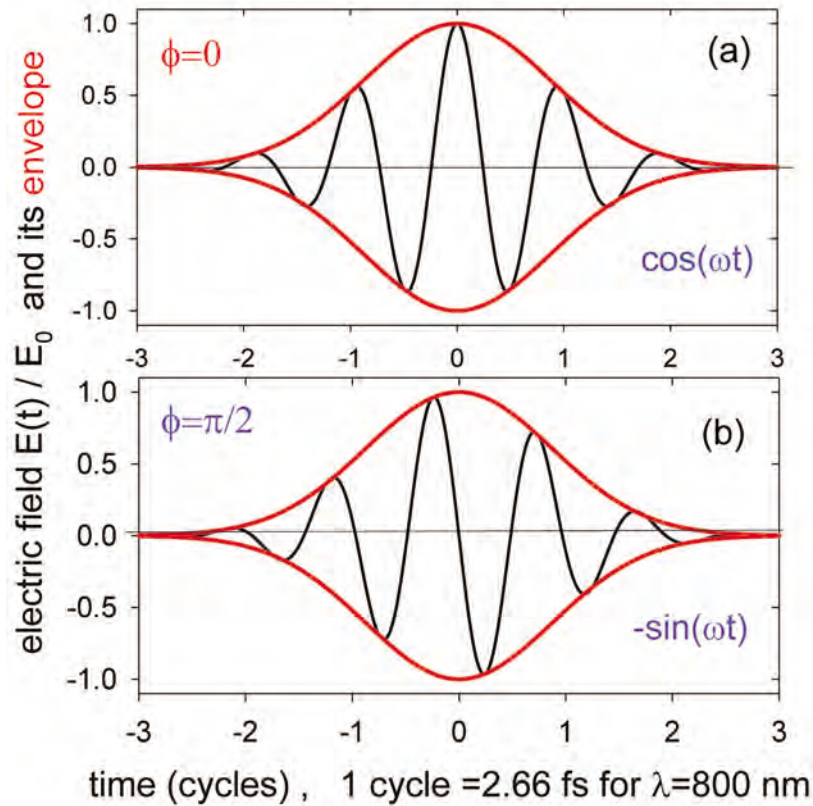

Figure 1. The shapes of the laser electric field E(t) used in our calculations for two C.E. phases $\varphi=0$ and $\varphi=\pi/2$.

For long monochromatic laser pulses the C.E. phase of the laser pulse does not induce any measurable effect. For example, the angular photoelectron distributions $f(\theta)$ are symmetric: i.e., $f(\theta)=f(\pi-\theta)$ (where θ is the angle between the photoelectron momentum and the laser polarization vector) because of the symmetry of the monochromatic electric field and of the atom. Considerable variation of the field envelope during one cycle and the nonlinear response of an atom lead to an asymmetry in photoelectron angular distributions, which can be used as a measurable signature of the C.E. phase of a few-cycle laser pulse. Figure 2 shows how such an asymmetry can be measured using two opposing detectors placed along the laser polarization (with laser focus in the center), with left/right detectors measuring the signals P_- or P_+ , respectively. We calculate these signals by solving numerically the 3D time-dependent Schrödinger equation (TDSE) describing the interaction of the laser pulse with a hydrogen atom (in spherical coordinates r, θ). Using well established numerical methods,[7,8] we obtained the time dependent wave function describing the ionizing electron $\psi(r,\theta,t)$ and the probability current of ionized electrons from which we calculated the signals P_+ and P_- registered by two detectors shown in Figure 2. Figure 3 shows the normalized asymmetry coefficient:

$$a=(P_+-P_-) /(P_+ + P_-)$$

as a function of the laser phase ϕ. To obtain each curve in Figure 3 we solved the TDSE 32 times (using 32 processors) for various 32 values of the phase ϕ in the interval $[0:\pi]$. Since the goal of our studies was to find the optimal experimental parameters we had to repeat calculations for many values of intensity, wavelength, and pulse duration which would be difficult to achieve without the access to a supercomputer. Figure 3 shows asymmetries for optimal range of intensities in which the asymmetry as a function of the C.E. phase ϕ is very sin-like. Most importantly zero's of the asymmetry occur in nearly the same place, i.e., at $\phi= \phi_0 =0.32$ π for intensities in the range: 3×10^{13} W/cm^2 $<I<10^{14}$ W/cm^2 , for the pulse durations between 3.6 fs and 6 fs and for various wavelengths between 780 to 1064 nm. See reference #8 for details. These simple patterns found in asymmetries as function of ϕ were in part already confirmed in recent experiments[6] and our results constitute an important piece of information for designing future experiments in which few-cycle pulses are used. Summarizing, our study shows the importance of numerical simulations based on TDSE in the non-perturbative regime and shows that analytic models, such as Strong Field Approximation Model[5] (or a tunneling model), yield correct value for the asymmetry coefficient only in a very narrow intensity interval above 10^{14} W/cm^2 .
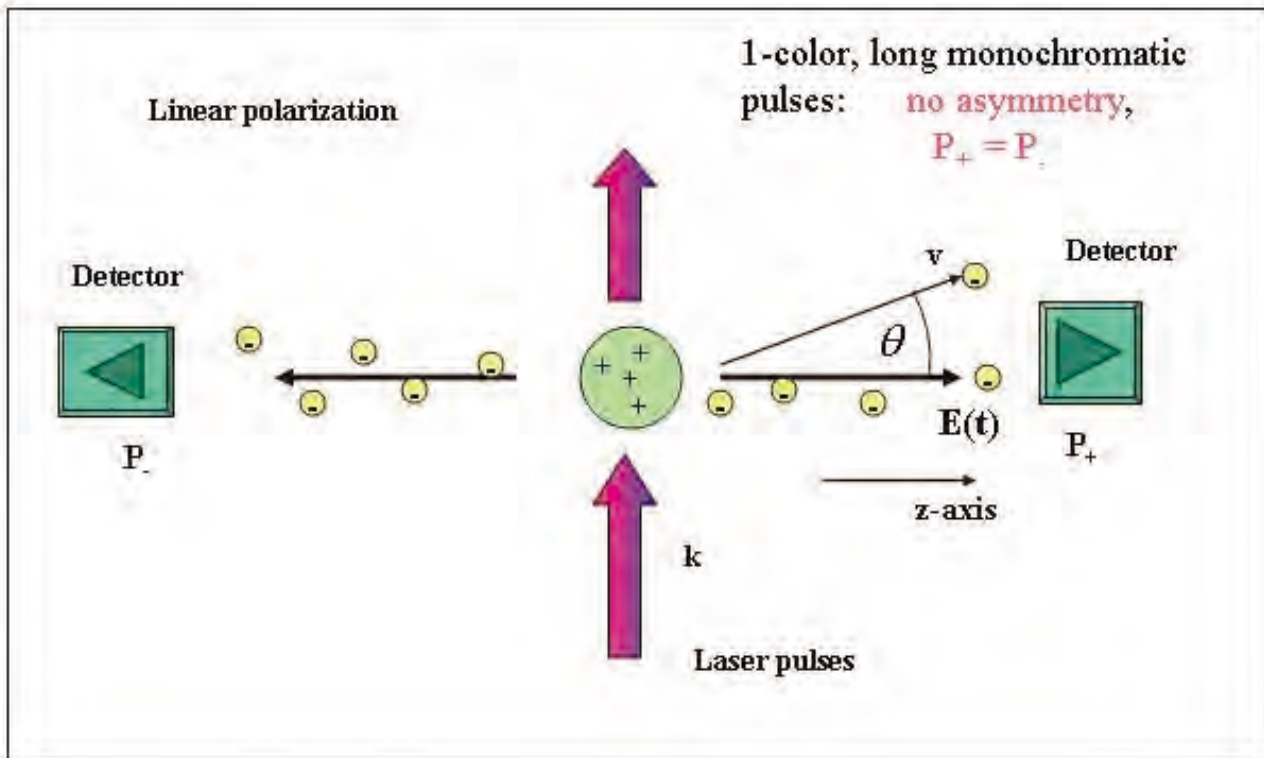

Figure 2. Experimental setup to measure the asymmetries in photo-ionization.

References:
1) T. Brabec and F. Krausz, Rev. Mod. Phys. 72, 545 (2000).
2) V. S. Yakovlev, P. Dombi, G. Tempea, C. Lemell, J. Burgd rfer, T. Udem, A. Apolonski, Appl. Phys. B 76, 329 (2003).
3) S. Chelkowski and A. D. Bandrauk, Phys.Rev. A 65, 061802 (2002).
4) S. Chelkowski, N. H. Shon, and A. D. Bandrauk, Las.Phys., 13, 871 (2003).
5) D. B. Milosevic, G. G. Paulus, and W. Becker, Optics Express 11, 1418 (2003).
6) G. G. Paulus, F. Lindner, H. Walther, A. Baltuska, E. Goulielmakis, M. Lezius, and F. Krausz, Phys.Rev. Lett.91, 253004 (2003); F. Lindner , private communication and Ph.D. Thesis, Max-Planck-Institute, Garching (Germany).
7) P. L. Devries, J. Opt. Soc. Am., B 7, 517(1990).
8) S. Chelkowski, A. D. Bandrauk, and A. Apolonski, Phys. Rev. A, accepted; Opt. Let., accepted.
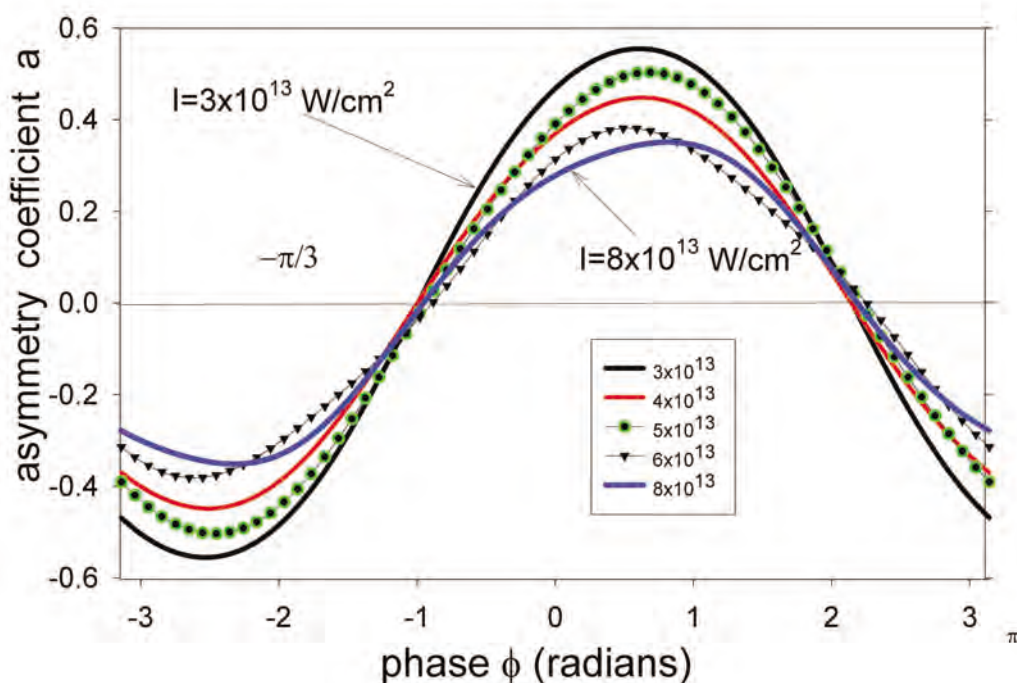
Figure 3. Asymmetry coefficient as a function of the C.E. phase for the wavelength $l = 800$ nm, $t_p = 3.9$ fs, for various intensities ranging from I= 3.1×10^{13} to I= 8×10^{13} W/cm^2 .

Author and Contact: Szczepan Chelkowski
Author: Andr D. Bandrauk
Organization: Laboratoire de Chimie Th orique, Facult des Sciences, Universit de Sherbrooke, Qu bec, JIK 2R1, Canada
Resources: 32 Processors of the *Tempest* System at MHPCC

Theater UnderSea Warfare (TUSW)

Robert Dant, Carl Holmberg, David Solomon, Lance Terada, Marie Greene, Thomas Meyer

A Linux Cluster is maintained and administered at the Air Force Research Laboratory Maui High Performance Computing Center (AFRL/MHPCC) for dedicated Theater Under Sea Warfare (TUSW) use. This TUSW cluster provides high performance computing resources to TUSW users for computationally intensive undersea warfare (USW) simulations. The cluster is designed to be easily expandable and has secure connectivity (via SIPRNet) to Pearl Harbor CTF-12 (Commander Task Force-12), allowing 'remote' access to the MHPCC computing resources for computationally intensive acoustic modeling. Modeling software is currently being integrated to demonstrate high performance computing 'reach back' during fleet exercises.

Research Objectives: The TUSW program objectives are: 1) developing and testing of a PC-based advanced USW workstation, 2) enhancing the design and implementation of an Undersea Warfare (USW) segment for the Net-Centric Collaboration Toolset, 3) engaging shore-based high performance computing power by porting operational databases and executing computationally intensive acoustic models within the AFRL/MHPCC processing environment, 4) creating TUSW Command Centers with automated knowledge management tools, 5) integrating air reconnaissance assets into the real-time USW net-centric environment, and 6) transitioning these new technologies to the acquisition community for eventual integration into the Navy's operational USW fleet and the Marine Corps warfighting inventory.

Methodology: Research efforts for the TUSW program (Year 2) at AFRL/MHPCC focused on: 1) integrating existing acoustic modeling and sonobuoy placement tools on a Linux cluster at MHPCC, 2) migrating from the legacy database application to a distributed object oriented database, and 3) developing a low latency manager/scheduler to load balance various computationally intensive models on the cluster.

To provide an initial USW processing capability, AFRL/MHPCC integrated a set of software tools, including the Scalable Tactical Acoustic Propagation Loss Engine (STAPLE) to calculate sound transmission losses through the ocean, and a Tactical Environmental Database Services (TEDServices) capability that provides continual updates to STAPLE's environmental data.
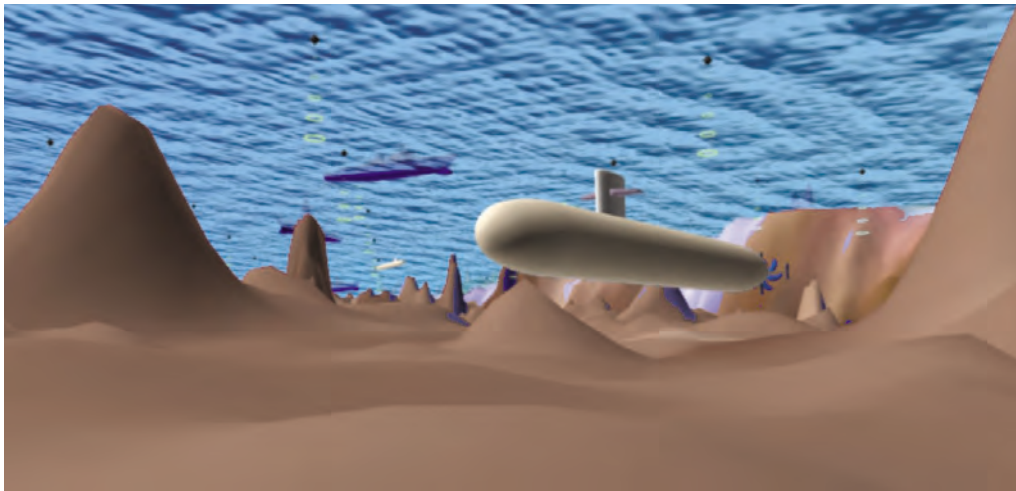

Figure 1. Display of actual bathymetry, contacts, buoy patterns and time-lapse sonar data are part of the research to augment existing USW graphical software.

Results: AFRL/MHPCC purchased and installed a 32-node (64 processor) Linux cluster system for exclusive TUSW use, as well as a stand-alone server/workstation and substantial disk storage. A traditional legacy Database Management System (DBMS) was replaced by a distributed object-oriented database that provided operational and environmental data to software models. The STAPLE transmission-loss modeling software was installed, its performance characterized, and then integrated with network access middleware to permit computational 'reach back' by existing PC-based client software.

AFRL/MHPCC also implemented a TUSW Manager/Scheduler that is responsible for managing user requests from CTF-12 (Pearl Harbor, HI). The Manager translates these user requests into appropriate TUSW application requests, which are presented to the TUSW Scheduler for execution. The Scheduler, which was designed for high-volume, short-duration jobs demanded by TUSW applications, then schedules and oversees the execution of the jobs on the cluster. The design of the TUSW Manager/Scheduler is concurrent in nature, so as to maximize job throughput and cluster resource utilization. The TUSW Manager/Scheduler also integrates knowledge of application resource demands and database bathymetry synchronization, so as to provide a robust and data-centric computing environment.
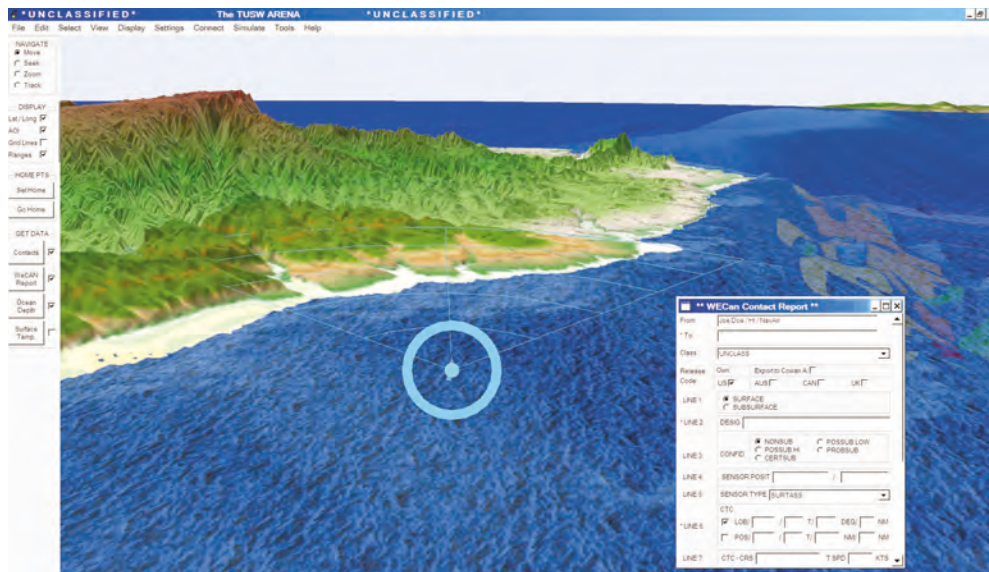
Figure 2. Ongoing USW research activities involved display of real world operational database information, such as the WeCAN (Web-Centric ASW Network) reports.

In addition, AFRL/MHPCC implemented a secure network interface between the Linux cluster and 'remote' TUSW users at CTF-12 (Pearl Harbor, HI). AFRL/MHPCC participated in TUSW code testing and in developing proof-of-concept demonstrations that highlighted initial TUSW program resources and capabilities.

Future TUSW developmental efforts will include testing of the high performance computation 'reach back' concept during fleet exercises, integration of the Manager/Scheduler, performance benchmarking, and installation of additional software models.
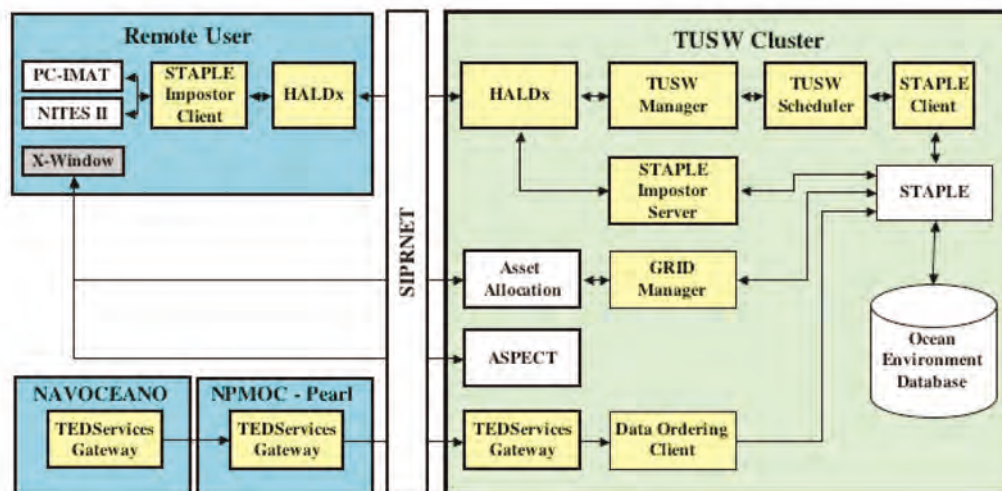
Figure 3. Legacy models, databases, and clients are linked over a wide area network using networking middleware that brings high performance computing to deployed naval units.

Visualization efforts include the development of a multi-platform interactive software application for viewing graphical representations of geo-referenced USW data within a three-dimensional geo-spatial environment.

Built into the interactive viewer are tools for navigating a global Synthetic Simulated Environment (SSE), defining and zooming to a geographic Area of Interest (AOI), using USW contacts and targets with Naval Tactical Data System (NTDS) symbology and models, and viewing Web-Centric Anti-Submarine Warfare (ASW) Network (WeCAN) reports.

High-resolution terrain and bathymetric data were converted into quad-tree geometries having multiple levels of detail and draped with geo-referenced aerial imagery to serve as the context for displaying data from USW databases.
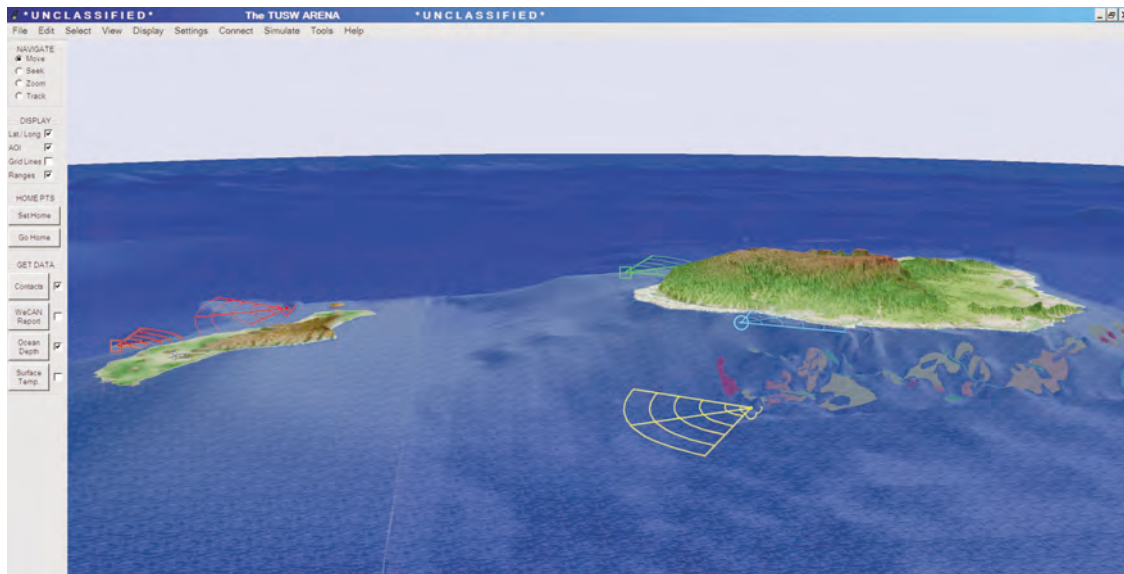
DoD

Figure 4. 3D geospatial data environments fused with interactive manipulation of contacts displayed with NTDS (Naval Tactical Data Systems) symbology provide better visualizations of warfare scenarios.

Integrated into this environment is the optional display of informational overlays comprised of geo-referenced data extracted from existing USW databases. These databases represent both historical and concurrent measurements, such as bathymetry, bottom loss, sound velocity, ocean temperature, and potentially any of the multitudes of other available measurements.

For visualization activities, future efforts will include the live integration of USW data obtained on demand from active USW databases to enable multiple asset tracking capabilities and near-real-time display of current oceanographic measurements for given global or local areas of interest.

Significance: The U.S. Navy has encouraged the identification, development, testing and deployment of technologies that enable undersea warfare decision makers to rapidly exploit the new advances in data fusion, knowledge management, high performance computing, and communications reach-back capabilities. The Office of Naval Research (ONR) - Code 35, Greater MIDPAC, has promoted research and development of innovations that will provide technology-based options for future U.S. Navy and Marine Corps capabilities. The goal for TUSW is to "Implement a 'leap ahead' command center for the future, for knowledge development, environmental analysis, and resource allocation for undersea warfare."

Author and Contact: Robert Dant
Authors: Carl Holmberg, David Solomon, Lance Terada, Marie Greene, Thomas Meyer
Organization: Maui High Performance Computing Center, 550 Lipoa Parkway, Kihei, HI, 96753
Resources: IBM Linux Cluster (96 Intel Processors), SGI Onyx 3900 (12 Processors) with Infinite Reality3 Graphics, DELL Dual Xeon (2 Processors) with nVidia QuadroFX 200G Graphics at MHPCC
Sponsorship: Office of Naval Research (ONR)

Resolving Closely Spaced Objects with Non Linear Image Processing Techniques

Keith Knox, Paul Billings, Bobby Hunt, Brian Kruse, Lewis Roberts

The Space Tracking and Surveillance System (STSS) Surrogate Test Bed (SSTB) Program is a risk reduction test bed for incorporating new technologies into the STSS program. This task will provide optical operations and infrastructure support, optical system design, and software design, and image processing optical algorithm research. The SSTB Team includes the MHPCC Contractor Team, MIT/LL, and Boeing MSSS Contractor Team.

Research Objectives: The objective of this task is to explore the requirements and feasibility of using super resolution image processing algorithms to resolve "closely-spaced objects" in a missile track using one or more image frames from an optical telescope.

Methodology: The MHPCC Contractor team has chosen to use NAPE (Nonlinear Algorithms for Parameter Estimation), a generalized optimization framework for estimating various quantities from noisy data. The parameters of an image formation forward model, including built on *a-priori* knowledge of the object (such as positivity and finite size), are adjusted until the best fit of the measured data to the model is achieved.

Results: In January 2004, the MHPCC contractor team, in association with the greater AMOS site, obtained observations of triple stars with the AEOS visible imager. The NAPE algorithm was applied to the images. The image of a single star (PSF in the image below) is used by the NAPE algorithm as reference information to increase the resolution of the unresolved binary star system. This produces a reconstruction of the double star, shown on the right in the diagram below. Additional computer simulations of the NAPE algorithm have demonstrated that this algorithm could achieve even greater increases in resolution, going beyond the diffraction limit of a telescope and thereby achieving super resolution. The team is continuing to explore possible multiple star systems that can be imaged and analyzed to demonstrate resolution beyond the diffraction limit with the NAPE algorithm.
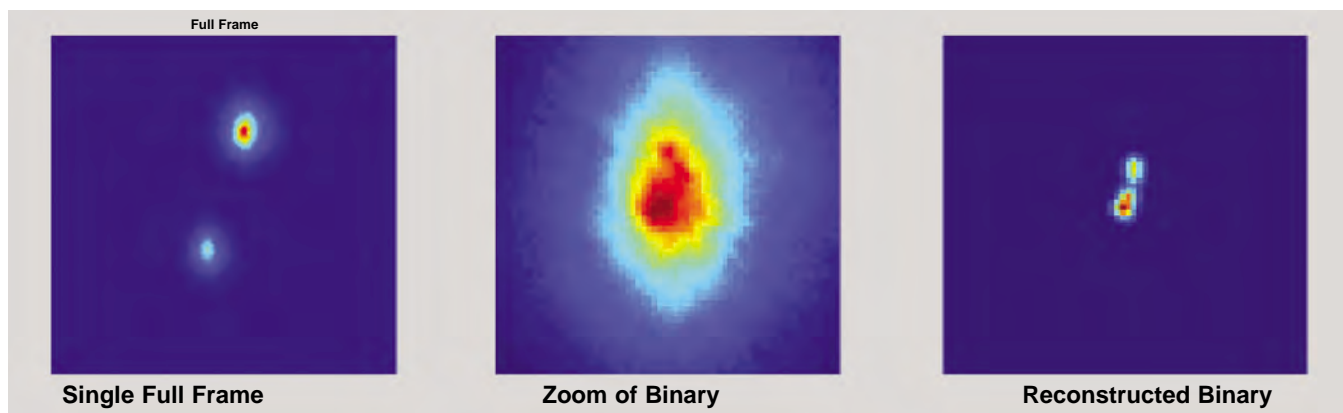

Full Frame

Single Full Frame   Zoom of Binary   Reconstructed Binary

Figure 1. Observations of Triple Stars.

Significance: The results of applying the NAPE experiments to triple star observations at 0.8 microns demonstrate that the NAPE super resolution algorithms are able to obtain very significant increases in object resolution. These increases, from the algorithm software, are beyond what is obtained even with the use of an Adaptive Optics system, which is considered the best that can be done in the application of optical hardware. When it is fully developed, this algorithm will provide resolved images of point objects, that are so closely spaced together they can only be seen as single unresolved spots of light.

Pan-STARRS Image Processing Pipeline Software Development

Bruce Duncan, Michael Berning, Robert DeSonia,
Eric Van Alst, Calvin Ross Harman

Pan-STARRS (Panoramic Survey Telescope and Rapid Response System) is an innovative new design for a wide-field imaging facility being developed for the Air Force Research Laboratory by the University of Hawaii (UH) Institute for Astronomy (IfA). UH IfA is the prime contractor and leader of the project. Massachusetts Institute of Technology Lincoln Laboratory (MIT/LL) is designing the charge-coupled devices (CCD) for the project. Science Applications International Corporation (SAIC) is a subcontractor to the IfA working on the database aspect of the project, and Maui High Performance Computer Center (MHPCC) is supporting IfA in the development of the data processing pipeline. By using four comparatively small co-located telescopes, the Pan-STARRS team plans to deploy an economical system that will be able to observe the entire available sky several times each month. The near-term goal is to discover and characterize Earth-approaching objects, including asteroids and comets that might pose a danger to our planet. The huge volume of images produced by this system will also provide valuable data for many other kinds of space scientific programs and products. This paper summarizes the overall project and the MHPCC contractor team development work performed to date.

Research Objectives: The full system, PS4, will be composed of four individual telescopes of 1.8-meter aperture observing the same region of sky simultaneously. Each telescope will have a three-degree field of view and be equipped with a CCD focal plane mosaic with 1 billion pixels. Pan-STARRS will cover 6,000 degrees squared per night in the survey mode searching for potential killer asteroids. The whole available sky as seen from Hawaii will be observed three times during the dark time in each lunation. Camera exposure times will vary between 30 and 60 seconds and IfA anticipates that Pan-STARRS will reach a limiting magnitude of 24. The focal plane will employ orthogonal transfer charge coupled devices (OTCCDs) that allow the shifting of charge along rows and columns, thus providing on-chip image motion compensation that is the equivalent of traditional "tip-tilt" image compensation, but without moving parts. Each raw image from a single Pan-STARRS camera will
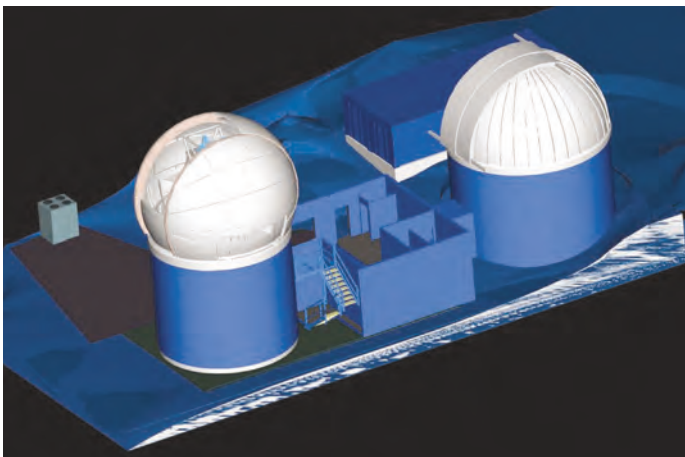
contain two Gigabytes of data and it is estimated that the raw data rate will be several Terabytes per night for the full telescope system. IfA decided in December 2003 to develop a one-telescope prototype system, PS1, which will be essentially one quarter of the total system and will be completed ahead of the full PS4 observatory. PS1 will have the same optics design and camera design as anticipated for the full version of Pan-STARRS. PS1 is being constructed inside the building that used to house the former Lunar Ranging Experiment (LURE) observatory atop Haleakala, Maui. A new dome will be placed on the building. Figure 1 shows an exterior pictorial for PS1, while Figure 2 shows how it will fit into its dome. PS1 will allow the team to test all the technology and subsystems that are being developed, including the telescope design, the cameras, and the data processing and reduction software. PS1 will be used to make a full-sky survey that will provide astrometric and photometric calibration data that will be used for the full Pan-STARRS survey. First light for PS1 is scheduled for January 2006, with deployment of the full PS4 system within two more years. Sites on Mauna Kea and Haleakala are being considered for the PS4 system, and site testing is being performed in parallel at both locations.

Figure 1. PS1 Telescope Facility installation pictorial (UH IfA).
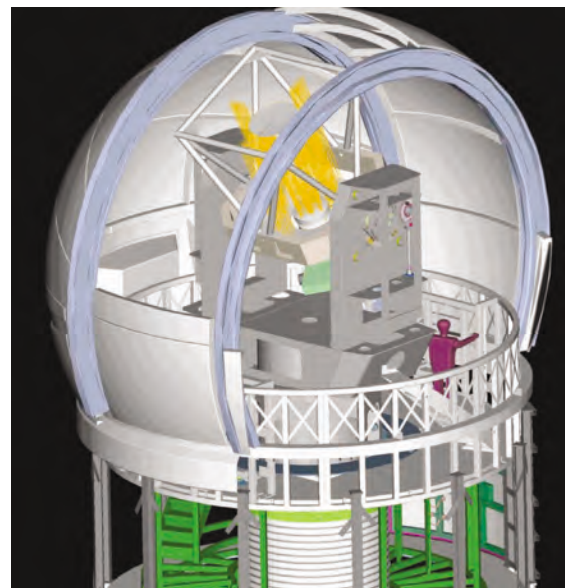

Figure 2. PS1 Telescope Dome installation pictorial (UH IfA).

Methodology: The MHPCC contractor team supported the UH IfA Pan-STARRS team during the first project year undergoing technology transfer from IfA, gaining knowledge and information on legacy image processing software and toolkits, and performing concept design studies, analysis, and benchmarking for the planned system. The collective IfA-MHPCC Image Processing Pipeline (IPP) Software Development Team, led by IfA, determined that it was in the best interests of the program to conduct a Pilot Project at the outset of the second year of program work. The primary purpose of the pilot was to not necessarily develop a major amount of the IPP software, but rather to drive out and exercise the collective IfA-MHPCC team in the software development process and the associated discipline, methods, procedures, and team communications that are needed while also developing modules that could be used in further software development for PS1 and the subsequent PS4 system. IfA and MHPCC also considered and assessed various software architectures during this time frame.

Upon successful completion of the Pilot Project, the MHPCC contractor team received direction from UH IfA to begin software development tasking for the PS1 IPP Data Handling Library. The first MHPCC task was to create a collection of functions and structures which define the basic data types, and which perform the wide range of basic analysis operations using those data types. This action was decided and planned by IfA to leverage existing libraries and provide software wrappers to them to minimize and localize the IPP dependency on external software sources. The necessary library functions were divided into four categories: system level operations, general data operations (such as basic statistics on a collection of data values), image handling operations (such as extracting a sub raster from an image), and object catalog handling operations (such as extracting a subset of objects in a spatial region). The end result of this new software package was planned to be the source code which could be compiled into a library of the basic IPP functions against which additional future programs can be linked and a header file, or set of header files, which would be included by those IPP functions needing access to the library functions. MHPCC was also tasked to provide code-description documentation and unit test software to the IfA. The library functions were to be written to use the public Application Program Interfaces (APIs) and data structures that IfA initially defined. IfA provided the requirements and design guidance documentation to MHPCC at the start of this work and MHPCC plans included the furnishing of an updated Software Design Document (SDD), a Software Version Description (SVD) document, and also HTML and Doxygen documentation along with the corresponding software package.

MHPCC work began with each software developer wrapping functions in assigned libraries and work sheets. Staff also coordinated memory management issues with IfA regarding reuse and/or modification of existing code. Our initial evaluation of the code provided indicated that it was not going to be totally reusable and bug free, but would require some significant customization and substantial new code development. The MHPCC team developed a status-tracking sheet to monitor the software development for system utilities, basic data collection, and data manipulation functions. This sheet was set up to capture and report status on: Wrapper Function, PS1 Library (Third Party, Pilot, Other, New), LOC Estimate, LOC Actual, Responsible Developer, Responsible Test Analyst, Coding Status, Peer Review Status, Development Completion Date, Unit Test Status, Unit Test Completion Date, Documentation Status, Documentation Completion Date, Configuration Management Status, and Open Issues/Comments. The MHPCC team developed an overall program-level WBS and schedule to monitor and control status for its work for this phase of the project. A preliminary Software Requirements Review was held in May. Items covered during this event included top-level requirements, architectural systems and hardware issues, data processing components, detailed computational and storage hardware requirements (presently estimated at 700 TB), data storage and data archiving operational needs, and developmental computing hardware.

As the software development progressed, MHPCC designed, developed, and created a test point life cycle tracking system and document describing procedures of test points, including steps and functions to provide for: navigation to test point tracker, creation of new test points, assignment of test points, implementation of test points, verification of test points, modification of test points, and the deletion of test points. MHPCC also developed a software metrics LOC counting template that uses automated tools to capture and track source file names (source lines, type definition lines, comment lines), header file names (type definition lines, comment lines, totals), make file names, test code function (source lines, type definition lines, comment lines), and a summary for source, header, and make files (executable, type definitions/instantiations, comments, and totals).

MHPCC subsequently began preparations to deliver the software package to IfA in mid-June. A features freeze on code development was enacted and the team initiated the package finalization and ship review process which involved unit testing completion and reviews, bug fixing and completion, and code and related documentation reviews. A comprehensive ship review checklist was developed. This 117-item list (with 23 major steps/categories/functions) included information that related to the requirement/guideline entries that were logged from the Pan-STARRS Coding Conventions and SRS-PSLib Software Requirements Specification documents received from IfA. MHPCC also loaded these requirements in a spreadsheet to allow personnel to correlate a checkpoint with a document. The MHPCC team also developed a spreadsheet using results from the Imagix 4D tool to describe the software content, productivity, and quality metrics.

Results: The MHPCC contractor team delivered Release 1.0 of the PS1 Image Processing Pipeline (IPP - Data Handling Library in June. The package was comprised of source, object, executable, and test codes; a comprehensive Software Design Description (SDD); a detailed Software Version Description (SVD); ManPages, and Doxygen software documents. Software metrics included (without comments): Source: 7,092; Header: 945; Make: 218; Unit Test Files: 7,378; and the Release 1.0 total lines of code count was 15,633. A review of the MHPCC team's software metrics revealed that its productivity level exceeded expectations, even though the work scope in terms of projected LOC exceeded the estimates also. MHPCC then began refinements, completion of open items, and bug fixes for the software package that was released. The team also began treating the Astronomy-specific functions software development task for the library. While some of the astronomy utilities are planned to be implemented through wrapping the Starlink organization's SLALIB Positional Astronomy Library, the majority will require totally new software development.

Significance: The delivery of the first release of PS1 IPP software represented a substantial milestone in the progression of the Pan-STARRS project. The MHPCC contractor team is continuing to support IfA in the execution of software development and documentation for the PS1 phase. The next near-term work will include software development support to complete the entire library development including the Astronomy functions. Future work here will include the treatment of projections (gnomic, orthographic, Cartesian, mercator, and Hammer-Aitof), tangent plane to sky, mosaic cameras, general astronomy functions, positions of major solar system objects, and offsets. MHPCC will also begin image modules and calibration construction image modules software development. The project team will continue working diligently toward the PS1 prototype system, with the longer term goal of fielding the full four-telescope PS4 system depicted in Figures 3 and 4.

The MHPCC contractor team wishes to express its thanks to UH IfA for its pioneering work on Pan-STARRS and its leadership of the project and support of the MHPCC team.
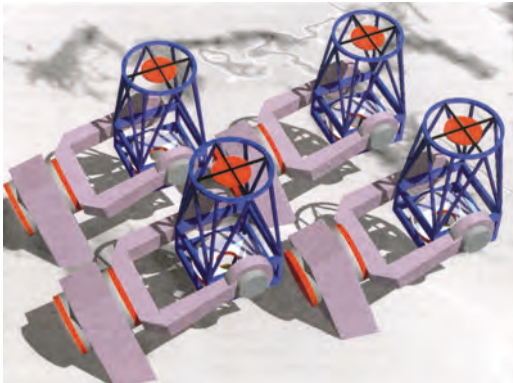
Figure 3. PS4 Candidate Design (UH IfA).

Figure 4. PS4 Pedestal Candidate Design (UH IfA).

Theoretical Study of the Insertion Reactions of Benzyne- and Carboryne- Ni Complexes

Eluvathingal D. Jemmis and Anakuthil Anoop

The reaction mechanism of the double insertion of acetylene to nickel benzyne complexes is studied in detail and compared and contrasted with a similar reaction with carboryne-nickel complexes using theoretical calculations at B3LYP/6-31G* level of theory.

Research Objectives: The attempt is to study the mechanism of the insertion reactions of alkyne to the Metal-benzyne bond in detail taking the example of Ni-benzyne complexes.[1] The study is extended to the 3-Dimensional counterparts, the carborynes. Polyhedral boranes and carboranes are being used in a variety of novel applications. Methods to develop chemistry of these polyhedral structures are much in need

Methodology: All calculations used the Gaussian 03 Program packages at MHPCC.[2] Geometry optimization was carried out at B3LYP/6-31G* level of theory. All the structures are characterized by frequency analysis.

Results: The scheme shows the proposed reaction mechanism. Various intermediates and transition states are optimized and the free energy change involved in each step is calculated. The reaction mechanism is found to be similar for the carborynes, with barriers that are within experimental reach.

References:

1) Bennett, M. A., Wenger, E., Organometallics 1995, 14, 1267.
   Bennett, M. A., Hockless, D. C. R., Wenger, E., Organometallics 1995, 14, 2091.
   Bennett, M. A., Wenger, E., Organometallics 1996, 15, 5536.
2) M. J. Frisch et al, Gaussian, Inc., Pittsburgh, PA, 2003.
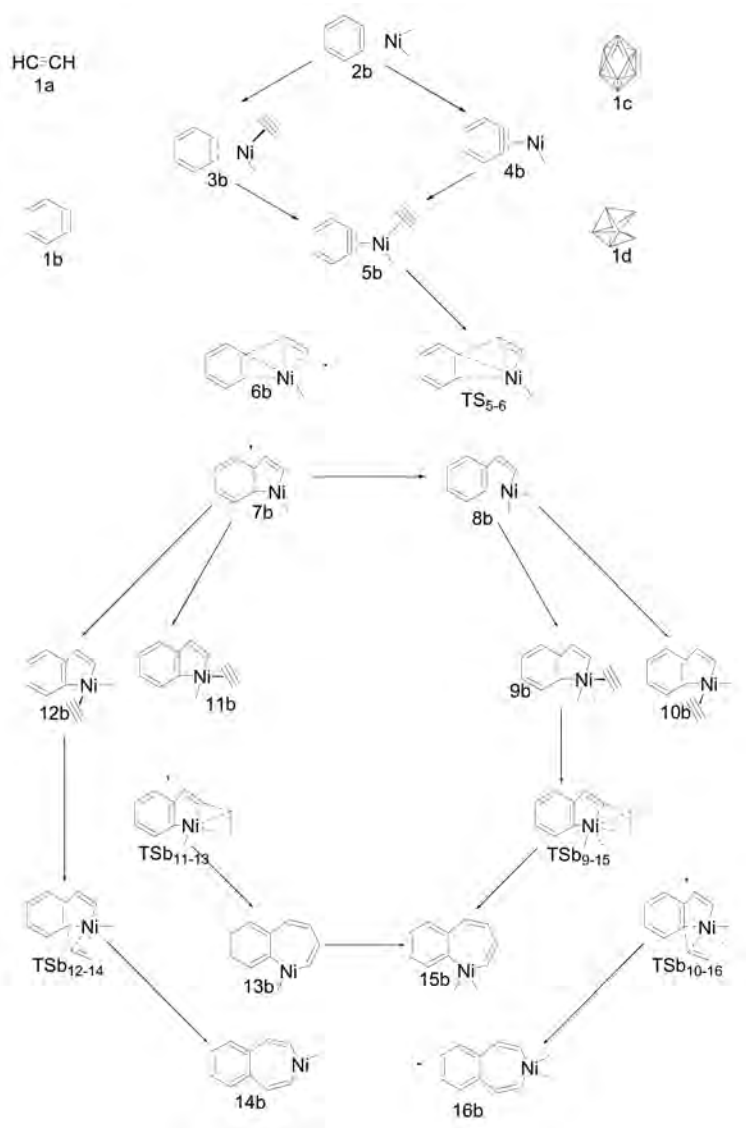
Electron-Impact Ionization of the C^{2+} Ion

Igor Bray

In this project we consider ionization of beryllium-like C^{2+} ions by fast electrons. In the experiment the production of C^{2+} ions occurs as an unknown mix of the ground 2^1S state and the long-lived metastable 2^3P state. We perform convergent close-coupling (CCC) calculations for the electron-impact ionization process and hence determine that the ratio of the two states is approximately 1:1.

Research Objectives: Carbon is the basis of known life and hence is of particular significance in extraterrestrial search for life. Accordingly, electron-impact spectra of carbon and its ions may be used to identify its outer-space abundance. For these reasons the study of electron-impact excitation and ionization of carbon and its ions is of current interest.

The production of ionic elements in a laboratory is a difficult task. Positively charged objects keep their charge for relatively short periods of time and are quickly neutralized by free electrons. Additionally, the method of production of the C^{2+} ion in a laboratory leads to it being in an unknown combination of the ground 2^1S state and the metastable 2^3P state. Here we show how a collision experiment coupled together with state-of-the-art theory can be combined together to determine the abundance of the various initial states of the target ion.

In the figure we present CCC calculations[1] for e-C^{2+} ionization. Given that the two cross sections lie approximately on either side of the experiment we can conclude that the ratio of the two initial states is approximately 1:1.
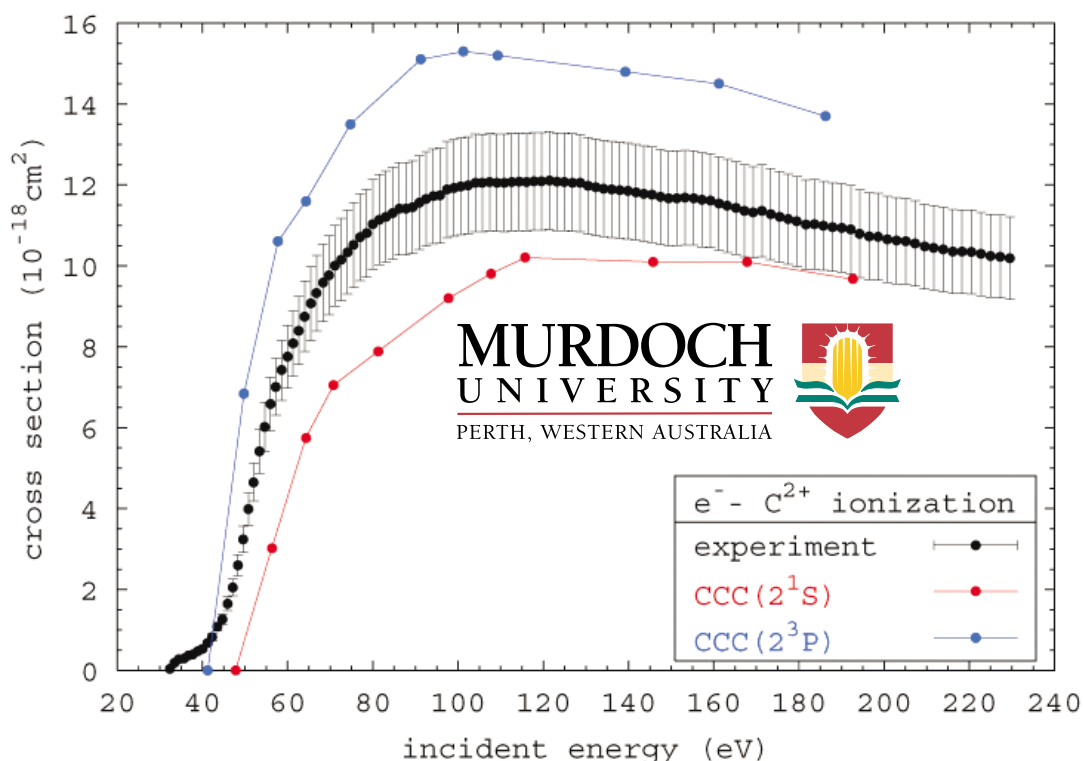
Figure 1. Total ionization cross section for electron-impact ionization of C^{2+}. The CCC calculations are for the two indicated possible initial target states.

References:
1) D. V. Fursa and I. Bray, Journal of Physics, B 30, 5895, (1997).

Author and Contact: Igor Bray
Organization: Murdoch University, Professional Fellow, Physics & Energy Studies, GPO Box S1400, Perth, Western Australia, 6849
Resources: IBM SP *Tempest* at MHPCC and SUN E450 at Murdoch University
Sponsorship: Australian Research Council

INDEX OF AUTHORS

INDEX OF ORGANIZATIONS